Vegetation change in response to climate extremes in Limpopo Province, South Africa

By

Thavhanyedza Humbulani

11612552

A dissertation submitted in fulfilment of the requirements for the Degree of Master of Environmental Sciences in Geography,

Department of Geography and Geo-Information Sciences
School of Environmental Sciences

University of Venda

Supervisor: Dr. N.S. Nethengwe
Co-Supervisor: Dr. H. Chikoore

February, 2020

DECLARATION

I, **Thavhanyedza Humbulani**, hereby declare that the dissertation for Master's degree in Environmental Sciences at the University of Venda submitted by me has not been previously submitted for any degree or examination at this or any other institution. This is my own work in design and execution, and all reference materials contained herein have been accurately acknowledged.

Signature :…  …… Date :……08/07/2020……..

DEDICATION

To my parents,

(The late**) Ndishavhelafhi Elton Thavhanyedza**

Ntshengedzeni Virginia Thavhanyedza

ACKNOWLEDGMENTS

First and foremost, praises and thanks to God, the Almighty for His showers of blessings throughout my life. I would like to express my deep and sincere gratitude to my supervisor Dr N. S. Nethengwe and co-supervisor Dr H Chikoore, for their patience, motivation, and immense knowledge in providing invaluable guidance throughout my research engagement. I would like to thank National Research Fund (NRF) and Department of Agriculture, Fisheries and Forestry for funding which made the study possible. I appreciate the rainfall and temperature data from South African Weather Service (SAWS). A special thanks to my research colleagues whose help motivated me immensely. Last but not least, I would like to thank my special friend and family, Murunwa Nemapate, Mukoni Kayla Thavhanyedza and others for their support throughout the research.

agriculture,
forestry & fisheries
Department:
Agriculture, Forestry and Fisheries
REPUBLIC OF SOUTH AFRICA

ABSTRACT

An increase in the level of greenhouse gases (GHGs) in the atmosphere, combined with climatic variability, is likely to bring about extreme climate events, such as tropical storms, heat waves, floods, and droughts. In addition, a small change in the variance and mean of climate parameters might result in a strong shift in the intensity and frequency of extreme climatic events. The climatic conditions over southern Africa are highly variable and, and as such, southern Africa region becomes highly vulnerable to changes in extreme climatic conditions. Changes in climate extremes exert much pressure on the vegetation cover, thereby threatening the ecological stability of an area. This study analysed changes in vegetation cover and responses to extreme climate and weather events in the Limpopo Province, South Africa. The specific objectives of the study are to determine the nature of climate extremes from 2000 to 2017; to examine vegetation change in the study area, and analyse vegetation responses and sensitivity to climate extremes. In order to achieve these objectives, various quantitative techniques were employed. Extreme climate characterisation was done using GPCP precipitation, maximum temperature, and standardized precipitation evapotranspiration index (SPEI), whilst MODIS satellite was used for land use/ land cover change and vegetation response. To analyse vegetation response to extreme weather events, MODIS vegetation indices i.e. NDVI, EVI, and LSWI were used to analyse vegetation conditions and sensitivity in relation to extreme climatic events. Using the interannual rainfall variability and anomalies, seasons with abnormal rainfall patterns were chosen and analysed. Season with anomalous heavy rainfall occurred in 1999/00 and 2005/06 over Limpopo Province, whilst the anomalous low rainfall occurred during the summer season (DJF) in 2002/03 and 2015/16. Over the region, heavy rainfall was observed to be negatively associated with maximum temperatures ($r = -0.66$). Severely dry or drought conditions were associated with very poor vegetation conditions due to excessive temperatures and increased evaporation rate resulting in land surface water loss ($LSWI < 0$) and vegetation stress, meanwhile, heavy rainfall had a strong association with good vegetation conditions. However, vegetation tends to lag by one month from heavy rainfall. Using the Pearson moment correlation coefficient, the vegetation conditions (NDVI and EVI) were correlated with Land Surface Water Index (LSWI) and climate variables i.e. GPCP precipitation and maximum temperatures, with correlation coefficient of LSWI against GPCP, Tmax, NDVI, and EVI ($r = 0.83$, $r = -0.78$, $r = 0.73$, $r = 0.87$ respectively), NDVI and EVI against GPCP precipitation and Tmax ($r = 0.31$, $r = -0.70$, $r = 0.53$, and $r = -0.73$ respectively). The study shows a link between extreme weather events i.e. drought/ floods conditions and vegetation conditions. The findings of the study could serve as a scientific baseline data for better

understanding the effects of drought and floods in relation to vegetation for sustainable management of the ecosystems. With enough details or information about the vegetation, it can be possible to generate policies and launch programs to save ecosystems and the environment. Foresters, biodiversity officers, and policymakers could also find the information important in the formulation of policies, and programs that require development planning.

Keywords*:* Limpopo Province, NDVI, EVI, LSWI, Vegetation Response

Table of Contents

DECLARATION i
DEDICATION ii
ACKNOWLEDGMENTS iii
ABSTRACT iv
LIST OF FIGURES x
LIST OF TABLES xiv
LIST OF ACRONYMS AND ABBREVIATIONS xv
CHAPTER 1: INTRODUCTION 1
1.1 Background 1
1.2 Problem Analysis and Motivation 2
1.3 Research Questions 3
1.4 Aim and Specific Objectives 3
1.4.1 Aim 3
1.4.2 Specific Objectives 3
1.5 Delimitation of the study and Description of the Study Area 3
1.5.1 Description of the Study Area 3
1.5.2 Delimitation of the study 7
1.6 Definition of Key Concepts 8
1.7 Dissertation Structure 8
CHAPTER 2: LITERATURE REVIEW 10
2.1 Introduction 10
2.2 Climate Dynamics of South Africa and Limpopo Province 10
2.2.1 Climate of South Africa 11
2.2.3 Climate of Limpopo Province 11
2.3 Climate Variability 11
2.4 Extreme Climate and Weather Events 12
2.5 Extreme climate and weather events classification 13
2.5.1. Heat Waves 13
2.5.2. Droughts 13
2.5.3. Floods 15
2.5.4 Impacts of Extreme climate and weather events 16
2.6 Synoptic Systems that causes extreme climate 17

2.6.1 Cut Off Lows 17
2.6.2 Tropical Cyclone (TCs) 18
2.7 Remote Influence of Extreme Climate Events 19
2.7.1 El Nino Southern Oscillation (ENSO) 19
2.7.2 Indian Ocean Dipole (IOD) 21
2.7.3 Southern Annular Mode (SAM) 23
2.8 ENSO Teleconnections and Impacts 23
2.9 Extreme indices 25
2.9.1 Extreme Value Theory (EVT) 25
2.9.2 El Nino Southern Oscillation (ENSO) 26
2.9.4 Standardized Precipitation Evapotranspiration Index (SPEI) 29
2.9.5 Palmer Drought Severity Index (PDSI) 30
2.10. Biomes of South Africa 30
2.11 Vegetation Dynamics 32
2.12 Vegetation Indices 33
2.12.1 Normalized Difference Vegetation Index 34
2.12.2 Enhanced Vegetation Index 34
2.12.3 Land Surface Water Index 35
2.13 Conceptual Framework 35
2.14 Summary 36
CHAPTER 3: METHODOLOGY 37
3.1 Introduction 37
3.2 Research design 37
3.3 Description of data 37
3.3.1 NASA Satellite Data 37
3.3.2 Meteorological Data 38
3.5 Methods of data analysis 39
3.5.1 Time Series Analysis 39
3.5.2 Climate extremes Identifications 40
3.5.3 Composite Analysis 40
3.5.4 Case Study 41
3.5.5 Land Use/ Land Cover Classification (LULC) 41
3.5.6 Vegetation Indices 43

3.5.7 Pearson's product-moment correlation coefficient 44
3.5.8 National Centers for Environmental Prediction (NCEP) 45
3.5.9 Standardized Precipitation Evapotranspiration Index (SPEI) 46
3.5.11 Change Detection 47
3.6 Quality Assurance 47
3.7 Summary 48
CHAPTER 4: EXTREME WEATHER EVENTS IN LIMPOPO PROVINCE 49
4.1 Introduction 49
4.2 Rainfall 49
4.3 Temperature 54
4.4 Extent and characteristics of extreme weather events using the Standardized Precipitation Evapotranspiration Index (SPEI) 57
4.5 Correlation of GPCP Precipitation and Temperature with ENSO Southern Oscillation (El Niño and La Niña) 65
4.6 GPCP Precipitation Composite (Summer) of La Niña and El Niño Events 67
4.7 Case Studies of extreme events over Limpopo Province 68
4.7.1 Case 1: 1999/2000 DJF over Limpopo Province 68
4.7.2 Case 2: 2002/2003 DJF over Limpopo Province 70
4.7.3 Case 3: 2005/2006 DJF over Limpopo Province 71
4.7.4 Case 4: 2015/2016 DJF over Limpopo Province 72
4.8 Summary 75
CHAPTER 5: VEGETATION CHANGE, RESPONSE, AND SENSITIVITY TO EXTREME WEATHER EVENTS 76
5.1 Introduction 76
5.2 Land cover extent and rate of change over Limpopo Province 76
5.2.1 Extent and distribution of Land Cover over Limpopo Province 77
5.2.2 Spatiotemporal Distribution of Land Covers 80
5.2.3 Land Use/ Land Cover Change 82
5.2.4 Land Use/ Land Cover Classification Quality Confidence 83
5.3 Vegetation Response and Sensitivity to extreme weather events 87
5.3.1. Normalized Difference Vegetation Index (NDVI) 87
5.3.2. Enhanced Vegetation Index (EVI) 93
5.4 Monitoring Vegetation Spatiotemporal Dynamics 98
5.4.1 NDVI and EVI 98
5.4.2 Land Surface Water Index (LSWI) 101

5.5 Pearson's Product-Moment Correlation Coefficient 102
5.6 Summary 110
CHAPTER 6: CONCLUSIONS AND RECOMMENDATIONS 111
6.1 Introduction 111
6.2 Synthesis of key findings 111
6.2.1 Climate drivers of vegetation response 111
6.2.2 Vegetation response 112
6.2.3 Vegetation Sensitivity 113
6.3 Conclusions 113
6.4 Recommendations 115
6.4.1 Biodiversity Management 115
6.4.2 Land Use/ Land Cover Management 115
6.5 Recommendations for Future Work 116
References 117

LIST OF FIGURES

Figure 1. 1: Map showing the study location over Limpopo Province, South Africa 4

Figure 1. 2: Vegetation condition map over Limpopo Province (Source USGS/EROS) 5

Figure 1. 3: Map showing the elevation over Limpopo Province 6

Figure 1. 4: Mean Annual Rainfall over Limpopo Province (Source: ARC-ISCW, 2014) 7

Figure 2. 1: Cut-off low circulation pattern at near surface at 500hpa levels. (Source: Tyson and Preston-Whyte, 2000) 18

Figure 2. 2: EL Nino Southern Oscillation 20

Figure 2. 3: Nino 3.4 Source 21

Figure 2. 4: Indian Ocean Dipole Source 22

Figure 2. 5: Rainfall patterns during El Niño events during DJF 24

Figure 2. 6: Rainfall patterns during La Nina events during DJF 25

Figure 2. 7: Time series of the ONI for the period 2000-2017 over Limpopo Province 27

Figure 2. 8: Time series of the Southern Oscillation Index for the period 2000-2017 over Limpopo Province 28

Figure 2. 9: Map showing the Biome types over South Africa (source, SANBI, 2018) 31

Figure 2. 10: Map showing Vegetation Cover over Limpopo Province 32

Figure 2. 11: Conceptual Framework 36

Figure 4. 1: Southern Africa mean summer (DJF) spatial GPCP rainfall distribution (mm/day) 49

Figure 4. 2: Mean annual cycles of rainfall over Limpopo Province based on South African Weather Services (SAWS) data 51

Figure 4. 3: GPCP Interannual summer rainfall (DJF) variability over Limpopo Province 52

Figure 4. 4: GPCP summer rainfall (DJF) anomalies over Limpopo Province 53

Figure 4. 5: Showing mean summer (DJF) spatial distribution of air temperatures over Southern Africa 55

Figure 4. 6: Annual cycles of maximum temperature over Limpopo Province based on South African Weather Service (SAWS) data 55

Figure 4. 7: Interannual summer maximum temperature variability over Limpopo Province 56

Figure 4. 8: Maximum temperatures anomalies over Limpopo Province for the period 2000-2017 56

Figure 4. 9: Lephalale Weather Station SPEI (SPEI 1, SPEI 3, SPEI 6 and SPEI 12) 60

Figure 4. 10: Mara Weather Station SPEI (SPEI 1, SPEI 3, SPEI 6 and SPEI 12) 61

Figure 4. 11: Polokwane Weather Station SPEI (SPEI 1, SPEI 3, SPEI 6 and SPEI 12) 62

Figure 4. 12: Warmbad Weather Station SPEI (SPEI 1, SPEI 3, SPEI 6 and SPEI 12) 63

Figure 4. 13: ONI/SOI vs GPCP Precipitation and ONI/SOI vs Temperature correlation in Limpopo Province 66

Figure 4. 14a+b: Composite mean GPCP precipitation anomaly (mm/day) for summer (December-February), for strongest events 2000-2017 for southern Africa during drought (a) and wet years (b) 68

Figure 4. 15a+b: Summer (DJF) rainfall (a) and maximum temperature (b) over southern Africa during 1999/00 wet condition. 69

Figure 4. 16a+b: Summer (DJF) rainfall (a) and maximum temperature (b) over Southern Africa during the 2002/03 drought condition. 70

Figure 4. 17a+b: Summer (DJF) rainfall (a) and maximum temperature (b) over Southern Africa during 2005/06 wet condition. 71

Figure 4. 18a+b: Summer (DJF) rainfall (a) and maximum temperature (b) over Southern Africa during the 2015/16 drought condition. 72

Figure 4. 19: Mean composite of summer (DJF) geopotential height at 500-hPa over Southern Africa, during extreme weather events. 73

Figure 4. 20: Mean composite of summer (DJF) OLR at 200-hPa over Southern Africa, during extreme weather events. 74

Figure 4. 21: Composite mean of summer (DJF) vector winds 500-hPa over Southern Africa, during extreme weather events. 74

Figure 5. 1: Map showing 2001 annual IGBP vegetation land covers over Limpopo Province, South Africa 77

Figure 5. 2: Map showing 2010 annual IGBP vegetation land covers over Limpopo Province, South Africa 78

Figure 5. 3: Map showing 2017 annual IGBP vegetation land covers over Limpopo Province, South Africa 79

Figure 5. 4: The annual IGBP spatiotemporal classification over Limpopo Province 81

Figure 5. 5: Temporal analysis of MODIS MCD12Q1 IGBP change detection over Limpopo Province.....82

Figure 5. 6: classification confidence (highest confidence 9 shown in red) for the IGBP land cover classifications. 84

Figure 5. 7: Spatial distribution of the NDVI over Limpopo Province during the wet condition of 1999/00.....88

Figure 5. 8: Spatial distribution of the NDVI over Limpopo Province during the drought condition of 2002/03.....89

Figure 5. 9: Spatial distribution of the NDVI over Limpopo Province during the wet condition of 2005/06.....91

Figure 5. 10: Spatial distribution of the NDVI over Limpopo Province during the drought condition of 2015/16.....93

Figure 5. 11: Spatial distribution of the EVI over Limpopo Province during the wet condition of 1999/00.....94

Figure 5. 12: Spatial distribution of the EVI over Limpopo Province during the drought condition of 2002/03.....95

Figure 5. 13: Spatial distribution of the EVI over Limpopo Province during the wet condition of 2005/06.....96

Figure 5. 14: Spatial distribution of the EVI over Limpopo Province during the drought condition of 2015/16.....97

Figure 5. 15: Time series showing mean NDVI values over Limpopo Province during droughts and floods conditions. 100

Figure 5. 16: Time series showing mean NDVI values over Limpopo Province during droughts and floods conditions. 101

Figure 5. 17: Time series showing mean NDVI values over Limpopo Province during droughts and floods conditions. 102

Figure 5. 18: Showing Matrix table of correlation coefficients using different visualizations.....105

Figure 5. 19 shows scatter plots showing the relationship between independent and dependent variables 107

Figure 5. 20: showing scatter plots showing the relationship between independent and dependent variables.....107

Figure 5. 21: Spatial distribution of the LSWI over Limpopo Province during the wet condition of 1999/00.....108

Figure 5. 22: Spatial distribution of the LSWI over Limpopo Province during the drought condition of 2002/03.....108

Figure 5. 23: Spatial distribution of the LSWI over Limpopo Province during the wet condition of 2005/06.....109

Figure 5. 24: Spatial distribution of the LSWI over Limpopo Province during the drought condition of 2015/16.....109

LIST OF TABLES

Table 2.1: ENSO events from 2000- 2017 based on SOI and INO 29

Table 3.1: depiction of MOD12Q1 annual IGBP land cover classes, adopted and modified from Friedl et al., (2010). 42
Table 3.2: Table showing categories of SPEI 46

Table 4.1: The ranks for selected droughts and floods over Limpopo Province, South Africa 54
Table 4.2: Table of SPEI 6, Extreme weather events classification over Limpopo Province 58
Table 4.3: Extreme weather frequency over Limpopo Province 64

Table 5.1: The spatial extent of annual IGBP land covers classes (Area_Km2) for 2001, 2010, and 2017 in Limpopo Province. 80
Table 5.2: Percentage of Post classification change detection over Limpopo Province. 83
Table 5.3: IGBP classification confusion matrix, commission, omission, producer's accuracy, and user's accuracy. 86
Table 5.4: P-values of correlated variables 106

LIST OF ACRONYMS AND ABBREVIATIONS

ARC	: Agricultural Research Council
ENSO	: El Nino Southern Oscillation
AVHRR	: Advanced Very High-Resolution Radiometer
EVA	: Extreme Value Analysis
EVI	: Enhanced Vegetation Index
FMC	: Fuel Moisture Content
GHGs	: Greenhouse Gases
GDP	: Generalized Pareto Distribution
GEV	: Generalised Extreme Value
GPCP	: Global Precipitation Climatology Project
IPCC	: Intergovernmental Panel on Climate Change
IOD	: Indian Ocean Dipole
LDA	: Limpopo Department of Agriculture
LSWI	: Land Surface Water Index
LULC	: Land Use/ Land Cover
MODIS	: Moderate Resolution Imaging Spectroradiometer
NCEP	: National Centers for Environmental Prediction
NDVI	: Normalised Difference Vegetation Index
NIR	: Near Infrared
ONI	: Oceanic Niño Index
PDSI	: Palmer Drought Severity Index
POT	: Peak Over Threshold
SAWS	: South African Weather Service
SPEI	: Standardised Precipitation Evapotranspiration Index
SPI	: Standardised Precipitation Index
SOI	: Southern Oscillation Index
SWIR	: Shortwave Infrared

TCs	: Tropical Cyclone
USGS	: United States Geological Survey

CHAPTER 1: INTRODUCTION

1.1 Background

Weather patterns are changing globally, increasingly driven by the rising atmospheric concentration of greenhouse gases (McElroy & Baker, 2012). The rise in the atmospheric concentration of greenhouse gases (GHGs), combined with climate variability result to critical changes in the climate of an area globally and regionally by bringing about more extreme weather events like tropical storms, floods and drought (Dangermond, 2010; McElroy & Baker, 2012).

Changes in the magnitude and frequency of extreme climate such as prolonged drought and periods of heavy rainfall have been identified as signs of climate change (Meehl & Tebaldi 2004; Meehl *et al.,* 2007). According to Easterling *et al.,* (2000); Jentsch and Beierkuhnlein (2008), much of the impacts of extreme climate and weather events are felt in all levels of ecological hierarchy, from organisms to ecosystems. Easterling *et al.,* (2000) reported that changes in the intensity and frequency of extreme climate are likely to impact the natural environment more.

Nicholls and Larsen (2011), defined extreme climate as the occurrence of a value of climate and weather variables that are above or below the normal threshold. Recently, changes in the intensity and frequency of extreme climate have aggravated the Impacts of weather hazards economically and socially (Easterling *et al.*, 2000), such as the 2015/ 2016 southern Africa drought and the tropical cyclone Dineo of February 2017. The occurrence, intensity, and character of many types of extremes are already changing and will very likely change in the future (time), as humans influence climate change (IPCC, 2013). Many studies in different regions prove that the frequency and impacts of extreme climates have changed already (Karl *et al*., 1995; Schar *et al*., 2004).

Limpopo Province is highly prone to extreme climate and weather events, which makes it more vulnerable to climate change impacts (Levey & Jury, 1996; Cook *et al*., 2004). The emphasis of the study is on extreme maximum temperature (Tmax), minimum temperature (Tmin) and above-normal precipitation and below-normal precipitation. Extremes climate and weather events also drive changes in vegetation cover much more than the average climate (Parmesan & Martens, 2008). However, most changes are often negative, but others can be beneficial, such as wildfires, which is an integral aspect of the perpetuation of some types of ecosystems (Nicholls & Larsen, 2011). Extreme climates can often determine how the ecosystems function, by determining the types of species that may exist in a certain ecosystem (Parmesan *et al*., 2000). For instance, it

can predict the role that drought plays in the forest dynamic, through influencing the mortality of tree species in the forests (Breshears *et al*., 2005).

According to van Vliet and Leemans (2006), over the last decade, most of the unexpected ecological changes observed were explained in relation to their response to extreme climates and weather events. Using GIS and Remote sensing techniques allows us to utilise complex statistical methods to view vegetation dynamics and responses to the changes in extreme climate and weather events at specific times or over periods of time (Dangermond, 2010). The study employed two vegetation indices, namely, Normalised Difference Vegetation Index (NDVI) and Enhanced Vegetation Index (EVI), to determine the sensitivity of vegetation in relation to extreme climate and weather events in Limpopo Province.

1.2 Problem Analysis and Motivation

Globally, the frequency and intensity of extreme climate are expected to increase due to climate change, thus making it very important to understand their ecological impacts (Smith, 2011). Extreme climate and weather events are statistically defined by their rarity in magnitude, frequency, and duration for a single climate parameter (temperature or precipitation) or combination of parameters for a particular ecosystem (Goodin, 2004). The analysis of the impacts of extreme climates (floods, heatwaves, drought, and tropical storms) on human societies has been privileged over-analyzing the impacts of extreme climate on vegetation structure and functioning. This is in spite of the importance of vegetation in influencing energy balance on the earth's surface and mitigating extreme local climate. According to Goodin (2004), extreme weather events can be identified and recognised based on the length of reliable observational data. Thus, the study determined the nature of extreme climate and weather events for the period of 18 years, from 2000-2017. Although many past studies were undertaken to investigate the impacts of climate extremes on ecosystem functioning, the emphasis of the study is on the changes and response of vegetation to extreme climate and weather events in Limpopo Province, South Africa. Using remotely sensed data namely, the Normalised Difference Vegetation Index (NDVI), Enhanced Vegetation Index (EVI), and Land Surface Water Index (LSWI) the study measured the vegetation responses to extreme climate events. In line with this, the research focuses on analyzing and quantifying the vegetation change and response to extreme climate and weather events in the study area.

1.3 Research Questions

- What is the nature of extreme climate events in the study area from 2000 to 2017?
- How has vegetation cover changed over time in the study area?
- How does the vegetation respond to climate extremes?
- How sensitive is vegetation to climate extreme?

1.4 Aim and Specific Objectives

1.4.1 Aim

The aim of the study was to analyse and quantify vegetation changes and the response to climate extremes in Limpopo Province, South Africa for the period 2000 to 2017.

1.4.2 Specific Objectives

The objectives of this study were to:

- Identify extreme climate events in the study area during the period;
- Examine changes in the vegetation cover in the study area; and
- Analyse the vegetation response and sensitivity to climate extremes.

1.5 Delimitation of the study and Description of the Study Area

1.5.1 Description of the Study Area

The study focuses on Limpopo Province as shown in Figure 1.1, which is located in the northern province of South Africa, lying between the borders of the countries of Botswana to the West, Zimbabwe, and Mozambique to the North and East respectively. The province has displayed vulnerabilities to the impacts of changing climate, as the region is prone to extreme weather events (Levey & Jury, 1996; Cook *et al.*, 2004). Limpopo Province (Figure 1.1) is subdivided into five district municipalities: namely, Vhembe, Greater Sekhukhune, Capricorn, Waterberg and Mopani Districts which are further subdivided into 25 local municipalities.

The Limpopo province is comprised of four (4) distinct climate regions; namely, the subtropical plateau, with flat elevated interiors which is characterised by hot and dry, with winter rain. The moderate eastern plateau has warm to hot and rainy summers and cold dry winters, while the

escarpment region has colder weather because of the altitude and rain all year round. The subtropical Lowveld region has hot-rainy summers and warm-dry winters, also known as the South African Bushveld (Tshiala *et al.*, 2011).

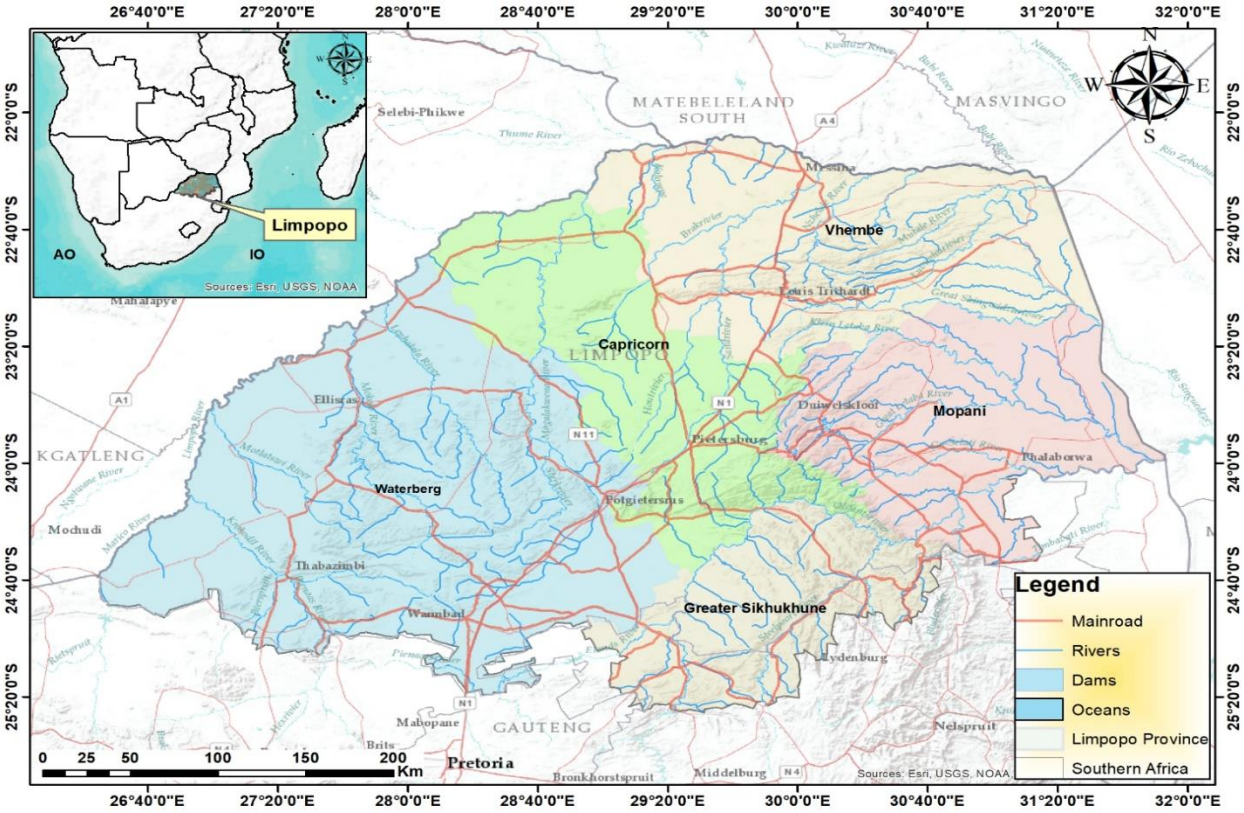

Figure 1.1: Map showing the study location over Limpopo Province, South Africa

- Vegetation Map

The NASA Moderate Resolution Imaging Spectroradiometer (MODIS) 250-meter resolution was used to generate the mean annual vegetation condition over Limpopo Province (Figure 1.2). The vegetation condition map shows that the vegetation in the region varies from sparse to dense vegetation condition, with sparse representing an area of no vegetation or poor vegetation and dense an area of good vegetation condition. over the region, dense vegetation is found in area of higher elevation with slope > 25% and is characterised by forests vegetation such as Evergreen needleleaf forest, Evergreen broadleaf forest, Deciduous broadleaf forest, and Mixed forest, whereas grassland, water bodies, and permanent wetlands are located in area of slope between 0 – 8% (see Figure 1.3 and Figure 5.1).

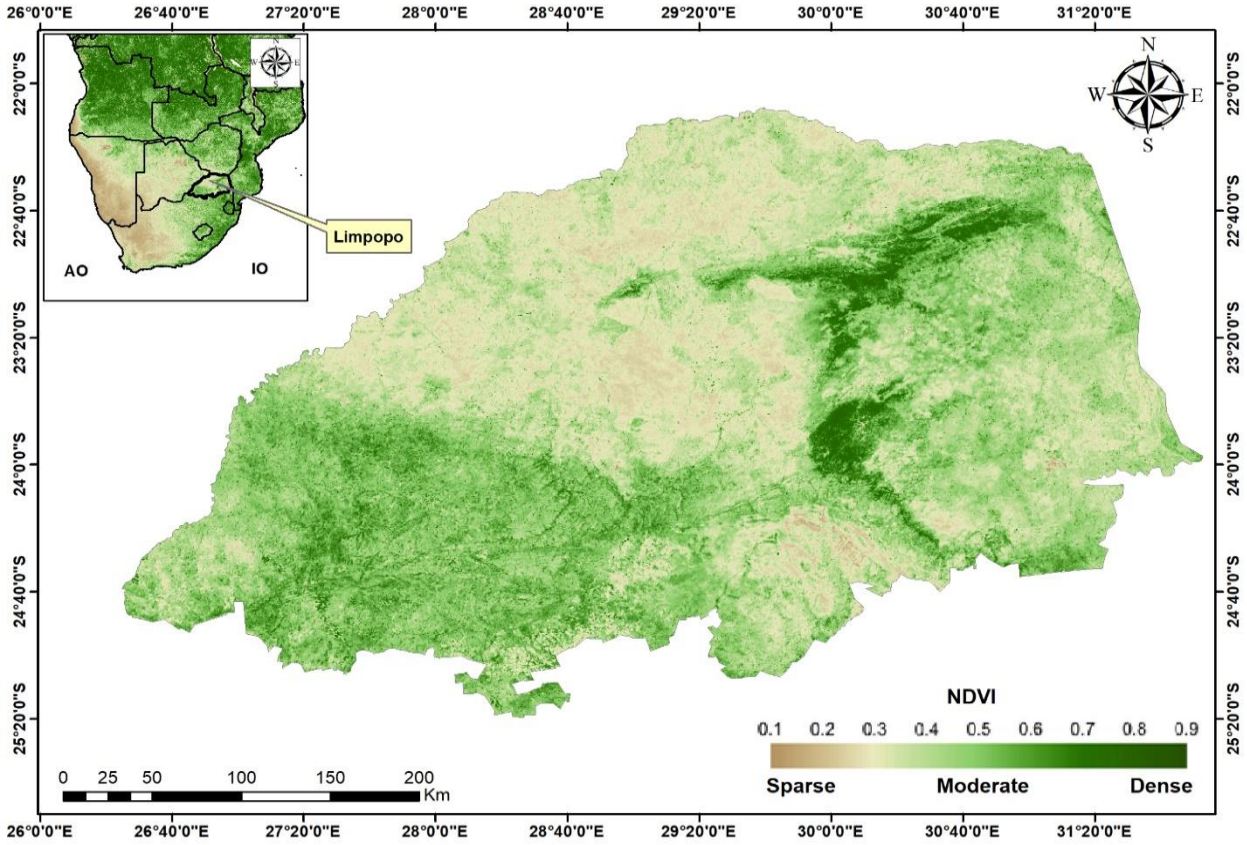

Figure 1.2: Vegetation condition map over Limpopo Province (Source USGS/EROS)

Figure 1.2 shows the annual vegetation cover over Limpopo province. The vegetation of the region shows that it depends on the climatic condition over the region; with dense vegetation conditions over the region of high rainfall (see Figure 1.4). Sparse vegetation condition is experienced over the region of low rainfall or fine climatic conditions. The region is composed of climate variability as well as vegetation variability, with the slope (Figure 1.3) playing an important role in the rainfall distribution over the region (Chikoore, 2016).

- Elevation of Limpopo Province

The Shuttle Radar Topography Map (SRTM) 30-meter spatial resolution was used to map the slope of the project (Figure 4.12). Based on the slope map, it showed that the province is dominated by flat slopes of about 0-8% from the sea level, and with the highest slopes of about >45% from the sea level.

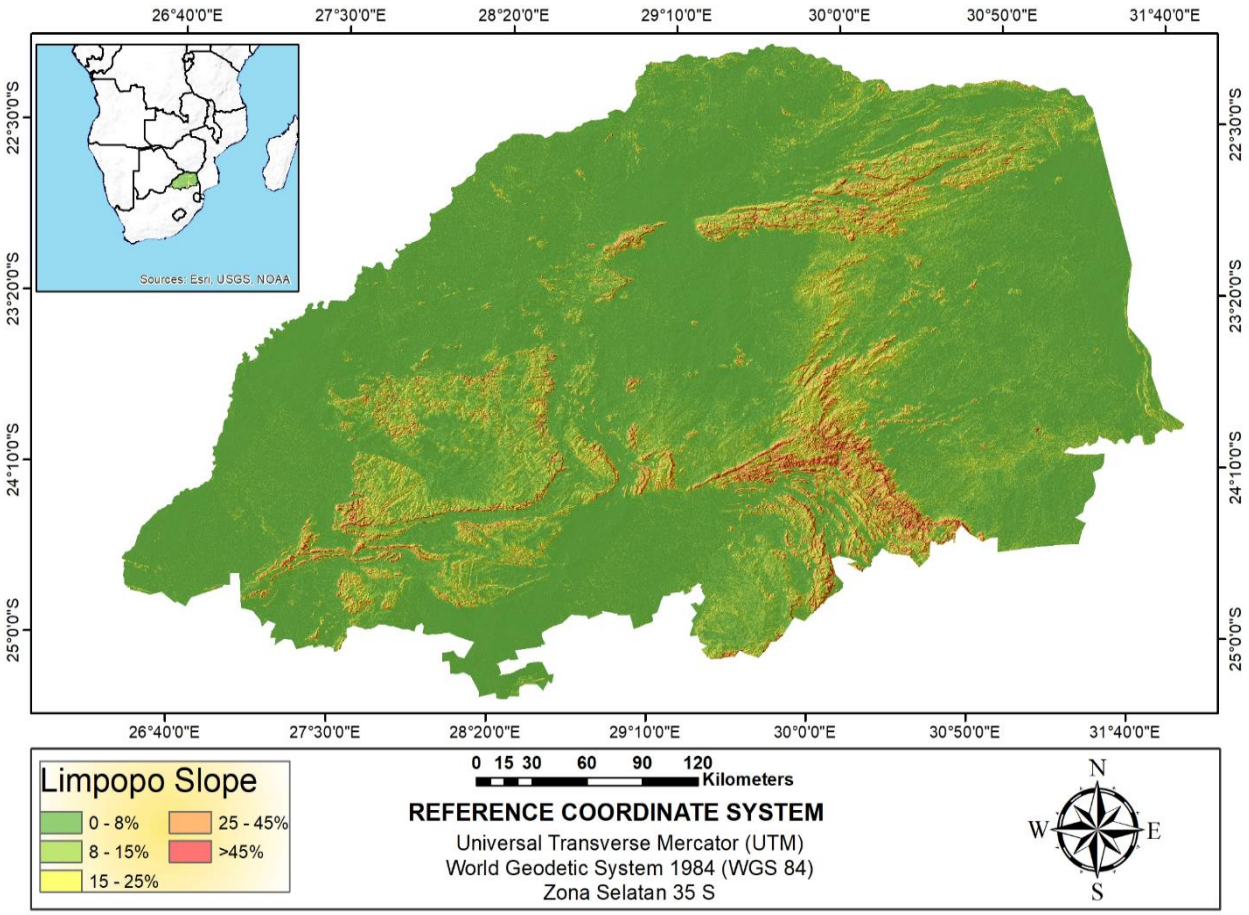

Figure 1.3: Map showing the elevation over Limpopo Province

The creation of an accurate map requires a clear understanding of the variation between the imagery and the ground to relate one another (Green *et al.,* 2017). The elevation such as the slope is one of the geological data layers that is used for thematic mapping of vegetation. The slope map created for Limpopo Province shows the area of lower elevation to higher elevation. From the elevation (Figure 1.2), integer values of percent slope were classified into 5 classes: Flat (0-8%), Gentle (8-15%), Moderate (15-25%), Steep (25-45%) and Very Steep (>45%).

- Rainfall Map of Limpopo Province

Figure 1.4 shows the mean annual rainfall map over Limpopo Province. The map shows that climatic condition over the region is highly variable, with the eastern part receiving higher rainfall and western part receiving lower rainfall. Limpopo province is located in the subtropical region, with high variability of the spatial mean annual rainfall.

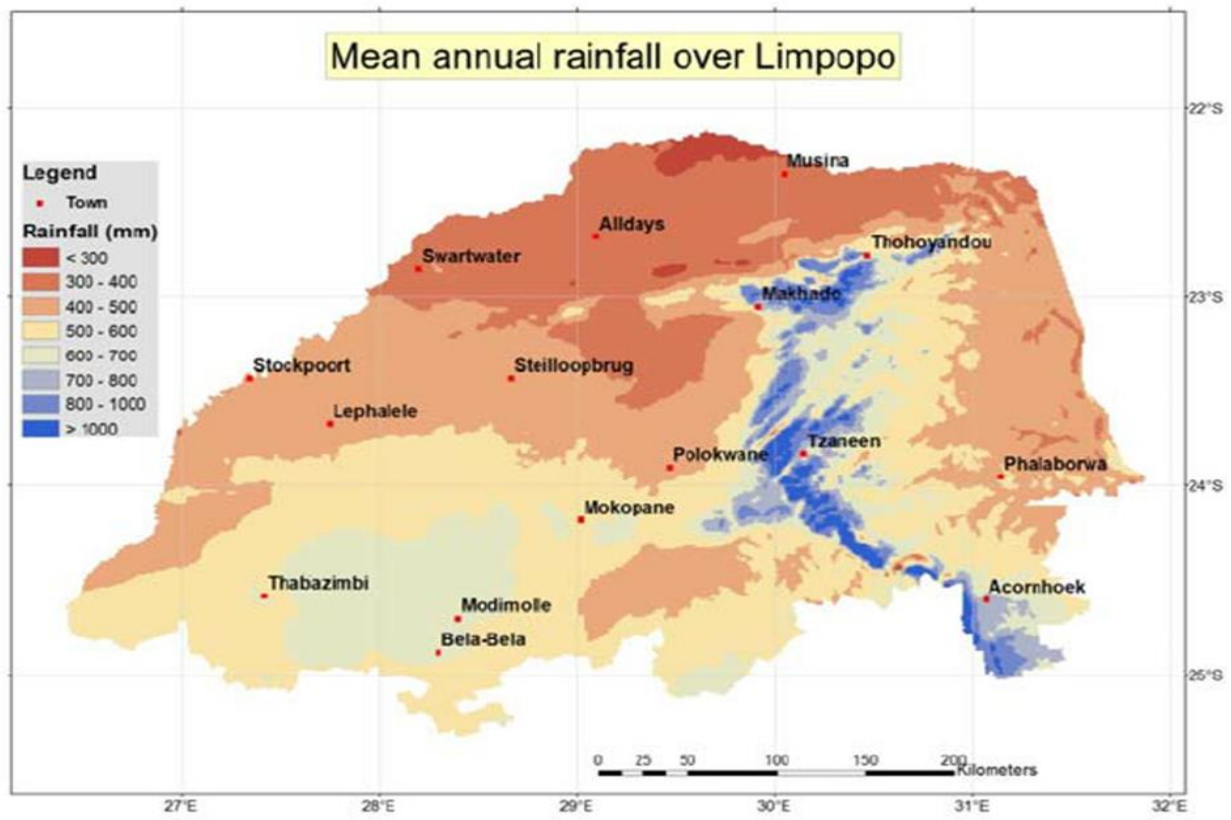

Figure 1.4: Mean Annual Rainfall over Limpopo Province (Source: ARC-ISCW, 2014)

Rainfall over the province is highly seasonal, with most of it occurring during summer season. The climatic conditions of the region vary significantly between the eastern part and the western part due to the escarpment barrier i.e. Soutpansberg mountain (Figure 1.3), with the eastern part receiving higher annual rainfall than the western part (Chikoore, 2016). The rainfall in the province is highly variable, with most of it recorded between October and April. Figure 1.4 illustrates the mean annual rainfall over Limpopo Province. The region is composed of an area of high rainfall and an area of low rainfall, with more than 1000 mm rainfall is recorded over the area of high rainfall and area of low rainfall receives below 300mm rainfall.

1.5.2 Delimitation of the study

The study focus is Limpopo Province, and various methods and datasets were used. During the period of heavy rainfall and availability of cloud covers over the region, certain areas were not clearly visible from other satellites such as LandSat, thus has influenced the selection and use of MODIS satellites to study the response of vegetation over the area. MODIS has the ability to cover a large area, with clear sky images were Landsat images, a mosaic of images is required.

Also, MODIS offers a better way of assessing vegetation using the MODIS MOD13Q1 vegetation composite indices at 16 days making it possible to study a short-term trend such as a single summer season (DJF).

1.6 Definition of Key Concepts

Extreme Climatic Events refer to periods of unusual, severe, and unseasonal weather extreme such as drought and floods which may lead to devastating consequences on the society, environment, and economy (Zhang *et al*., 2015).

NDVI is defined as a satellite-based indicator with the aim to characterise and monitor the vegetation conditions across the globe from space (Saleska *et al.*, 2007).

EVI is defined as a vegetation condition indicator designed to optimise vegetation signal by improving sensitivity in the area of high biomass and improved vegetation monitoring through reducing atmospheric influences and de-coupling canopy background (Jiang *et al.*, 2008).

LSWI is defined as the measure of the amount of liquid in the vegetation canopies that interact with solar radiation and soil background (Gao, 1996; Chandrasekar *et al.*, 2010).

Vegetation response refers to the photosynthetic activity which is characterised by estimating the fraction of absorbed photosynthetic active radiation, determining the vegetation growth using NDVI obtained with multispectral radiometric data such as Landsat, MODIS, and AVHRR (Menenti *et al*., 2010).

1.7 Dissertation Structure

Chapter 1, introduces the setting of the study, whilst outlining the purpose and objectives, and defining the key concepts. The relationship between extreme weather events and vegetation indices is explained, while also outlining the impacts of extreme climate on vegetation conditions. The study area selection, vegetation condition of the region, the climate of the region, and elevation were also outlined.

Chapter 2 gives a brief outline of the literature review, outlining the extreme weather events associated with changing climate and their impacts on vegetation conditions. It also gives a clear explanation or characterisation of indices that are used for the identification of extreme weather events and vegetation conditions.

Chapter 3 presents the research methodology followed in the study. The type of research design and methods of data collection and analysis were clearly stated. Steps used for data collection and archives data extracted from were shown. The methods and steps followed in the assessment of the impacts of extreme weather events were covered.

Chapter 4 presents the results and discussion of extreme weather events in Limpopo Province and their frequencies and intensity. Using the web-based tool, mean patterns of GPCP precipitation and maximum temperature were displayed showing an overview of climatic conditions. Case studies of extreme weather events over the region were explained.

Chapter 5 outlined the impacts of extreme weather events on vegetation conditions over the region. Using Normalised Difference Vegetation Index, Enhanced Vegetation Index, and Land Surface Water Index, the impacts of vegetation conditions are shown. Also, the Pearson moment correlation coefficient was used to relate the extreme weather events and vegetation conditions.

After clear identification of extreme weather events and their impacts on vegetation conditions, chapter 6 concludes and makes recommendations. All chapters include a short summary outlining the findings, with detailed findings of this study presented together with the synthesis of the key findings, conclusions, and recommendations.

CHAPTER 2: LITERATURE REVIEW

2.1 Introduction

This section reviews relevant literature for the study. The review compiles and evaluates the nature, characteristics, and impacts of extreme climate on vegetation, whilst disclosing materials that are necessary to examine and identify extreme climate and weather events as well as their impacts on vegetation ecosystems.

2.2 Climate Dynamics of South Africa and Limpopo Province

Climate is essentially defined as the distribution of weather variables (particularly the precipitation, temperature, and humidity) that an area/ region experiences over a long period of time (McElroy & Baker, 2012). Generally, it is often estimated using an observational experience of thirty years. Climate represents the accumulation of daily and seasonal weather events (the average range of weather) over a long period of time (Zhang *et al.*, 2015); thus, it can be viewed as a synthesis of the aggregate of weather.

A large-scale change in temperature and precipitation that happens over a decade or less are typically described as climatic change, which results in substantial disruptions in most of the social, economic and environmental costs, due to an increase in the frequency and severity of extreme events (Karl *et al.*, 2008). Climate change involves an increase in the global mean temperature, with an intensification of extreme precipitation events, high frequency of longer storm period and longer-lasting dry periods such as drought (Easterling *et al.*, 2000; IPCC, 2007; Groisman &Knight, 2008). The globe has been characterised by the successive warming of the earth's surface from the past three decades (IPCC, 2013).

Globally, the land and ocean surface temperature data showed a warming linear trend of 0.85 (0.65 to 1.06)°C for the period between 1880 to 2012 (IPCC, 2013), with the total increase being averaged to 0.78 (0.72 to 0.85) based on the period 1850 – 1900 and 2003 – 2012. A warming climate in many regions is associated with a significant intensification (increase) of extreme climate events (Easterling *et al*., 2000; Alexander *et al*., 2006).

Climate change primarily impacts the environment and society by increasing the intensity and frequency of extreme climate events (Song *et al.*, 2014). Changes in the extreme climate events are strongly influenced by climate variability (Katz & Brown, 1992; Song *et al.*, 2014).

2.2.1 Climate of South Africa

Different studies have shown that southern Africa is prone to the occurrence of hydrological extreme conditions such as droughts and floods (e.g. Kruger & Shongwe, 2004). According to Ziervogel *et al.,* (2014); South Africa over the past five decades, has experienced an increase in the intensity of extreme rainfall events. However, this is due to an increase in the mean annual temperature and the global average temperature observed of (0.65°C) has increased by 1.5 times. Engelbrecht, (2015) reported that South Africa is expected to continue warming at a higher rate than 0.15 °C per decade as observed over the 20th century. According to the Department of Environmental Affairs (DEA, 2013), due to changes in climate across the country, maximum and minimum temperatures have increased whilst rainfall showing interannual variability with the number of rain days reduced almost everywhere around the country. Climate variability can result in extreme climate events such as drought or floods and these extreme conditions can be very destructive leading to loss of infrastructure, life and could also damage ecosystems and its functions.

2.2.3 Climate of Limpopo Province

According to the Limpopo Department of Agriculture (LDA, 2008), the province is described as relatively warm on most of the days, with long sunny days and dry weather conditions. The province receives summer rainfall with semi-arid on the western and sub-tropical on the eastern part. However, the western and far northern part of the region is prone to drought conditions. Around summer, it often receives short-lived thunderstorms which disturb the warm days of the season. The rainfall for the province ranges from 200mm in the hot dry areas to 15000mm in the high rainfall areas, with most of the rainfall happening between October and April (Tshiala *et al*., 2011). According to Kruger and Shongwe, (2004), observations show strong evidence about the warming trend over southern Africa. Warming trends within the country are driven by changes in the maximum and minimum temperatures which result in a high levels of evaporation rate.

2.3 Climate Variability

Climate change is responsible for changes in the intensity, frequency, duration, timing and spatial extent of extreme climates which result in unprecedented extremes (Nicholls & Larsen, 2011). Globally and regionally, changes in precipitation and temperature are often described as the relevant aspects of climatic change in the warming world (Markus *et al*., 2016), with little consensus on the expected and observed changes in temperature and precipitation patterns. The

spatial patterns of changing climate are heterogeneous, with different regions displaying opposing trends from observed patterns (Donat *et al*., 2013). Extreme climates and weather events exhibit substantial variability. Vegetation mortality regionally is also believed to be influenced by climate change (McDowell *et al*., 2008). However, there is little consensus on the impacts of extreme climate and weather events on the natural environment (Easterling *et al*., (2000). Global warming simulations intensifications of extreme weather events such as precipitation in tropics and extratropical regions (Kharin *et al*., 2013 and O'Gorman and Schneider, 2009). Meanwhile, due to the warming climate, uncertainty remains (O'Gorman, 2012), probably because of the sensitivity in simulation models of extreme precipitations in the tropics such as convective parameterization (Wilcox & Donner, 2007).

Studies from the past indicate that globally, climate change continues, along with the intensification and changes in the total annual precipitation and the number of measurable days with precipitation (Zhang *et al.,* 2010). Globally, observed precipitation data show that the number of heavy precipitation events have intensified in most regions, rather than decreased. Thus, there is considerable variability in spatial trend patterns (Lenderink & Van Meijgaard; 2008; Westra *et al*., 2013; Donat *et al*., 2013,). The intensification and frequency of extreme climate are expected to change under the influence of climate change (Meehl *et al*., 2000). An increase in global temperatures is expected to cause or exacerbate the increase in extreme weather events, which in turn, affects the ecosystems and society.

2.4 Extreme Climate and Weather Events

Changes in the intensity and frequency of extreme events, such as drought, heatwave and heavy precipitation, have attracted a lot of attention because of their devastating consequences on society, economy and environment. Extreme weather events include very high temperatures, high rainfalls, and droughts or extreme weather events (Rosenzweig *et al*., 2001). It also includes unusual, severe or unseasonal weather, and weather at the extreme of the historical distribution (Zhang *et al*., 2015). Globally, the changing climate alters precipitation and temperature patterns (IPCC, 2013). This has been predicted to intensify extreme climate events, with considerable impacts on vegetation ecosystems.

Despite an increase in temperature, global prediction models predict more and frequent severe extremes, such as floods, drought and heatwaves (Easterling *et al*., 2000; Schar *et al*., 2004).

The classical parametric method, such as the Generalized Extreme Value (GEV) theory, is used to analyse extreme events (Zhang *et al*., 2015),

2.5 Extreme climate and weather events classification

2.5.1. Heat Waves

An increase in temperature variance is likely to influence the chances of extreme high-temperature events over and above what could simply be expected from mean increase alone (Meehl *et al*., 2000). Temperature is associated with several types of extreme, such as human health, the physical environment and vegetation ecosystems (Seneviratne *et al*., 2012). However, past analysis of temperature extreme regionally and globally shows a consistent change with a warming climate, supported by previous assessment in AR4. Finally, temperature extremes also result in the formation and intensification of heatwaves.

The heatwave is a period of at least three days where the combined effect of excess heat and heat stress is unusual with respect to the local climate (Nairn & Fawcett, 2011). Heat waves are generally driven by large-scale synoptic events such as quasi-stationary anticyclonic circulation anomalies or atmospheric blocking (Meehl & Tebaldi, 2004; Nairn & Fawcett, 2011). Heat waves around the globe have been shown to be responsible for more deaths than any other extremes, and its impacts include bush fires, storms, tropical cyclones and floods (Coates, 1996).

Different scholars globally, have projected more heatwaves due to climate change from global warming (Alexander *et al*., 2007; CSIRO and Bureau of Meteorology, 2007). Nairn and Fawcett, (2011) reported that severe impacts of heatwaves globally, can either be direct or indirect. However, they are accountable for damage to vegetation ecosystems and crops. Heatwaves occasionally occur in mid-summer, with less intense heatwaves being experienced in spring and early autumn and are sometimes referred to as the period with exceptional and unusually hot weather (Nairn & Fawcett, 2011). McBride *et al*., (2009), concluded that surface heating is the dominant contributor to heatwave formations.

2.5.2. Droughts

Globally, changes in precipitation patterns have been identified as the relevant aspect of a warming climate in the world (Donat *et al*., 2017), yet there is little understanding about observed and expected changes in spatial precipitation patterns. Allen and Ingram (2002), reported that due to the warming climate, the intensifications of hydrological cycles are expected.

Alexander *et al*., (2006), Min *et al*., (2011) and Westra *et al*., (2013), all reported that increases in precipitation extreme can result, whilst Sillmann *et al*., (2013) and Kharin *et al*., (2013) further projected an intensification in the extremes for the future. According to Seneviratne *et al*., (2012), drought is influenced by the reduction in a mean or total precipitation. According to O'Gornam (2015), climate models have observed and simulated the intensification of extreme precipitation as a result of a warming climate. Other studies have found that increased concentrations of greenhouse gasses result in heavy daily precipitation events (Gordon *et al.*, 1992).

Drought is generally the period of the prolonged dry season or abnormal dry weather which causes hydrological imbalance (Seneviratne *et al*., 2012). Lack of precipitation, which is called meteorological drought, often results in drought and influences the intensification of evapotranspiration induced by enhanced wind speed, radiation and vapor pressure reduction.

Regional-scale forest mortality has been associated with severe drought worldwide (McDowell *et al*., 2008). However, such widespread mortality events are known to have long-term impacts on the forest dynamic and interaction between species and may also impact atmospheric CO_2 and climate. Due to extreme climatic events, regional drought is increasing in terms of frequency and severity, with significant impacts on eco-social, with increased interest in the impacts of extreme climate to ecology (Royer *et al.*, 2011).

Drought is a gradual process which intensifies as a period of the prolonged dry season continues over a time (Lei & Duan., 2011). Globally, extreme drought is responsible for growth reduction and vegetation mortality in the ecosystems (Allen *et al*., 2010). Drought, according to the remote sensing community, is defined as a complex phenomenon characterised by abnormal dry weather period which influences vegetation cover change (Tucker & Choudhury, 1987; Heim, 2002). Drought is characterised into three different categories, namely meteorological drought, hydrological drought and agricultural drought.

Types of Drought

- **Meteorological Drought**

Droughts are the results of deficiency of precipitation over a period of time which results in the shortage of water for the environmental sector or some activities. Meteorological drought is mainly due to deficiencies of the natural precipitations and excessive evapotranspiration over a time period at different areal extent (Wang *et al.*, 2016). Different types of drought display specific characteristics, although hydrological drought and agricultural drought start as a result of meteorological droughts. Meteorological drought can be characterised simply using standardised

precipitation index (SPI), standardized precipitation evapotranspiration index (SPEI) which have been found to be an effective in analysis (Zarch *et al.*, 2015). Drought development involves a variety of interacting climate variables with various land-atmosphere feedback (Wang *et al.*, 2016).

- **Hydrological Drought**

Hydrological drought persists due to a shortage of precipitation associated with excessive temperatures and higher evaporation rates. As such, soil moisture declines to a point were terrestrial ecosystem or crops are affected, leading to hydrological drought (Van Lanen *et al.*, 2016; Wang *et al.*, 2016). Normally, hydrological drought is often defined by the frequency and severity of watershed or river basin scale. Although all droughts are the results of precipitation deficiency (Wang *et al.*, 2016), hydrological drought is more concerned with the hydrological cycle or system.

Hydrological drought normally lags in occurrence of meteorological droughts and agricultural droughts (Wang *et al.*, 2016), as it takes a longer period for precipitation deficiency to show up in components of the hydrological system such as soil moisture, reservoir levels, or stream flows.

- **Agricultural Drought**

The agricultural drought interlinks various characteristics of both meteorological droughts or hydrological droughts to agricultural impacts (Wang *et al.*, 2016), focusing on soil moisture depletion, shortage of precipitation, excessive temperatures and increased evapotranspiration and decline of reservoir levels. Deficiency of precipitation leads to a decline in the topsoil moisture at planting which may hinder crop development, resulting in low crop per area hectare and a reduction of the final production (Van Lanen *et al.*, 2016). Agricultural drought is referring to period of declining soil moisture and consequently leading to crop failure (Mishra & Singh, 2010).

2.5.3. Floods

Floods are defined as the accumulation of waters over areas that are not normally submerged or an overflow of normal confines of streams and other water bodies (Seneviratne *et al*., 2012). Extreme climate events are expected to be altered by climate change, such as floods (Death *et al*., 2015). Meanwhile, future changes in the intensity and frequency of extreme climatic conditions are expected to vary according to region. Floods are caused by an intensification of snow, long-lasting rainfall or a combination of both or intense local storms (Smith & Ward, 1998).

Intense or extreme wind speed consequently threatens human safety, and the integrity of infrastructure and vegetation (Seneviratne *et al*., 2012). Trends of average wind speed influence increased evaporation rate and the availability of water by bringing intense local storms and drought (McVicar *et al.*, 2008).

- **River Floods**

A river floods is due to an overflow of water over the banks of the riverbanks, outside its natural or artificial made. As surface water from runoff introduced or added into streams and river, it exceeds the river or stream's capacity to accommodate the flow. River flows are considered normal or not hazard unless it threatens human life, and property (Burby, 2001). According to Ives (1989), the dynamics and intensity of river floods varies depending on the terrain of an area, with mountainous areas floods occurs after heavy rainfall, and low flat areas characterised by shallow and slow-moving floodwater. River flows normally occur when the river exceeds it carrying capacity, either at meanders or bends.

- **Flash Floods**

These are floods caused by excessive or copious heavy rainfall at a short period of time. Flash floods are associated with heavy rainfall due to thunderstorms, tropical cyclones, hurricane or melting of ice (Weather, 2007). This can be related to the 2000 floods that have affected most of southern Africa countries due to TCs Eline. It is associated with the creation of gullies and large volume of water flowing with debris. The flash floods can be distinguished from regular floods due to the time scale between heavy rainfall and the onset of flooding.

- **Urban Floods**

Urban areas are constituted by artificial surfaces which cannot absorb water from rainfall, such as pavement, parking lots, roads and buildings (Ramachandra *et al.*, 2009). The urban floods are the result of excessive runoff developed in areas of hard surface where water doesn't have anywhere to go. Urban floods are usually linked to major natural disasters, such as tropical cyclones.

2.5.4 Impacts of Extreme climate and weather events

- **Impacts of drought**

Drought is the naturally occurring disaster and it is critical that it be monitored. Wherever drought strikes, it leaves a wide-ranging trail of effects, such as in economy, agriculture, social, and

environmental (Vose *et al*., 2016). The physical characteristics of droughts drive the economy, social, agriculture and environmental effects, which include the severity, spatial extent, and duration. Most impacts of drought are based on social and economic activities.

Economically, the effects of drought can either be direct or indirect, with direct effects associated with the water services, and timber productions. The indirect effects can be interlinked with agricultural drought and changes in the ecological conditions (Vose *et al*., 2016). The effects of drought lead to the reduction of water use for community and agriculture. Due to a shortage of water, it results in crop failure and an economic loss. The effects of drought are complex to monitor because they interplay both social, physical and technological responses. Vose *et al.,* (2016), reported that the effects of drought on the ecosystem in more complex, with some biota being negatively affected.

- **Impacts of Floods**

Extreme precipitation also has large societal and environmental impacts and appears to be increasing with climate change in many regions globally. This is because a change in the intensity of precipitation is accompanied by an increase in daily extreme precipitation amounts during the growing season. Floods display both direct and indirect impacts.

Floods have devastating effects on society, ecosystems, economy, and agriculture. During heavy rains, the river spills water in the flood plains causing water to move downstream and impose a threat on crops, plants, and animals resulting in an ecological disturbance.

2.6 Synoptic Systems that cause extreme climate

2.6.1 Cut Off Lows

Cut-off Lows (COLs) are baroclinic temperate disturbances that take place on the westerlies as deep troughs that are associated with a cold-cored depression (Tyson & Preston-Whyte, 2000). Globally, it is known that COLs are associated with extreme precipitation events (Sabo, 1992; Zhao & Sun, 2007; Muller *et al*, 2008). According to Sabo (1992), COLs are responsible for long-lasting heavy precipitation in large areas of Austria. COLs are regarded as South Africa's most important synoptic weather systems that are responsible for bringing widespread rainfall in the country, with some resulting in flood events (Taljaard, 1985; Roux & Van de Vyver, 1988; Singleton & Reason, 2007). From 1973 to 1982 and 1973 and 2002, studies conducted by Taljaard (1985) and Singleton and Reason (2007) both recorded 11 average COLs occurring per year. For instance, the 300 mm of rainfall in 24 hours at East London in August 2002, was reported

by Singleton and Reason (2006) to be associated with COLs which was situated over the South African's western interior. According to Taljaard (1985) Singleton and Reason (2007), about 20% of the floods in South Africa are a result of COLs.

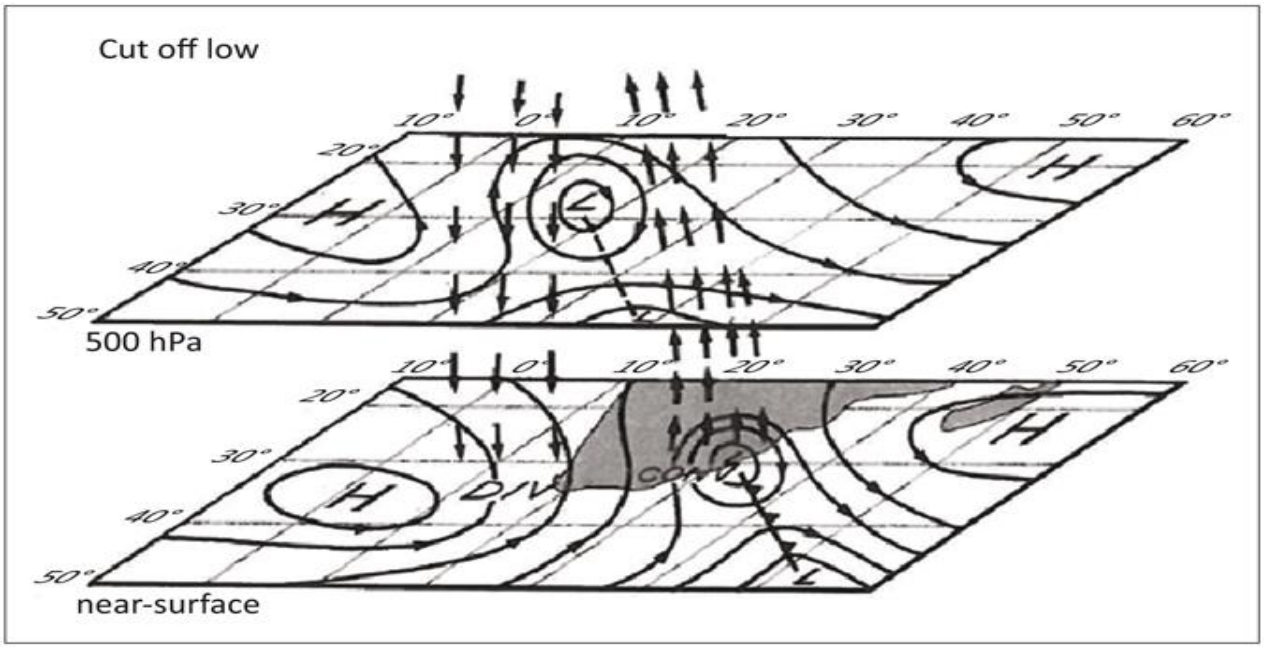

Figure 2.1: Cut-off low circulation pattern at near surface at 500hpa levels. (Source: Tyson & Preston-Whyte, 2000)

2.6.2 Tropical Cyclone (TCs)

Tropical cyclones (TCs) are the rotating systems which are characterised by a low-pressure center with strong winds and heavy rainfall that results in severe damage both inland and outland (Córdoba *et al*., 2018). TCs are defined as intense, cyclonically rotating, low-pressure weather systems that form over the tropical oceans. In the South Indian Ocean, TCs form to the west of Australia where they are carried westward in the tropical easterlies before recurving southward in the South Indian Anticyclone before reaching land, and they often move south along the Mozambique Channel (Tyson & Preston, 2000). In the Australian, Indian and Pacific, 97 % of TCs form in the Monsoon Trough between the equatorial westerlies and tropical easterlies overlaid by 200 hPa ridge. TCs in the Indian Ocean are mainly a summer and autumn phenomenon. TCs storms are always associated with heavy rainfall and flooding and are maintained by the release of latent heat. TCs have negative impacts on the environment along with places it passes as it produces heavy rainfall and strong winds (Kubota & Wang, 2009). Different scholars have reported that the amount of extreme precipitation influenced by TCs are increasing as they

increase the frequency and extreme precipitation associated with each TCs (Knight & Davis, 2009). TCs produce heavy rainfall in a short period of time (extreme precipitation) which results in flooding (Denniston *et al.*, 2015). Denniston *et al.*, (2015) reported that recent ENSO are dominant controllers of interannual TCs activities globally as they influence the surface ocean gradients and atmospheric circulation. ENSO tends to influence the formation of TCs, for example, the tropical cyclone Eline resulted in most of southern Africa countries flooding in 2000. According to Reason and Keibel (2004), much of the January-February-March (JFM) 2000 extreme rainfall in the southern Africa regions resulted from the TCs system. TCs Eline was recorded to be the longest-lived tropical storm in the Southwest Indian Ocean (SWIO) which penetrated far inland over the interior of southern Africa (Reason & Keibel, 2004). Another example is tropical cyclone Dineo, which brought extreme precipitation to some parts of the southern African countries, such as Mozambique, Zimbabwe, and some parts of South Africa, in Limpopo and Mpumalanga Provinces.

2.7 Remote Influence of Extreme Climate Events

2.7.1 El Nino Southern Oscillation (ENSO)

ENSO is defined as the natural fluctuation of the global climate system as a result of equatorial atmospheric-ocean interaction in the tropical Pacific Ocean (Philander, 1992). ENSO is the dominant phenomenal mode of coupled atmosphere-ocean variability on interannual time scales in several regions of the world (Trenberth & Stepaniak, 2002). The ENSO cycles consist of three phases: El Nino, neutral phase and La Nina (Hanley *et al*., 2003). ENSO is defined as the irregular periodical variations in winds and SST in the equatorial Eastern Pacific Ocean and is associated with strong year to year climate variability around the globe (Climate Prediction Center, 2016 & Meehl *et al*., (2000). The phenomenon is one of the key factors that influence the interannual variability of precipitation (Panalba & Rivera, 2016). In the southern hemisphere, the Eastern Pacific Ocean atmospheric pressure conditions are affected due to SST which generates the ENSO, and substantially influences precipitation distribution (Mason & jury, 1997; Nicholson, 1997).

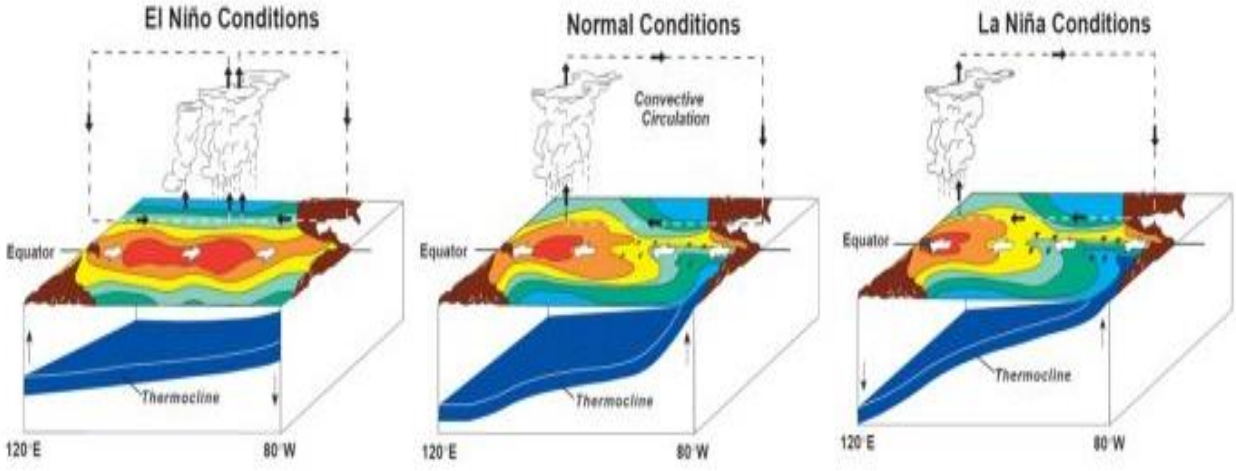

Figure 2.2: EL Nino Southern Oscillation Source (https://www.smhi.se/polopoly_fs/1.10208.1490013686!/image/Fig%201_nina_normal_nino.jpg_gen/derivatives/Original_1256px/image/Fig%201_nina_normal_nino.jpg)

ENSO is the dominant force of tropical climate variability at interannual timescales and is characterised by SST and surface pressure anomalies across the Pacific Ocean (Williams & Hanan, 2011). The two extreme phases of this oscillation are known as El Nino and La Nina. An El Niño episode is one phase of the ENSO phenomenon and is associated with abnormally warm central and eastern equatorial Pacific Ocean surface temperatures (Seneviratne *et al*., 2012). In the other phase, La Niña episode is associated with abnormally cool ocean temperatures in this region. The ENSO phenomena are best explained by the Walker Circulation (WC). The WC features the trade winds blowing from east to west across the central Pacific, rising motion over the warm water of the western Pacific, returning flow from west to east in the upper troposphere, and sinking motion over the cold water of the eastern Pacific (Bjerkness, 1966). According to Overpeck and Cole (2006), El Nińo/ Southern Oscillation is more energetic and can influence climate anomalies globally.

Both ENSO phases are characterised by spatial patterns of extreme events such as droughts and floods. Recent studies have suggested that both different phases of ENSO are associated with different frequencies of short-term weather extremes such as heavy rainfall events and extreme temperatures (Alexander *et al.*, 2009).

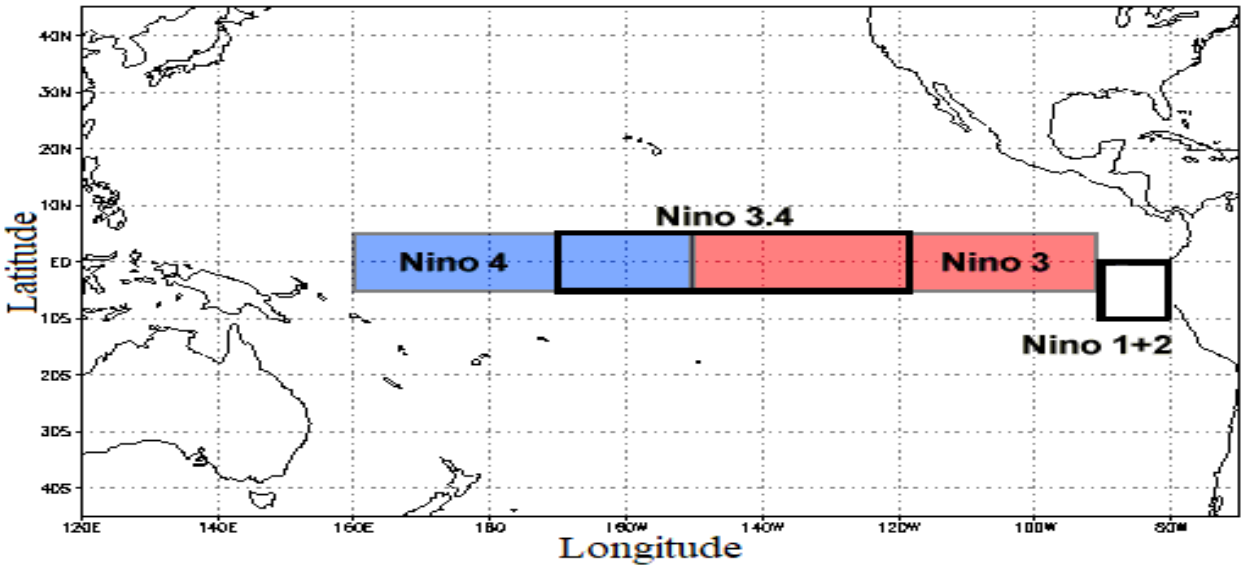

Figure 2.3: Nino 3.4 Source (https://www.ncdc.noaa.gov/monitoring-content/teleconnections/nino-regions.gif)

To characterise the frequency and intensity of ENSO events, Oceanic Niño Index (ONI) in the Niño 3.4 region is used. ONI is the average in sea surface temperature anomaly in Niño 3.4 region by 5°N-5°S from 150° - 90°W. An anomaly SST in the Pacific is either referred to as El Niño or La Nina event when the 5-month running mean of the ONI index exceeds +0.5°C for El Niño or -0.5°C for La Nina for at least 6 consecutive months (Trenberth, 2000).

2.7.2 Indian Ocean Dipole (IOD)

Indian Ocean Dipole is a coupled ocean-atmospheric phenomenon in the Indian Ocean with the difference in the sea surface temperature (SST) between two areas/ poles, a western Indian ocean is sometimes referred to as western pole in the Arabian Sea and an eastern pole in the eastern Indian Ocean south of Indonesia. The SST difference usually develops and peaks between June and October. Indian Ocean Dipole has been established as the dominant influence over ENSO, as it exerts much of the influence on East African rainfall behaviour, particularly during the short rainy seasons of September, October and November (SON) [Black, 2005; Behera *et al*., 2005].

During the dry season of May-October, IOD events bring more changes in the interannual rainfall (Hamada *et al.*, 2012). The Indian Ocean Dipole (IOD) is divided into two phases, the negative phase (wet season) and the positive phase (dry season) see Figure 2.8. The negative IOD is characterised by warmer than normal SST in the eastern equatorial Indian Ocean and cooler than

normal SST in the western tropical Indian ocean (Saji *et al.*, 1999). Whilst the positive IOD is characterised by cooler than normal SST in the western equatorial Indian Ocean and warmer than normal SST in the eastern tropical Indian Ocean.

A positive IOD is associated with above-average sea surface temperature and increased precipitation in the western Indian Ocean region with a corresponding cooling of water in the eastern Indian Ocean. The reverse effects prevail during negative IOD conditions, with the cooling of water in the western Indian Ocean region associated with increased precipitation in the eastern Indian Ocean.

The negative IOD and El Niño happen together in the dry season and they are associated with below normal rainfall, resulting in drought conditions. On the other hand, positive IOD tends to bring wet seasons with or without the influence of La Nina (Hamada *et al.*, 2012). The IOD tends to have an influence on the intensity and frequency of rainfall on the continent (Saji *et al.*, 1999) During the phases of IOD (negative and positive), the sea surface temperature (SST) surrounding the continent tends to be cooler or warmer, influencing large-scale convergence and divergence (Hamada *et al.*, 2012). This results in the suppression and induced rainfall on the continent.

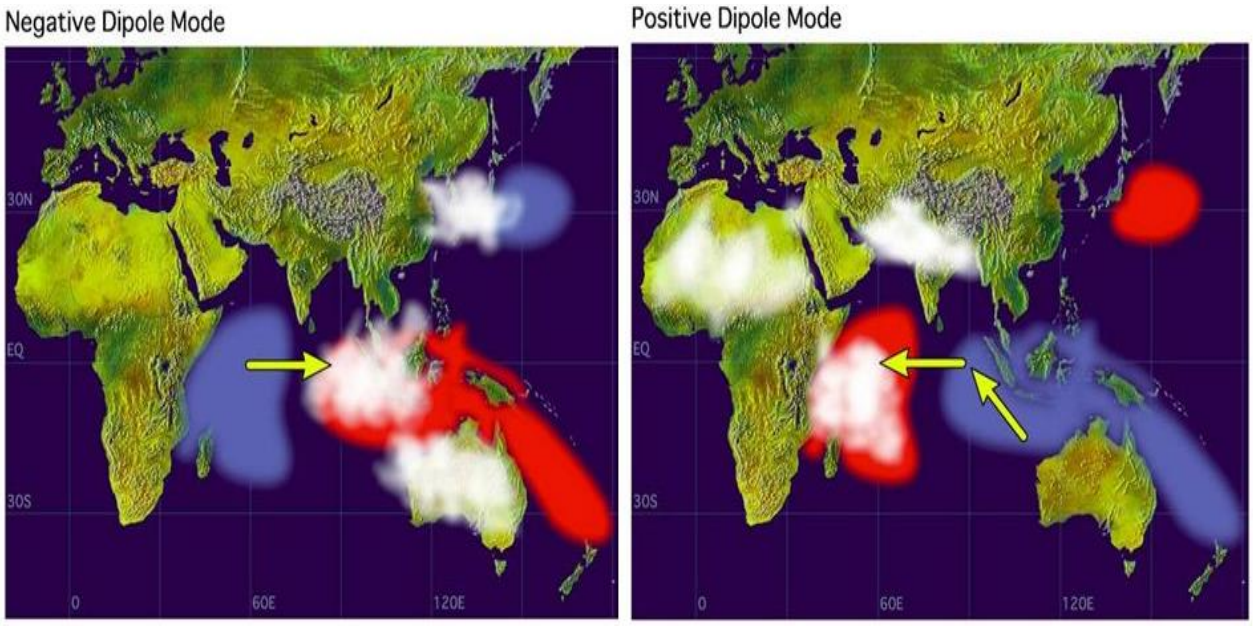

Figure 2.4: Indian Ocean Dipole Source (http://upscfever.com/upsc-fever/en/geog/indgeo/images/slide_24.jpg)

2.7.3 Southern Annular Mode (SAM)

Southern Annular Mode (SAM) is referred to as the largely zonally symmetric mode of variability in the southern Hemisphere, characterised by opposing perturbations of geopotential height with opposing signs over the Antarctic and zonal band (Gillett *et al*., 2006). SAM is defined as the ring of climatic variability circling the south pole. SAM describes the position of the westerly wind belt which in turn influences the strength and position of cold fronts, windiness and storm activity between the middle latitudes (40-50°C) and higher latitudes, over the southern oceans and Antarctic sea ice zone (50-70°C). SAM is associated with pressure anomalies centered over Antarctica, the relative influence of SAM is considered more dominant over the South Island than the North (Ummenhofer & England, 2007).

The positive phase of SAM is characterised by a decline in geopotential height over the polar cap, with an increase in geopotential height over area of midlatitudes, strengthening poleward shifts of storm track over Southern Ocean (Thompson & Wallace, 2000). A positive phase of SAM results in anomalously cold surface temperatures over Antarctica, with the warming of the Antarctica Peninsula (Thompson & Wallace., 2000). The positive phase of SAM is associated with cool and wet conditions over Australia and South Africa and dry and warm conditions over Tasmania, New Zealand, and southern South America due to the southward shift of the storm track (Gillett *et al*., 2006). The positive phase of SAM is relatively associated with light winds and settled weather conditions. Kidston et al, (2009) reported that, wind anomalies over summer season are easterly, becoming northeasterly over the North Island and the northwesterly over the southern South Island in winter. The negative phase of SAM is associated with more unsettled conditions with increased westerly winds.

2.8 ENSO Teleconnections and Impacts

The El Niño and Southern Oscillation (ENSO) is the powerful atmospheric and oceanic phenomenon coupled with the interannual variability on earth, contributing to the temperatures, rainfall, and extreme weather events. The ENSO alternates between anomalous cold (La Niña) and warm (El Niño) sea surface temperatures. During an El Niño episode, the surface air temperatures over the western pacific become warmer and higher than the eastern pacific compared to a normal year, leading to weak trade winds (Yeh *et al*., 2018). The weak prevailing wind reduces the upwelling intensity, leading to shifting of rainfall patterns farther than normal to the eastern side (see Figure 2.5). During the period, southern Africa is typically warm and dry

whilst eastern Africa is cool and warm. The effects are largely revered during La Niña, with trade winds in the pacific become more stronger than normal resulting in increased upwelling intensity from South America. This results in shifting of rainfall pattern farther west (see Figure 2.6), leading wet and cool conditions southern Africa.

ENSO has numerous impacts on humans and natural systems such as agriculture, public health, forestry, hydrologic cycle, marine, and terrestrial ecosystems. The ENSO impacts in areas outside of the Pacific occurs due to atmospheric and oceanic teleconnections (Yeh *et al*, 2018; Frischknecht *et al*, 2015). According to Yeh *et al*., (2018), teleconnections is referred to the remote response either current of after time, which is the case of ENSO. Extreme heat at the Australia coast is caused by ENSO oceanic teleconnection.

Over the southern Africa region, during the El Nińo movement of walker circulation to the east attributes to anomalous subsidence and warming of the Indian Ocean region leading to less summer monsoon rainfall (Yeh *et al*., 2018). During this period, the region is subjected to warm and dry or drought conditions which also affect the economy, people, agriculture and terrestrial ecosystems (Figure 2.5). The impact on agriculture are through crop failure. The ENSO and atmospheric teleconnection also play a role in influencing climate and weather conditions over the world (Alexander *et al*., 2000).

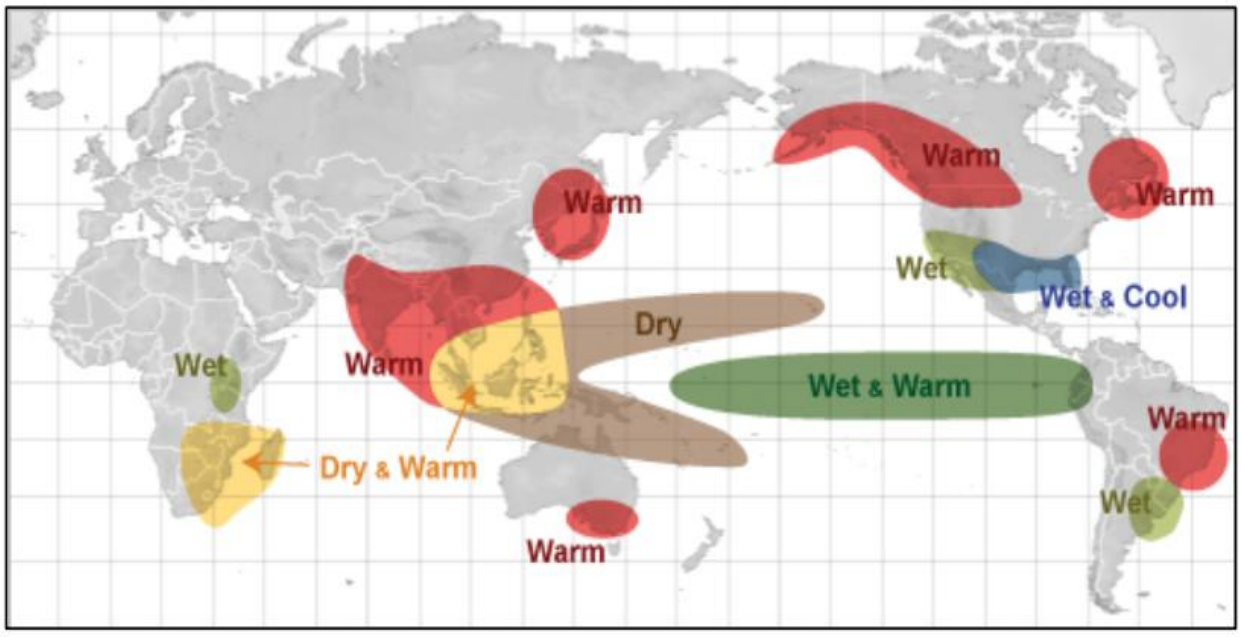

Figure 2.5: Rainfall patterns during El Nińo events during DJF (Source: http://www.srh.noaa.gov/jetstream/tropics/enso_impacts.htm NOAA)

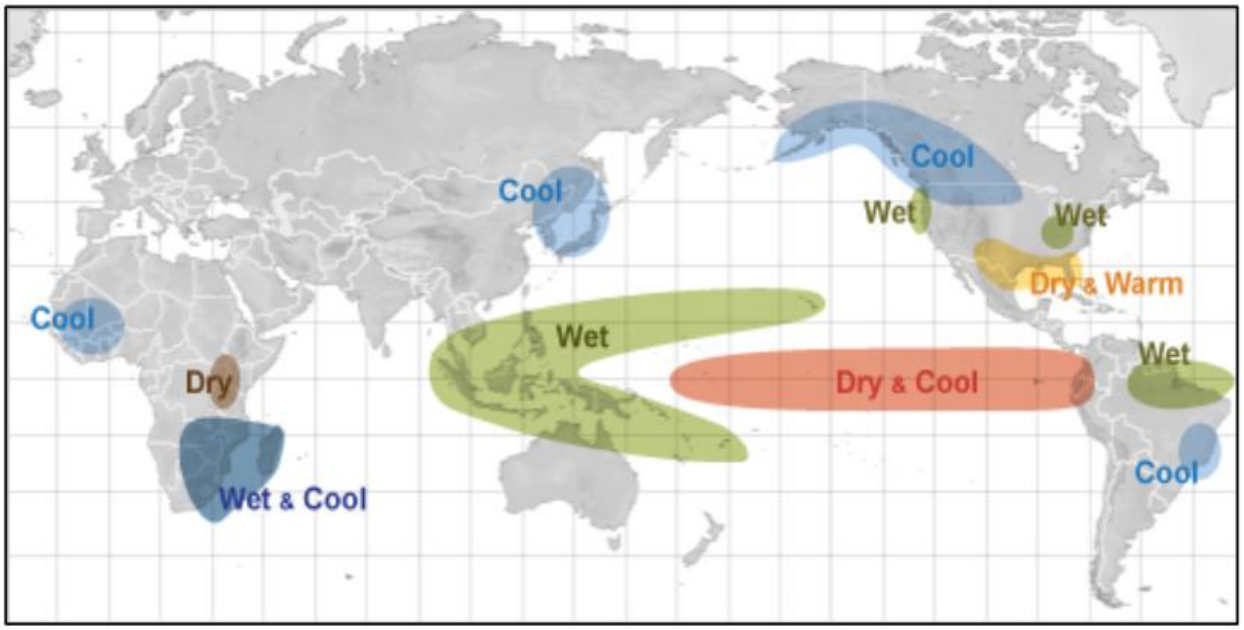

Figure 2.6: Rainfall patterns during La Nina events during DJF (Source: http://www.srh.noaa.gov/jetstream/tropics/enso_impacts.htm NOAA)

2.9 Extreme indices

2.9.1 Extreme Value Theory (EVT)

Extreme Value Theory (EVT) is defined as a statistical branch representing the behaviour of observational data (Fisher & Tippett, 1928; Coles, 2001). The theory has been applied in many different studies to solve problems in finance, hydrology and recently in climate studies (Embrechts *et al.*, 1997; Coles, 2001). According to Coles (2001), EVT requires an estimation of the probability of events that are more extreme than any that have been observed before, such that the observation is a very high maximum and a very low (minimum). EVT can be used as a method to disclose the knowledge and behaviour of extreme value (Rahayu, 2013). The theory is characterised by two statistical approaches; namely, the block maxima and peak over the threshold. Block Maxima from the theory is classically modeled by GEVD.

Many researchers have used the EVT and studied the theory widely (Coles, 2001). The Natural Environment Research Council (NERC, 1975), have recommended that GEVD be used to analyse floods and rainfall frequency. Martins (2000) reported that GEVD in practical is used to model different natural climate extremes such as wind speeds, floods, drought, rainfall and other maxima. However, the distribution patterns of those natural climate extremes either follow one of the extreme values (EV types I, II, and III) types joined by GEVD. Rahayu in 2013 used the GEVD approach to identify climate change, and concluded that there is no climate change in the area.

Another study using the GEVD was conducted by Husna in 2012 using a 10-year period to model extreme temperatures in Penang.

2.9.2 El Nino Southern Oscillation (ENSO)

When studying ocean processes that determine ENSO phases, sea-surface temperatures (SSTs) are considered. Different ENSO indices exist depending on different variable inputs (Hanley *et al*., 2003). The study employed ONI and Southern oscillation Index (SOI). ONI are calculated from SSTs anomalies over the tropical Pacific Ocean basin [5°N – 5°S, 170°W – 120°W]. While SOI is considered from changes in sea-level pressure between Darwin and Tahiti.

- Oceanic Nino Index (ONI)

To compute Nino 3.4, long term means SSTs for Niño regions were calculated from long records of SSTs data (Trenberth & Stepaniak, 2002). If the ocean is colder than the mean, it has a negative anomaly, while warmer than the mean ocean surface is a positive anomaly. The study used ENSO indices that correspond to times when SST anomalies in the Nino-3 region (5°N-5°S, 150° - 90°W) exceed ±0.5°C or when sea surface temperature anomalies exceeds ±0.5°C in the region (5°N-5°S, 170°-120°W), which is evidently enough to cause perceptible impacts in the pacific rim countries (Trenberth, 2000). ENSO indices for ONI employ a threshold of ±0.5 (Ropelewski & Halpert, 1987). A negative value (<-0.5) indicates that values are cooler than usual, hence a La Nina episode. The positive value (>0.5) indicates values that are warmer than usual, hence an El Nino episode, whereas a neutral phase corresponds to values between ±0.5.

Based on the HadISST Oceanic Niño Index (ONI) from the Niño 3.4 region (5°N-5°S from 150° - 90°W), a composition of ENSO cycles is constructed from 2000-2017 (Figure 2.7). Sea Surface Temperature (SSTs) departures from Niño 3.4 region that exceeds 0.5 (less than -0.5) are selected and considered as they represent ENSO seasons (Dahlman, 2009). As presented in Figure 2.7 and Figure 2.8, during the study period of 2000-2017 an average of 6 El Niño events and 8 La Niña events are observed using ONI and SOI (Table 2.1).

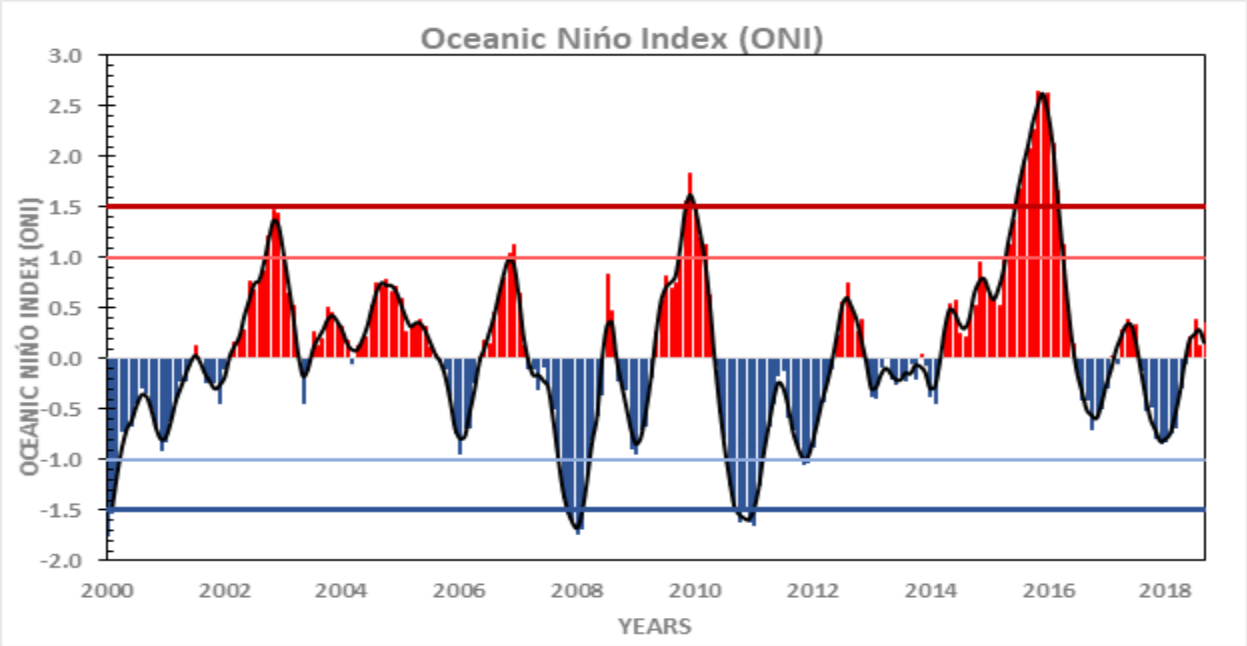

Figure 2.7: Time series of the ONI for the period 2000-2017 over Limpopo Province

The Oceanic Niño Index (ONI) time series from 2000-2017 shows the fluctuation between the positive and negative phases (El Niño and La Niña respectively). The ENSO (El Niño and La Niña) have been found to influence the droughts and humid conditions over Southern Africa. ONI employs a threshold range between -0.5 and +0.5, with at or below -0.5°C anomaly for cold (La Niña) events and at or above +0.5°C anomaly for warm (El Niño) events (Trenberth, 2000). However, for the study, the threshold was further broken down into weak (with a ±0.5 to ±0.9 SST anomaly), moderate (±1.0 to ±1.4) and strong La Niña (≤ -1.5) or strong El Niño at (≥ +1.5) events respectively.

The ONI time series presented in Figure 2.7, show an active ENSO cycle for the time frame 2000-2017. The period was featured by years of El Niño episode which were associated with drought and La Niña episodes, associated with floods events. During the period, six dry years were recorded over the ocean (2002/03, 2004/05, 2006/07, 2009/10, 2014/15 and 2015/16) and eight wet years (1999/00, 2000/01, 2005/06, 2007/08, 2008/09, 2010/11, 2011/12 and 2015/16). ENSO cycles that occurred over the area for the period 2000-2017 are presented in Table 2.1.

- Southern Oscillation Index SOI

Southern Oscillation Index (SOI) displays the intensity /strength of the phase of difference in sea level pressure (SLP) between Tahiti and Darwin (Ropelewski & Halpert., 1987). A negative value

usually indicates that the oscillation has entered an El Nino phase while a positive value usually indicates a La Nina episode. SOI values range from below -8 hPa to +8 hPa (Deser and Wallace, 1999; Harrison and Larkin, 1996). SOI values between +1 and -1 indicate neutral conditions, whilst condition above +1 indicates La Nina condition and below -1 indicates El Niño conditions. The Southern Oscillation Index (SOI) is defined as

$$SOI = 10 \times \frac{SLP_{Tahiti} - SLP_{Darwin}}{\sigma} \qquad \text{---------- eq1}$$

Where σ is the standard deviation of the pressure difference. The time series of this index for the period from 2000 – 2017 is shown in Figure 2.8.

The SOI (Figure 2.8) showing the time series of sea level pressure (SLP) anomalies for the time frame 2000-2017. Like the SST, the SLP shows clear interannual fluctuations over the region for the time scale. The spatial structure of SLP variation is revealed by displaying SLP departures from 2000-2017.

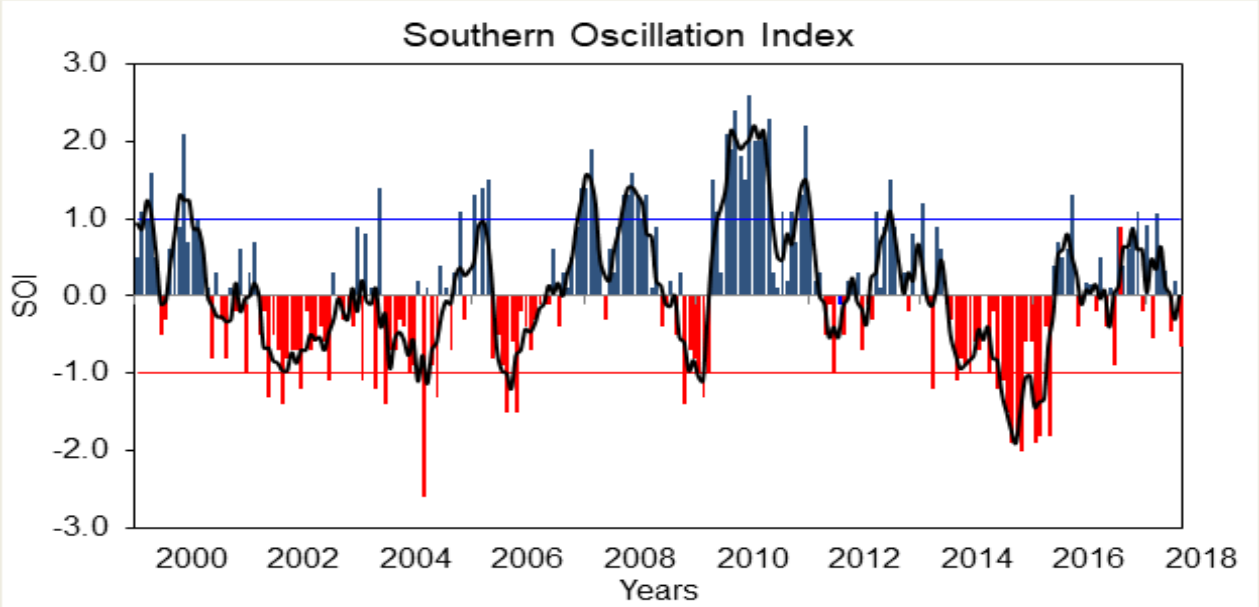

Figure 2.8: Time series of the Southern Oscillation Index for the period 2000-2017 over Limpopo Province

The Southern Oscillation Index (Figure 2.8) time series from 2000-2017 shows the fluctuations of the ENSO cycle from positive departures (La Niña) to negative departures (El Niño) phases. The average period of ENSO cycle is about four years, although the period varies between 2-7 years

(Marshal & Plumb, 1989; Tyson & Preston-Whyte, 2000). SOI gives an indication of the development and intensity of El Niño and La Niña events in the Pacific Ocean.

The time series of SOI features SLP anomalies with an active ENSO cycle during the period with six El Niño episodes (2002/03, 2004/05, 2006/07, 2009/10, 2014/15 and, 2015/16) and eight La Niña episodes (1999/00, 2000/01, 2005/06, 2007/08, 2008/09, 2010/11, 2011/12 and, 2016/17). The SLP variability is an indicator of variability in climate conditions (Marshall & Plumb, 1989). The negative departures exceeding -1.0 indicate El Niño events and positive departures exceeding +1.0 indicate La Niña events. Generally, the ENSO coincides with the summer rainfall of Southern Africa, beginning around May-June and peaks during December-January (Chikoore, 2016). The period was featured with two of the most prolonged periods and consecutive warmings events of the century (2014/15 and 2015/16). Table 2.1 presents the ENSO cycles that occurred during the 2000-2017 (Period). The ENSO cycles from the study correspond to that of Chikoore, (2016).

Table 2.1: ENSO events from 2000- 2017 based on SOI and INO

ENSO Events					
El Niño Events			La Niña Events		
Weak	Moderate	Strong	Weak	Moderate	Strong
2004/05	2002/03	2015/16	2000/01	2011/12	1999/00
2006/07	2009/10		2005/06		2007/08
2014/15			2008/09		2010/11
			2016/17		

2.9.4 Standardized Precipitation Evapotranspiration Index (SPEI)

Drought is the most damaging and complex natural disaster to understand, as it is difficult to predict when it will start and when it will end (Tan *et al*, 2015; Mckee *et al.*, 1993; Serrano *et al.*, 2010). Drought conditions result in some severe impacts on the environment, society, water resources and agricultural production (Chen *et al.*, 2013; Zhang *et al.*, 2015; Wang *et al*. ,2014; Wang and Meng, 2013). According to Tan *et al.*, (2015) the SPEI has been developed with many other drought indices that are used to monitor, assess and predict the severity of drought on the natural environment or society. Among the developed indices we have Palmer Drought Index, SPI and SPEI.

The SPI and SPEI indices are used to calculate the time scale to indicate the status of drought severity on the environment (Tan *et al.*, 2015). SPI and SPEI indices have proven to be a reliable index for monitoring and predicting the drought severity, by studying the temporal-spatial variation of drought.

2.9.5 Palmer Drought Severity Index (PDSI)

Droughts are naturally occurring events that are negatively associated with impact people or the environment. They are recognised as environmental disasters that have attracted attention from hydrologists, ecologists, environmentalists, and agricultural scientists. Several drought indices have been developed in recent decades (Mishra & Singh, 2010). A drought index is defined as the prime variable that is derived to assess and quantify the effects of drought, which include the duration, severity, intensity and spatial extent. Of the developed indices, PDSI (Palmer, 1965) is among them. PDSI is perhaps the most widely used drought index to monitor drought by illustrating the extent and severity of drought episodes. However, several limitations have been documented about PDSI (Mckee *et al*., 2005). The limitations of PDSI includes, mountainous terrains or areas of higher elevations are often questionable, and area of frequent climatic extreme, along with assuming all precipitation is rain (Mishra & Singh, 2010).

2.10. Biomes of South Africa

Gonzalez *et al.*, (2010) have reported that changes in the concentration of greenhouse gasses and climate in the atmosphere are drastically altering the distribution of biomes in South Africa. The observed changes in the forest covers, tree covers, and fire regimes are driven by climate change and intensification of extreme climate (Masubelele *et al.*, 2014). Changes in the distribution of plant life are determined by climate (Schmiedel *et al.*, 2010). According to Rutherford and Westfall (1994), biomes over southern Africa are based on their relation to temperature and rainfall. Many scholars have projected that global climate change by 2050 will result in changes from grassland dominated biome to shrub-dominated biome (Masubelele, 2014). South Africa consists of nine (9) biomes (Figure 2.9), namely, Albany Thicket, Azonal Vegetation, Forest, Fynbos, Grassland, Nama Karoo, Succulent Karoo, Savanna and Savanna (Rutherford & Westfall, 1994). South Africa is dominated by Savanna biome, constituting almost 46% of the land.

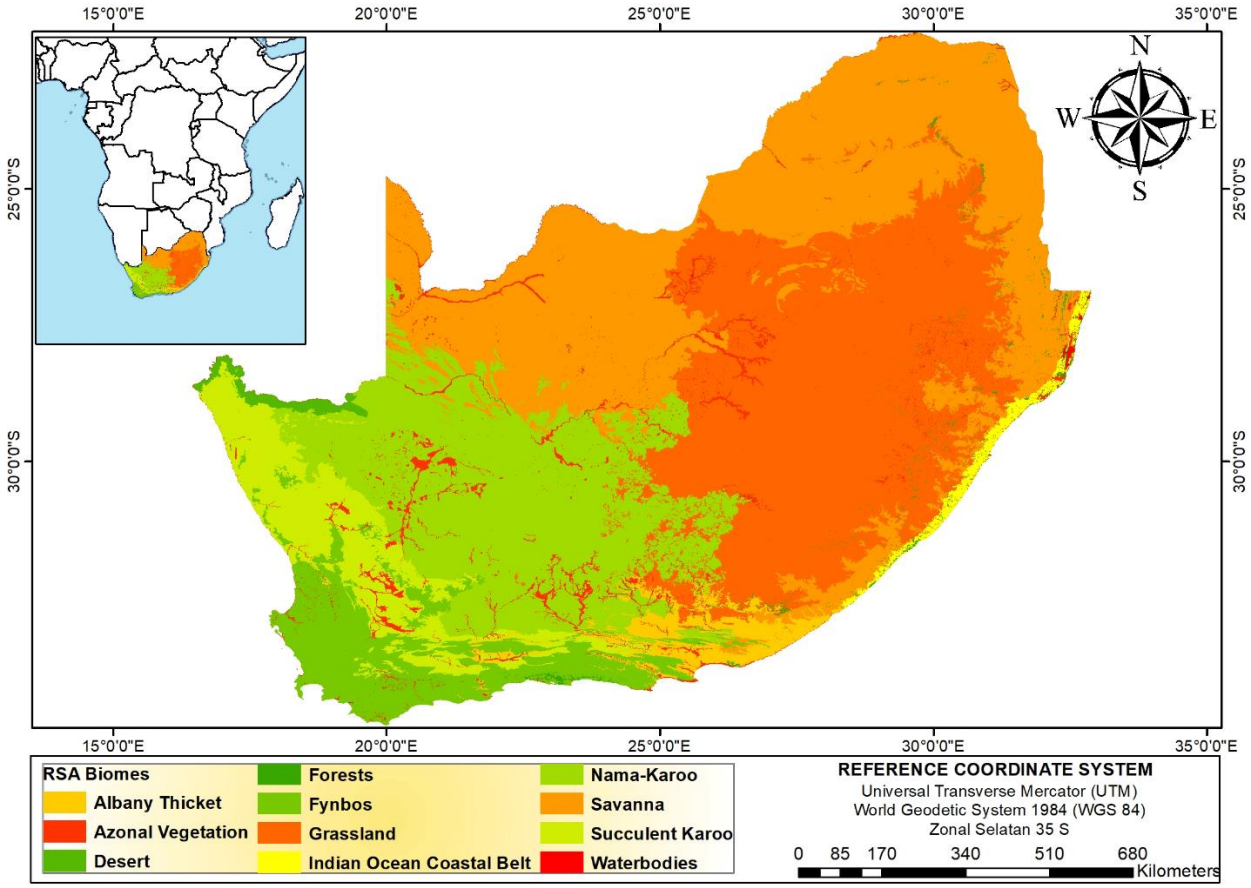

Figure 2.9: Map showing the Biome types over South Africa (source, SANBI, 2018)

- **Limpopo Province vegetation**

As shown in Figure 2.9, Limpopo Province lies in the savanna biome, which is mostly dominated by mixed grassland and small trees known to be bushveld (Limpopo Department of Agriculture, 2008; Tshiala *et al.*, 2011). The region is characterised by summer rainfall, with hot and humid summers and mist in the mountain areas and eastern and northern areas as subtropical.

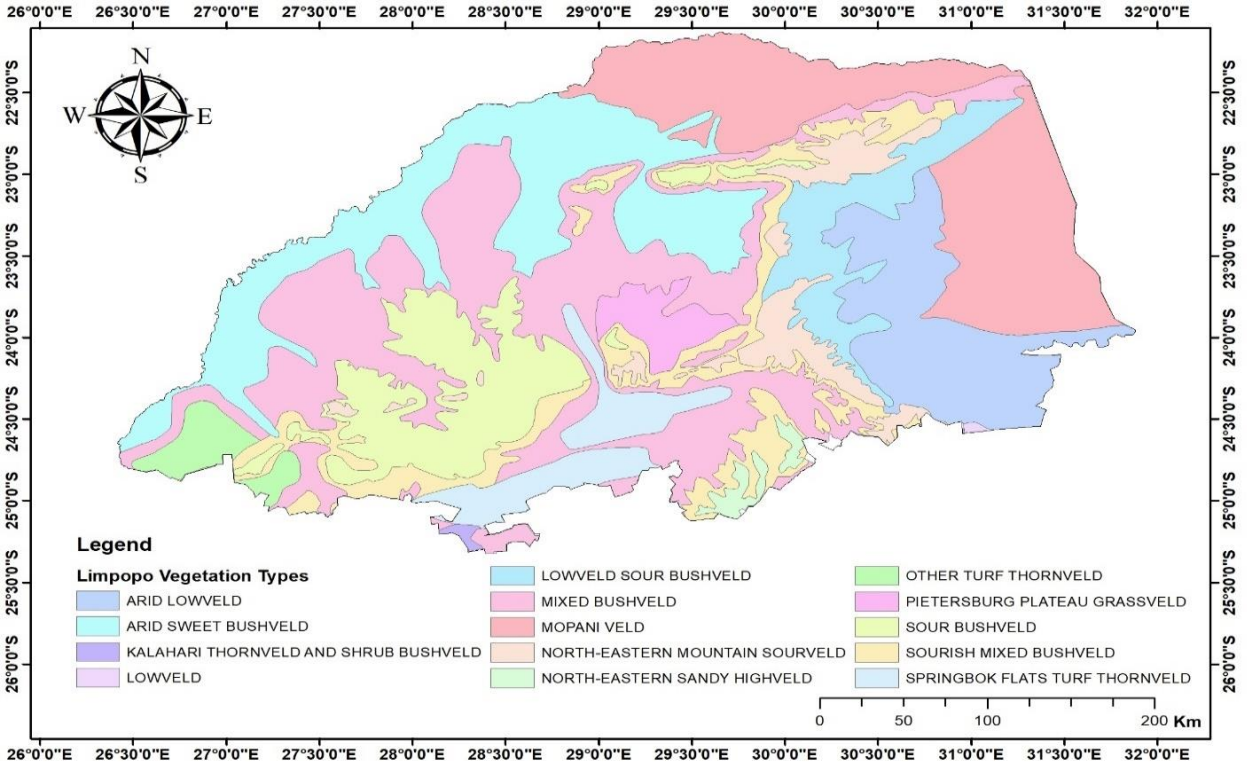

Figure 2.10: Map showing Vegetation Cover over Limpopo Province

2.11 Vegetation Dynamics

Globally, climate plays a role in the vegetations functioning of an area, however, extreme climate events such as floods, severe drought and heat waves consequently impact the ecological functioning of an area (Smith, 2011). According to Huang *et al*., (2014), extreme climatic events in a changing climate are expected to intensify, thereby increasing the chances of research to evaluate environmental risk by vegetation response.

Furthermore, climate extremes are likely to alter the vegetation functioning and structure and to transform its associated ecosystems properties (Gutschick & BassiriRad 2003; Gitlin *et al*., 2006; Jentsch *et al*., 2007; Overpeck & Cole 2006; Smith 2011), thereby reducing the uppermost canopy and increasing near-ground solar radiation (Royer *et al*., 2011), this directly affects the abiotic and biotic processes. According to Royer *et al*., (2011), the extreme climate can potentially affect the entire region very rapidly.

According to Smith (2011) and McDowell *et al*., (2008), drought is some of the extreme climatic events with severe impacts on the ecosystem. These events have the potential to extensively and rapidly alter the structure of vegetation and the functioning of the ecosystem as a result of drought-

induced mortality of uppermost plants. In response to extreme climatic events, forest and woodland plants mortality can have a large-scale shift in the ecosystem functioning and structure (Allen & Breshears, 2007; Breshears *et al*., 2005; Shaw *et al*., 2005; Berg *et al*., 2006; Gitlin *et al*., 2006). Auclair (1993); Allen and Breshears, (2007), both reported about the observation of climate-related vegetation mortality in six vegetated continents, biomes and plant functional types.

According to Jentsch *et al*., (2011), the current knowledge about an ecological response to extreme climate is based on the effects that are posed by climate trends, such as gradual warming of the atmosphere, changes in precipitation patterns and GHGs increase. As a result, to the context of extreme climate, ecology responds in the context which ranges from little to no response (Arnone *et al*., 2011; Jentsch *et al*., 2011), to responses that are large or 'extreme'.

A study of vegetation response to extreme events helps to forecast vegetation dynamic, as future average conditions will be close to current extreme events (Prus-Glowacki and Stephan, 1994). Meehl *et al*., (2007) projected that extreme temperature and heat waves are likely to increase in their intensity and frequency and they could also last longer than the current extremes.

According to Singh (1989), vegetation change can be measured by remote sensing, thus vegetation change detection, which is used to identify differences in vegetation cover through observations at different times. As reported by Lu *et al*., (2004), it requires the application of multi-temporal datasets, such as MODIS, SPOT and Landsat satellite imagery to quantitively investigate the temporal impacts of vegetation.

2.12 Vegetation Indices

From the past, the intensity and frequency of extreme climate have been increasing in many regions of the world (IPCC, 2013). However, these recurring changes negatively impact vegetation responses. Thus, due to the environmental ramification of extreme climate (Owrangi *et al.*, 2011), satellites have been used to monitor and detect vegetation changes and respond to extreme climate events. According to Owrangi (2011), the most efficient methods to monitor vegetation changes involve using remote sensing techniques such as NDVI, EVI and LSWI.

According to Lillesand and Kiefer (2002), these vegetation indices are based on spectral reflectance on the visible and infrared bands, which help to inform about the absence and presence of vegetation. Huete *et al.*, (2002) have reported that these vegetation indices help to intercompare vegetation activities by isolating green photosynthetic active signals from the spatial and temporal mixed pixels. Vegetation indices in the study include NDVI, EVI and LSWI. Beck *et*

al., (2006), have reported that NDVI is commonly the most used and relied on, as it focuses on the absorption of red radiation by the chlorophyll and other leaf pigments in the red spectrum, and strong scattering in the infrared spectrum.

2.12.1 Normalized Difference Vegetation Index

Satellite vegetation index products are commonly used applications aimed at monitoring and characterising vegetation cover and conditions from space. As a result of changing climate and land use/ land covers, continuous and long-term consistent satellite data are needed to monitor and quantify the rate of change to the terrestrial ecosystems (Jiang *et al.*, 2008). NDVI generally provides an overview of global vegetation conditions and their spatial distribution, and is widely used for monitoring vegetation conditions to the impacts of extreme weather events. it proves to be a useful tool for monitoring vegetation (Byuiyan., 2004). Based on the remote sensing data developed to effectively detect extreme condition over the world.

Extreme weather events cause stress to vegetation, the extent of drought and floods can be reflected using changes in the vegetation condition index. The NDVI is based on the normalised difference between near-infrared (NIR) and red reflectance (Karnieli *et al.*, 2010; Chang *et al.*, 2017). NDVI is the most widely used vegetation index to detect vegetation stress to extreme. NDVI is the mostly used indicator for vegetation growth conditions and the degree of change between land covers, and it ranges from -1 to +1. If the vegetation condition of an area I covered by vegetation, then it displays positive values and increases as vegetation cover increases as well (Aihui, 2004).

2.12.2 Enhanced Vegetation Index

Vegetation indices plays an important role in monitoring and mapping the variations in vegetation. The NDVI is considered used satellite-based vegetation index, however with few defects that enables NDVI to cancel out large proportion of noise forms as a result of topography and atmospheric conditions leading to large source of errors and uncertainty over the canopy background conditions and atmospheric variables (Matsushita *et al.*, 2007).

Based on the defects of NDVI, the Enhanced vegetation Index (EVI) was proposed and developed on the bases of the feedback-based approach incorporating background adjustments and atmospheric variable resistance into the NDVI. EVI is considered an improved version of NDVI, with modified sensitivity to high biomass regions and improved vegetation monitoring capability through the reduction of atmospheric influences and de-coupling of canopy background. The EVI

vegetation indices, was adopted by Moderate resolution Imaging Spectroradiometer (MODIS) as a global vegetation index for monitoring the world ecosystem photosynthetic vegetation activity.

Although with improved features such as reduced effects of atmospheric conditions and soil background, EVI does not consider topographic effect (Matsushita *et al.*, 2007). Unlike the NDVI, for EVI to reduce effects of environmental factors, it includes the soil adjustment *L* as its denominator. This makes EVI not to ignore topographic effects, like NDVI.

2.12.3 Land Surface Water Index

The Land Surface Water Index (LSWI) is a satellite-based monitoring vegetation index that uses shortwave infrared (SWIR) and near infrared band. LSWI is used to measure the amount of liquid water in soil background and vegetation (Chandrasekar *et al.*, 2008). Due to the ability of shortwave Infrared (SWIR) to absorb light by liquid water, it has been widely used to monitor the influence of drought and floods on the analysis of vegetation stress. The LSWI is used as a water related vegetation index to evaluate the sensitivity to assess the impacts that droughts and floods are associated with (Bajgain *et al*., 2015).

Although NDVI and EVI have been the most popular satellite-based tools for drought and floods monitoring, LSWI indices have proven to be an effective tool for monitoring water content of vegetations (Bajgain *et al*., 2015). More studies have reported that, water-related vegetation indices are more sensitive to climate variability than greenness related vegetation indices (Chandrasekar *et al*., 2010; Zhang *et al*., 2013; Bajgain *et al*., 2015). Satellite remote sensing is considered an effective tool for monitoring vegetation conditions of an area to climate variability, considering large spatial area coverage Zhang *et al*., 2013).

2.13 Conceptual Framework

The conceptual framework (Figure 2.11) shows key concepts that have guided the study. Extreme weather events are naturally occurring phenomena associated with devastating impacts on people, agriculture, marine and terrestrial ecosystems across the world. Various indices were produced to measure and quantify the magnitude, severity, and duration of such extreme, along with remote sensing indices to measure extreme climatic impacts of marine and terrestrial ecosystems. In this case, the conceptual framework is introduced as a guide to be followed when studying their vegetation response to extreme weather events in Limpopo Province. In general, to the overall flow of the study.

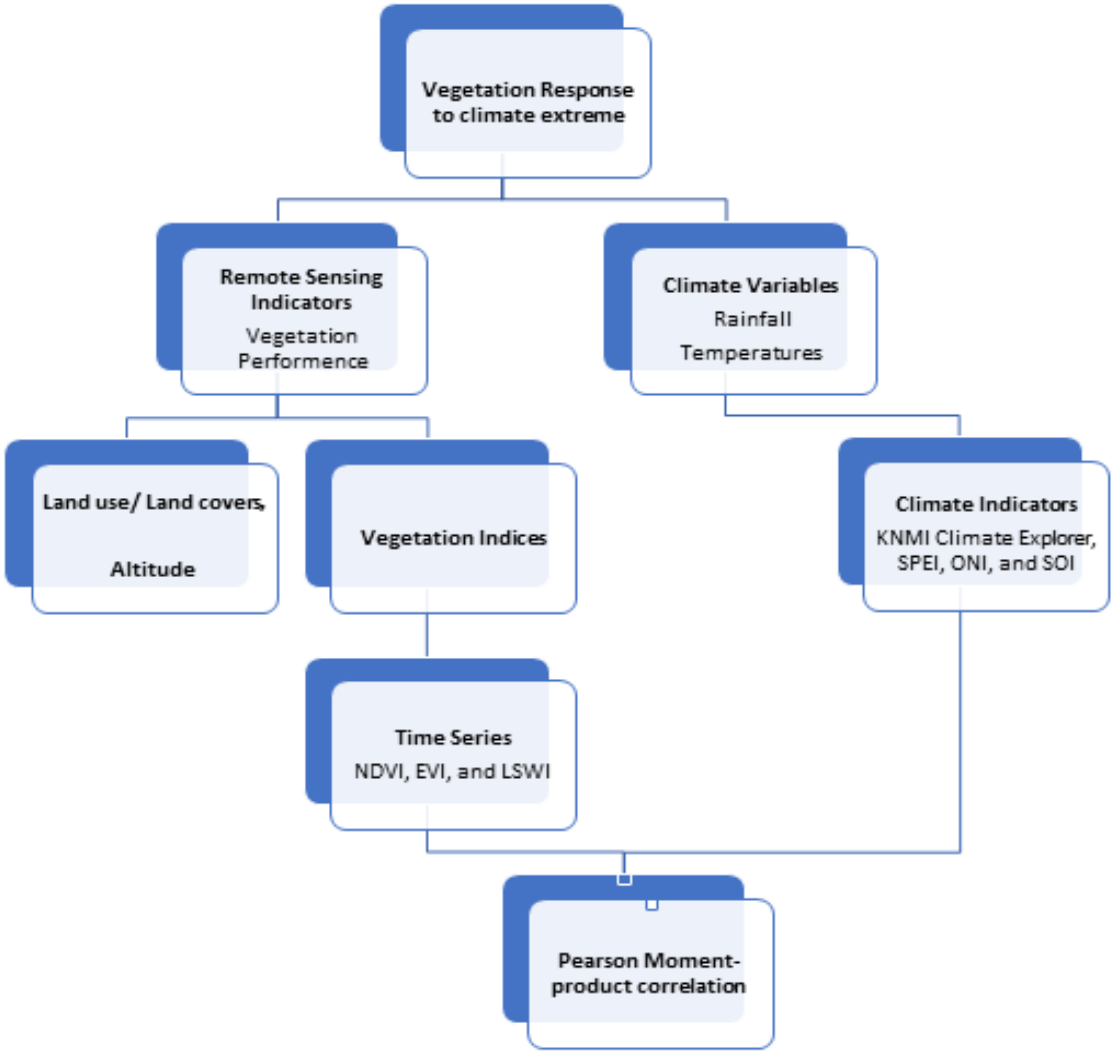

Figure 2.11: Conceptual Framework

2.14 Summary

The chapter covered the comprehensive literature from different studies about vegetation analysis and characteristics in relation to extreme climate and weather events such drought and wet conditions. Numerous droughts, wet condition and vegetation indices have been developed and used to analyse the impacts of drought and wet conditions on vegetation, response and sensitivity. The section revealed different vegetation indices that are used to analyse the impacts of a climate extremes to vegetation and the conceptual framework followed. NDVI, EVI and LSWI were identified as suitable indices to study drought and wet conditions.

CHAPTER 3: METHODOLOGY

3.1 Introduction

This chapter entails the research methodology applied in the study. It describes the design (research) covered and methods of data collection. It also describes the analysis methods outlined in order to achieve the objectives of the study. Extreme value theory and its components are explained, along with the vegetation indices for analysing vegetation change.

3.2 Research design

To achieve the main objective, the study adopted a quantitative approach. Raw data from South African Weather Services (SAWS), and satellite images from the US Geological Survey (USGS) and NASA were used to achieve the study. NOAA-NCEP reanalysis model, KNMI Climate Explorer, ground station data and satellite images for the period of 2000 to 2017 were used.

The study aimed to use remotely-sensed indicators for vegetation condition, primarily the normalized difference vegetation index (NDVI), Enhanced Vegetation Indices (EVI), and climatic measurements from ground weather stations as well as the meteorological models such as NCEP and ERA-INTERIM to analyse the vegetation's response to climate extreme in Limpopo Province. These methods have been used to analyse the extreme climate and weather events by Zhong *et al*., (2017).

3.3 Description of data

3.3.1 NASA Satellite Data

- Land Use/ Land Cover

The MODIS MCD12Q1 land use/ land cover product (MCD12Q1/ Terra Land Use/Land Cover product 500-meter spatial resolution) were used to map the distribution of land use/ land cover types of Limpopo Province. The MCD12Q1 land use/ land cover product was acquired from Land Processes Distributed Active Archive Center (LP DAAC). The MODIS Land Cover Type Product (MCD12Q1) provides global land cover maps at annual time steps from 2001-present.

- Vegetation Indices

The NASA Moderate Resolution Imaging Spectroradiometer (MODIS) was used to characterise the vegetation response and sensitivity over time. MODIS MOD13Q1 vegetation Indices product (MODIS/ Terra vegetation indices, 250-meter spatial resolution) datasets were used to determine vegetation response and sensitivity over Limpopo Province for the period 2000-2017. The vegetation indices product was used to calculate the Normalised Difference Vegetation Index (NDVI) and Enhanced Vegetation Index (EVI). The MODIS MOD13Q1 vegetation Indices Product was acquired from the Land Processes Distributed Active Archive Center (LP DAAC). From MODIS MOD13Q1, for NDVI calculation two bands were used, red band and near-infrared band, whilst for EVI calculation three bands were used, red band, blue band, and near-infrared band.

3.3.2 Meteorological Data

The study involved determining the nature of the climate extremes i.e. meteorological drought, and floods; therefore, climate parameters required for the study included temperature and rainfall. The study used different climate indices to monitor, detect and attribute changes in extreme events. Raw data for the study period was requested from the South African Weather Service (SAWS).

- Temperature

Raw data for temperature was requested from the SAWS for 18 years period. The temperature data was helpful in determining the heat level, whether its normal, below normal or above normal. The study used daily and monthly maximum temperature and minimum temperature data in order to detect and monitor changes in extreme events. Temperature data were subjected to EVA to detect extreme events that occurred.

NCEP-NCAR reanalysis datasets were used to show annual temperature data which is available in a global grid of 2.50 $_{x}$ 2.50. Data were analysed based on the case of extreme conditions. The reanalysis model was used to quantify extreme events occurring in Limpopo Province namely, the temperature $°C$ and precipitation (mm) in relation to vegetation response.

- Precipitation (Rainfall)

Monthly rainfall data was requested from SAWS to be used to measure the scale of rainfall, whether it is above or below normal rainfall. Rainfall data was requested from the South African Weather Services for Limpopo Province for 17 years period, from 2000 to 2017. The precipitation

data helped to quantify droughts, floods and normal rainfall experienced in the study area. Global Precipitation Climatology Project (GPCP) data was analyzed from NCEP reanalysis in the study. The data covered the period from 2000 to 2017.

3.5 Methods of data analysis

Changes in vegetation cover and responses caused by extreme climate and weather events were analysed using various methods discussed below. Remote sensing techniques were employed to examine vegetation response to extreme climate. Vegetation and atmospheric variables were studied through GIS, remote sensing, KNMI Climate Explorer and NOAA-NCEP reanalysis models.

Rainfall and precipitation raw data from SAWS based on various ground stations in Limpopo Province were used for analysis. The project El Niño Southern Oscillation (ENSO) indices were employed in the study to analyse climate extreme occurring in the study area for the period of 17 years from 2000 to 2017. The ENSO indices involve Oceanic Niño Index (ONI) and the Southern Oscillation Index (SOI).

Changes in vegetation cover and responses were analysed and mapped using ArcGIS and Remote Sensing Techniques and Standardized Precipitation Evapotranspiration Index (SPEI). The study used different vegetation indexes, namely, NDVI and EVI to determine the vegetation response and change due to extreme climate events.

3.5.1 Time Series Analysis

Over time, the time series modeling has attracted attentions of researchers. Time series modeling aims to collect and rigorously study the past observations to develop an appropriate model describing the structure of the series (Adhikari & Agrawal, 2013). A time series refers to sequential sets of data points typically observed and measured over successive time and is considered important in the field of climate analysis (Modelsee, 2010). In this study, time series analysis was used to compose trend, outlier / extreme and variability of rainfall data and temperature data.

The time series approach is used for forecasting, past rainfall and temperature observation and develop a suitable mathematical modeling. It is an important forecasting application in many fields (Adhikari & Agrawal, 2013). A time series analysis was employed for the period 2000 to 2017 to analyse seasonal rainfall and temperature trends in Limpopo Province.

$$Y_t = T_t + S_t + C_t + R_t \text{ ---------- eq2}$$

Where: Y_t = Time series

- T_t = Trend
- S_t = Seasonal
- C_t = Cyclical
- R_t = Random

3.5.2 Climate extremes Identifications

- **Anomalies**

From the precipitation and temperature data, anomalies were used depicting abnormal or non-conforming patterns such as anomalies or outliers. Anomalies aim to detect patterns that do not conform to a well-defined motion of expected behaviour of data (Chandola *et al.*, 2009). The technique was used in the study, to identify or find a non-conforming pattern of data. Anomalies are classified into three categories namely; point anomaly, contextual anomalies, and collective anomalies.

Point anomalies occur when an individual data is considered anomalous with entire data record, contextual anomalies associated with data anomalous in a specific context, while collective anomalies relate to a collection of related data being anomalous with the entire data record.

3.5.3 Composite Analysis

Several cases of extremely heavy rainfall (floods) and extremely low rainfall (drought) were studied to identify common characteristics of weather systems influencing floods and drought in the area. The study used composite analysis to visualise GPCP precipitation, wind vector and geopotential height for the period of 2000 to 2017. In studying the effects of extreme weather events, composites can be useful for exploring the large-scale impacts of teleconnections from modes of atmospheric variability such as El Niño and La Nina and Southern Annular Mode (SAM). Composite of the weather over southern Africa was produced to study how precipitation and temperature variations due to ENSO.

3.5.4 Case Study

The case study approach was applied to sample extreme climatic events in Limpopo Province. The study sampled cases according to their extremal events (anomalous wet departure i.e. floods conditions and anomalous dry departure such as meteorological drought) in order to facilitate the exploration of a phenomenon within its contexts. A case study is defined as a set of related events that aim at describing and explaining a phenomenon of interest through identifying structures, forms, and variables (Bromley, 2002; Starman, 2013). Analysis of vegetation cover and response was studied based on extreme cases identified and sampled. The study reviewed and reported on the extreme event cases identified.

3.5.5 Land Use/ Land Cover Classification (LULC)

Timely and accurate background knowledge on LULC of an area is important for management activities and is considered an essential element for understanding and modeling the earth as a system (Lillesand *et al.*, 2014). The MODIS MCD12Q1 LULC product provides detailed characteristics for global coverage from the quality data of intermediate spatial resolution (500 m).

Table 3.1: Below depicts MOD12Q1 annual IGBP land cover classes, adopted and modified from Friedl et al., (2010).

Broad Cover Type	Name	Value	Description
Natural Vegetation	Evergreen Needleleaf Forests	1	Land dominated by evergreen conifer trees (canopy >2m) and tree cover >60%. Almost all trees remain green all year and the canopy is never without green foliage.
	Evergreen Broadleaf Forests	2	Land dominated by evergreen broadleaf and palmate trees (canopy >2m) and tree cover >60%.Almost all trees and shrubs remain green year round. Canopy is never without green foliage.
	Deciduous Needleleaf Forests	3	Dominated by deciduous needleleaf (larch) trees (canopy >2m). Tree cover >60%. Consists of seasonal needleleaf tree communities with an annual cycle of leaf-on and leaf-off periods.
	Deciduous Broadleaf Forests	4	Land dominated by deciduous broadleaf trees (canopy >2m) and tree cover >60%. Consists of broadleaf tree communities with an annual cycle of leaf-on and leaf-off periods.
	Mixed Forests	5	Dominated by neither deciduous nor evergreen (40-60% of each) tree type (canopy >2m) and tree cover >60%. Consists of tree communities with interspersed mixtures or mosaics of the other four forest types. None of the forest types exceeds 60% of landscape.
	Closed Shrublands	6	Land dominated by woody perennials (1-2m height) >60% cover. The shrub foliage can be either evergreen or deciduous.
	Open Shrublands	7	Land dominated by woody perennials (1-2m height) 10-60% cover. The shrub foliage can be either evergreen or deciduous.
	Woody Savannas	8	Lands with herbaceous and other understory systems, with forest canopy cover between 30% and 60%. The forest cover height exceeds 2 m.
	Savannas	9	Lands with herbaceous and other understory systems, and with forest canopy cover between 10% and 30%. The forest cover height exceeds 2m.
	Grasslands	10	Dominated by herbaceous annuals (<2m). Tree and shrub cover is less than 10%.
	Permanent Wetlands	11	Permanently inundated lands with 30-60% water cover and >10% vegetated cover. The vegetation can be present in either salt, brackish, or fresh water.
Developed & Mosaic Lands	Croplands	12	Lands covered with temporary crops followed by harvest and a bare soil period mosaic lands (e.g., single and multiple cropping systems). At least 60% of area is cultivated cropland
	Urban and Built-up Lands	13	At least 30% impervious surface area including building materials, asphalt, and vehicles and other man made structures.
	Cropland/Natural Vegetation Mosaics	14	Mosaics of small-scale cultivation 40-60% with natural tree, shrub, or herbaceous vegetation.
Non Vegetated Lands	Permanent Snow and Ice	15	At least 60% of area is covered by snow and ice for at least 10 months of the year.
	Barren	16	At least 60% of area is non-vegetated barren (sand, rock, soil) areas with less than 10% vegetation.
	Water Bodies	17	At least 60% of area is covered by permanent water bodies.

The MCD12Q1 product is created using the supervised classification of MODIS reflectance data (Friedl *et al.*, 2010). MODIS MOD12Q1 annual IGBP supervised classification at 500-meter resolution was employed to identify the LULC in terms of vegetation covers. The MOD12Q1

identifies classes into 17 as displayed in Table 3.2 above. MCD12Q1 data were used to analyse IGBP land use/ land covers for the period 2001, 2010, and 2017 over Limpopo Province.

3.5.6 Vegetation Indices

- Normalized Difference Vegetation Index (NDVI)

According to Chen *et al.*, (1998), Normalized Difference Vegetation Index (NDVI) is defined as vegetation indices that allow the study of vegetation conditions by generating satellite imagery displaying greenness such as relative biomass. NDVI is constantly used to monitor vegetation conditions (Tucker, 1979). MODIS MOD13Q1 vegetation product, terra at 16-days were used to extract NDVI from February-2000 to 2017. The NDVI is computed using the near-infrared and red, and is calculated using the formula,

$$NDVI = \frac{(\rho_{NIR} - \rho_{RED})}{(\rho_{NIR} + \rho_{RED})} \quad \text{---------- eq3}$$

Where ρ represents spectral reflectance measurements in the RED and NIR regions of the electromagnetic spectrum, respectively. This spectral reflectance represents the ratio of reflected radiation to incoming radiation from each spectral band, with values ranging between 0.0 and 1.0. Theoretically, the NDVI values range between -1.0 and +1.0, typically ranged from vegetation and other earth surface materials between about -0.1 (less NIR than RED) for non-vegetated surfaces and as high as 0.9 for dense vegetation canopy.

- Enhanced Vegetation Index (EVI)

MODIS MOD13Q1 EVI was used for the assessment of increased sensitivity over a wide range of vegetation conditions and the removal of soil background influences and removal of atmospheric effects that are present in the NDVI. Vegetation indices recently have proven to be very useful in terms of indicating extreme events such as drought in terms of vegetation conditions. This is because they can cover the globe at relatively high spatial resolution (Jinghua *et al*., 2012). Satellite imagery data were employed in the study to determine the impacts that extreme climate events have on vegetation cover and dynamics. A series of images were used to calculate the EVI from 2000 to 2017. EVI is computed by the equation given below:

$$EVI = 2.5 \times \frac{P_{NIR} - P_{Red}}{P_{NIR} + (6 \times P_{Red} - 7.5 \times P_{Blue}) + 1} \quad \text{----------eq4}$$

where P_{NIR}, P_{Red} and P_{Blue} are the reflectance in the near infra-red (NIR), red and blue channels, respectively; 2.5 is a gain factor, 6 and 7.5 are coefficients designed to correct for aerosol scattering and absorption and 1 is a canopy background adjustment (Huete *et al*., 1994; 1997).

- Land Surface Water Index (LSWI)

LSWI is a satellite-based tool that is used to measure and monitor the amount of liquid content in the vegetation canopy (Chandrasekar *et al*., 2010). MODIS MOD09A1 terra LSWI at 500m spatial resolution for month was derived from NOAA satellite for 2000 -2017 period. By using a combination of shortwave infrared (SWIR) and near infrared (NIR), LSWI were proposed and considered advanced and direct vegetation moisture indicators (Zhang et al., 2013). Using MODIS satellite data, the NIR and the SWIR bands as band 2 and band 6 are used and defined as the this LSWI. LSWI follows the equation:

$$\text{LSWI}=\frac{(P_{NIR}-P_{SWIR})}{(P_{NIR}+P_{SWIR})} \quad \text{----------} \quad \text{eq5}$$

Where ρ represents spectral reflectance measurements in the NIR and SWIR regions of the electromagnetic spectrum, respectively.

3.5.7 Pearson's product-moment correlation coefficient

The correlation coefficient between the climate variables and vegetation indices was calculated to analyse the effects that temperature and precipitation have on the vegetation conditions over Limpopo Province from 2000 to 2017. The Pearson product-moment correlation coefficient was used to study the relationship between vegetation indices and climate variables. The study analysed the correlation between NDVI and temperature ($P_{NDVI-TMax}$), NDVI, precipitation (P_{NDVI-P}) and NDVI and LSWI ($P_{NDVI-LSWI}$), EVI and temperature ($P_{EVI-TMax}$), precipitation (P_{EVI-P}), and LSWI ($P_{EVI-LSWI}$) respectively.

This method of Pearson Correlation Coefficient was used to validate a change in the relationship between climatic variables with NDVI (Chen *et al*., 2015). It summarises the relationship between two variables creating the correlation coefficient. The correlation coefficient is given by the symbol r and it ranges from -1 ≤ r ≤ 1. Pearson correlation follows the equations:

$$r = \frac{\sum(X_i-\bar{X})(Y_i-\bar{Y})}{\sqrt{\sum(X_i-\bar{X})^2\sum(Y_i-\bar{Y})^2}} \quad \text{----------} \quad \text{eq6}$$

When computing the correlation coefficient r, it is useful to test the significance of the correlation coefficient. It gives the researcher a view on how large the correlation coefficient must be to demonstrate the relationship between two variables.

- **Hypothesis Tests**

The formula for hypothesis tests depends on the correlation coefficient calculated, whether it is tested against 0 or against other values.

Testing H_0: $p = 0$

$$t = \frac{r}{\sqrt{\frac{1-r^2}{n-2}}} \text{ ---------- eq7}$$

3.5.8 National Centers for Environmental Prediction (NCEP)

NCEP reanalysis was employed in the study to map different types of mean synoptic circulation fields. This involves observations conducted at different sources, such as ground stations and satellites. The reanalysis model was used to reconstruct the past of the atmosphere incoherent way by combining numerical models with available observation (Solomon *et al*., 2007), as well as developing a comprehensive record through graphs of how mean synoptic circulation fields are changing. According to Compo *et al*., (2011), NCEP reanalysis reconstructs the past using similar methods, such as those of numerical weather predictions, for instance, the model base assimilation data methods. The circulation fields computed using the NCEP model includes 500-hPa geopotential heights, 500-hPa wind vector, and 200-hPa OLR, all available from 1948 (Chikoore, 2016). The composite of seasonal NCEP reanalysis data sets of geopotential height, vector winds and outgoing longwave radiation were analysed.

3.5.10 KNMI Climate Explorer

The KNMI Climate Explorer is a web-based climate analysis application used for data statistically. Statistical analysis performed using KNMI Climate Explorer includes maximum temperature and GPCP precipitation from ECMWF (ERA-int). Seasonal absolute mean precipitation and maximum temperature were investigated. The KNMI Climate Explorer has been a widely used tool for extracting and performing statistical analysis (e.g. Chikoore., 2016). Based on extreme weather events cases identified, precipitation and maximum temperature plots were produced using KNMI Climate Explorer.

3.5.9 Standardized Precipitation Evapotranspiration Index (SPEI)

Vincente-Serrano *et al.,* (2010) were the first to propose the use of standardized precipitation evapotranspiration index (SPEI) as an improvement to drought index suited to study the impacts of a warming climate on drought severity. SPEI is designed similarly to the Palmer Drought Severity Index (PDSI). However, it considers the effects of evapotranspiration on drought severity and identifying different types of drought and its impacts on the diverse systems (Vicente-Serrano *et al*., 2012).

Table 3.2: Table showing categories of SPEI

Categories	SPEI Value
Extremely Dry	< -2
Severe Dry	-1.99 to -1.5
Moderate Dry	-1.49 to -1.0
Mild Drought	0 to -0.99
Mildly Wet	0 to 0.99
Moderate Wet	1.0 to 1.49
Severe Wet	1.50 to 1.99
Extremely Wet	> 2

SPEI was applied in the study to identify types of drought and its value. According to Huang *et al*., (2014), the method can be used to characterize types of extremes. Two sets of meteorological station data, namely, precipitation and temperature, are used in the study.

According to Potop and Mozny (2011), the SPEI is based on a monthly (or weekly) climatic water balance (precipitation minus evapotranspiration) that is adjusted using a three-parameter log-logistic distribution, to consider common negative values. However, the selected record for the study covers the period from 2000 to 2017. To measure drought severity, this study applied a SPEI.

The SPEI follows the equations (Abramowitz and Stegum, 1965):

$$SPEI = W\ \frac{C_0+C_1W+C_2W^2}{1+d_1W+d_2W^2+d_3W^3} \quad \text{---------- eq8}$$

Where $W = \sqrt{-2In(P)}$ for p ≤ 0.5

and *P* is the probability of exceeding a determined *D* value, $P = 1 - F(x)$. If $P > 0.5$, then *P* is replaced by 1 - *P* and the sign of the resultant SPEI is reversed. The constants are C0 = 2.515517, C1 = 0.8022853, C2 = 0.010328, d1 = 1.432788, d2 = 0.189269, and d3 = 0.001308.

3.5.11 Change Detection

The change detection technique was used to identify the type of change and to quantify the amount of change. The study employed the post-classification approach using MODIS MCD12Q1 IGBP classification at 500m annually to detect land use/ land cover changes between two images from 2001 to 2017. Post-classification change detection consists only of comparing the “from-to” information for each pixel or segment (Coppin *et al*., 2004; Yuan *et al.*, 2005), to define the rate of change and location for land cover have transformed. However, due to the availability of MODIS MCD12Q1 data, land use and land cover were performed from 2001 to 2017, as well as change detection. Post classification change detection is the most widely used approach for identifying land use and land cover change and displays good accuracy (Lu *et al.*, 2004).

3.6 Quality Assurance

The accuracy assessment of all satellite imagery products was conducted, depending on referenced data collected in the study area, called ground-truthing (Jensen, 1996). Reference data is known to represent high accuracy information about the accuracy assessment site or a specific area which can be theoretically 100 percent accurate. The referenced data is obtained through site visits or photographic interpretation or videos. It is represented generally in grouped pixels or polygons. It involves comparing site categorized data with the reference data of the visited sites (Jensen, 2007). For accuracy assessment over Limpopo Province, a total of 80, 110 and 220 random pixels were selected from each land use and land cover and compared with original pixels in the corresponding images. To calculate the accuracy assessment, the total correct pixels (diagonal elements) are divided by the total number of pixels in the referenced image (Campbell, 2007). Accuracy assessment also involves the calculation of the kappa coefficient to reveal the map results in relation to total labeling of imagery pixels (Congalton, 1991; Jensen, 1996; Lillesand and Kiefer, 1994). The user accuracy, producer accuracy, commission, omission, kappa coefficient, and overall accuracy were calculated.

3.7 Summary

This chapter provided a description of the various methods used to collect and analyse the data. The study used precipitation and temperature data from South African Weather Service (SAWS) and web-based tools, along with remote sensing indices. A time-series analysis and anomalies methods were used. The impacts of extreme weather events, namely drought and floods were analysed using NDVI, EVI, LSWI. Pearson moment-product correlation was used to assess the level of association between climate variables and vegetation indices.

CHAPTER 4: EXTREME WEATHER EVENTS IN LIMPOPO PROVINCE

4.1 Introduction

The chapter presents the climatological variables over Limpopo Province. The section addresses the frequency of extreme weather events, dry or drought conditions and floods conditions within the austral summer (DJF), and their interannual variability for the 2000-2017 period. The characteristics and consequences of drought and floods events in the region were identified and their impacts were discussed. The occurrence of extreme weather events in the Limpopo region was characterised using GPCP Precipitation, maximum temperature, and the SPEI.

4.2 Rainfall

4.2.1 Mean Spatial Pattern

Figure 4.1 shows a spatial distribution pattern in austral summer rainfall (DJF) for the southern Africa region from GPCP precipitation for the 2000-2017 period. The study region is located on the far North-Eastern part of South Africa and displays west to east rainfall gradients.

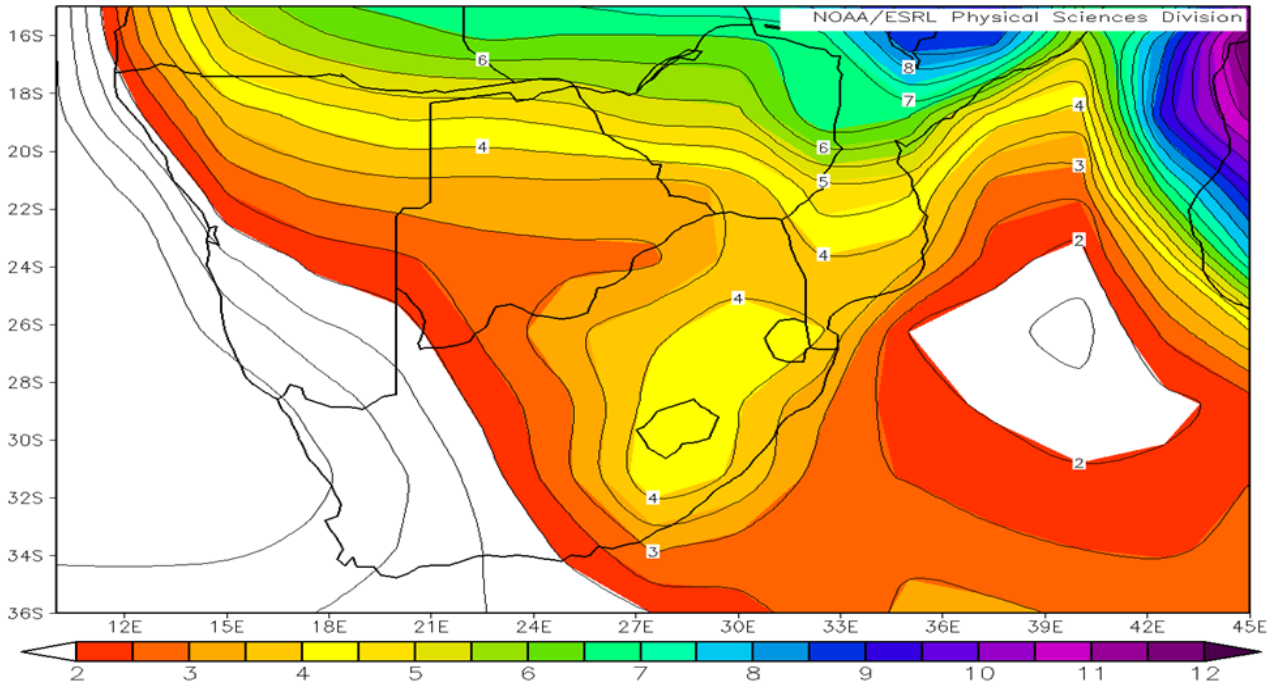

Figure 4.1: Southern Africa mean summer (DJF) spatial GPCP rainfall distribution (mm/day)

The mean spatial distribution pattern of summer rainfall (DJF) is highly variable in the southern Africa region, there is west to east gradient in the rainfall distribution over the region (Figure 4.1).

Rainfall varies from west to east with the highest rainfall in the eastern part of the region and lowest in the western part. The western part of the region is associated with the lowest rainfall, covering most of the region's deserts (Chikoore, 2016). Limpopo Province is in the northeast part of South Africa and receives summer rainfall (DJF). From 2000 to 2017 the region received less than 2 mm/day of rainfall in the western part, while in the eastern part received average rainfall greater than 4 mm/day.

The South Western Indian Ocean (SWIO) and warm Agulhas current may be attributed to the occurrence of eastern rainfall due to the onshore moisture from the Indian Ocean. The western part of South Africa receives low rainfall due to the offshore prevailing winds, making the western region dry. The province is a subject of distinct climatic conditions due to mountain ranges (Soutpansberg mountain) which extends from Drakensberg mountain. Due to the escarpment barrier, climate variability exists between the western part and eastern side of the escarpment, with the eastern part of the escarpment receiving higher annual rainfall exceeding 1500 mm than the western part (Chikoore, 2016).

Tropical cyclones regularly form over the Indian Ocean in summer and are always associated with copious heavy rainfall and flooding (Tyson & Preston-Whyte, 2000; Chikoore *et al.*, 2015). During TCs conditions in southern Africa, heavy rainfall occurs only across the eastern coast and adjacent inland areas, with fine and dry conditions prevailing over the central and western coast (Tyson & Preston-Whyte, 2000). The rainfall distribution associated with tropical cyclones may have devastating effects as was the case with Eline (1999/00), Dando (2011/12) and the latest TC Idai 2018/19. The southern Africa region is vulnerable to the impacts of TCs (Chikoore *et al.*, 2015). Tropical cyclone (TC) Dando which developed in the south western Indian ocean resulted in flooding, eliciting damage in the eastern part of South Africa, Swaziland and Mozambique (Chikoore *et al.*, 2015).

4.2.2 Annual Cycles of Rainfall in Limpopo Province

Figure 4.2 presents the mean annual cycles of rainfall for four weather stations from South African Weather Services (Mara, Lephalale, Polokwane & Warmbad Towoomba Weather Station, respectively). The rainfall distribution over Limpopo Province is strongly seasonal, with the highest recorded during the austral summer from October to March, with more of its wet years and dry years experienced during the austral summer. The stations present different annual cycle patterns; however, they depict the same sequence of austral summer rainfall (DJF).

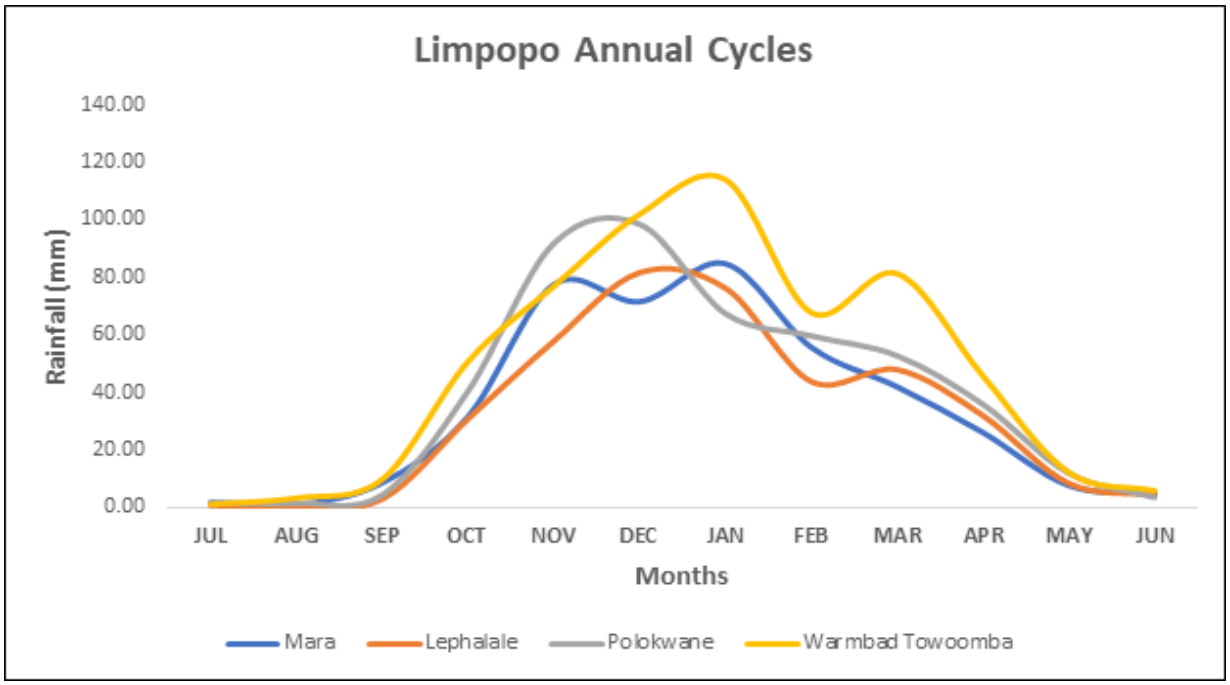

Figure 4. 2: Mean annual cycles of rainfall over Limpopo Province based on South African Weather Services (SAWS) data

The climate of the region is semi-arid with droughts and floods are a distinct and recurring feature of the summer climate (Chikoore, 2016), and are associated with the normal-dry winter season and wet summer seasons (Mpandeli, *et al.*, 2015). The mean annual cycles of rainfall in the Limpopo region shows that the region receives most of its rainfall during austral summer months from October to March, with its peak from December to February (Figure 4.2). From the annual cycles above (Figure 4.2) Mara peaks during January (81 mm), Lephalale peaked during December (80 mm), Polokwane peaked during November (100 mm) and Warmbad peaked in January (120 mm). Since rainfall in the region peaks at different months, this shows that there is a strong seasonal rainfall variability over the area.

4.2.3 Interannual Variability

The interannual rainfall variability over Limpopo shows a high variability from season to season. Figure 4.3 shows the interannual rainfall variability over the region for the 2000-2017 period.

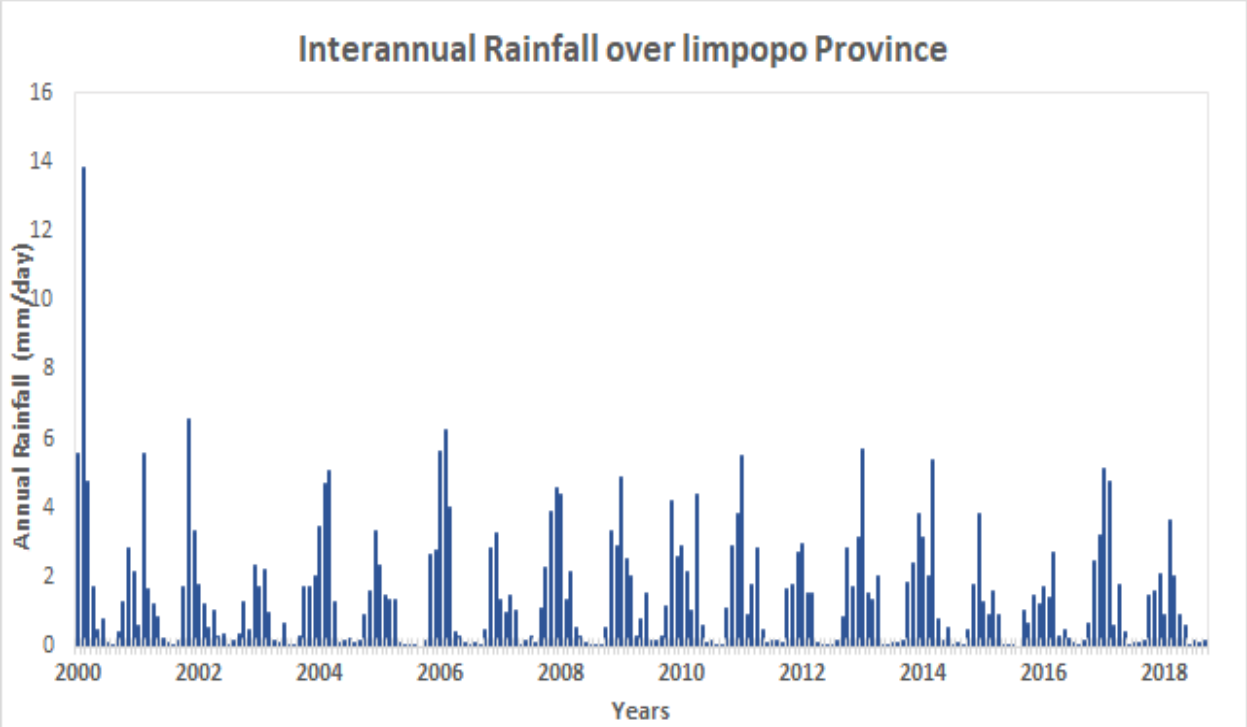

Figure 4.3: GPCP Interannual summer rainfall (DJF) variability over Limpopo Province

The inter-annual rainfall distribution of Limpopo Province is highly gradual with an increase in the occurrence of extreme events. Interannual rainfall varies a lot over Limpopo with the region experiencing events of different intensity (different from one another) and receiving its rainfall during austral summer season (DJF) with the highest rainfall peak of about 14 mm/day during the year 2000, 6 mm/day for the year 2006. The lowest rainfall was recorded in 2002/03 (2 mm/day) and 2015/16 with rainfall less than 2 mm/day received. The year 2000 experienced the highest rainfall due to the occurrence of landfalling of tropical cyclone Eline formed over the southwest Indian Ocean and traversed southern Africa bringing historic floods (Dyson & Van Heerden, 2001; Reason & Keibel, 2004; Chikoore *et al*., 2015)). As a result of cyclone Eline, the year 2000 was recorded as the wettest year (Reason & Keibel, 2004). The lowest rainfall received in 2002/03 and 2015/16 of about 2 mm/day (of rainfall) was due to the El Nino induced drought that occurred, resulting in less rainfall over the region (see Figure 2.7 and Figure 2.8).

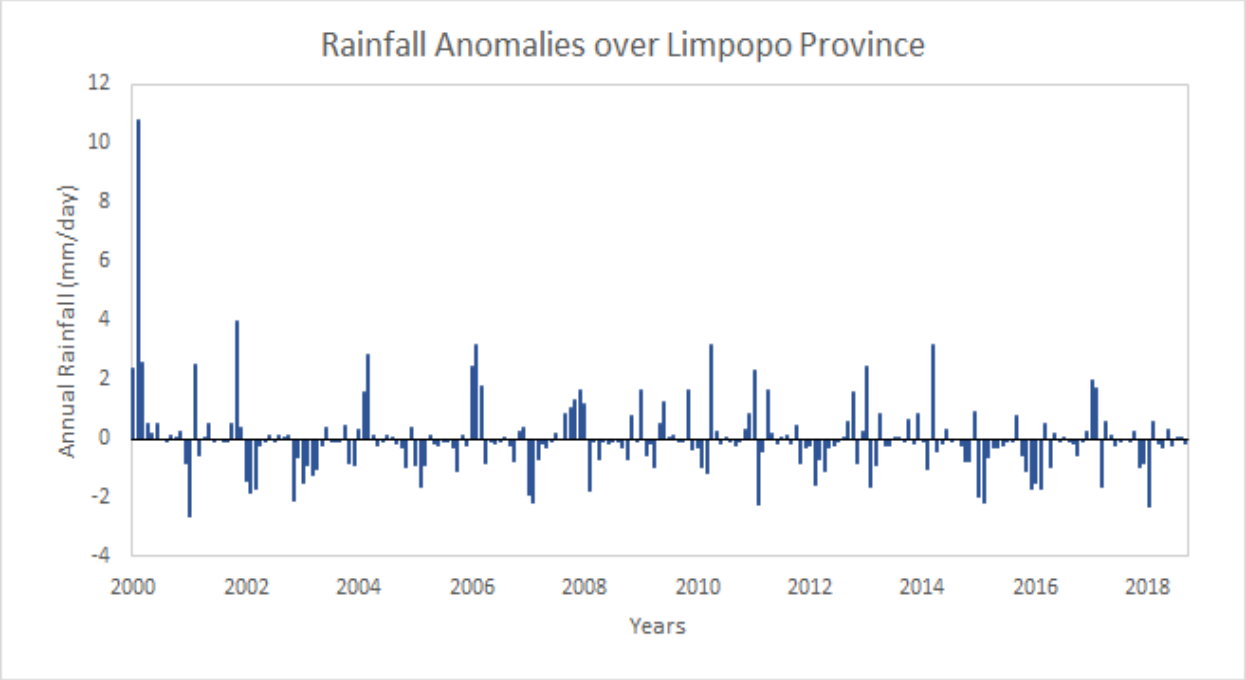

Figure 4.4: GPCP summer rainfall (DJF) anomalies over Limpopo Province

Figure 4.4 presents austral summer (DJF) rainfall anomaly over Limpopo Province for the study time frame. Anomalous heavy rainfall events occurred over the region during the austral summer season (DJF) 1999/00 and 2005/06, whilst the anomalous low rainfall occurred during the austral summer season (DJF) 2002/03 and 2015/16 (Figure 4.4). The anomalous wet seasons in the case of 1999/2000 floods were caused by tropical cyclone Eline over the southwest Indian Ocean. Tropical cyclones have been found to influence the severe heavy rainfall and flooding in Limpopo (Chikoore, 2015). From the displayed Figure 4.4, it is evident that extreme floods and droughts are frequent in the region.

Rainfall anomaly (Figure 4.4) provides evidence that the region is prone to frequent dry spells (droughts) and wet spells (floods). The ENSO cycle corresponds to wet years and dry years over the region (see Figure 2.7 and Figure 2.8). Wet years in the region are associated with floods whilst dry years are associated with droughts. Figure 4.4 shows that the region has a high occurrence of extreme weather events coming in every two to four years. The region was exposed to one of the successive hottest and driest years in 2014/15 and 2015/16, with negative anomalies of about -2mm/day respectively.

The oceanic interaction with the atmosphere leads to intense weather conditions, which has considerable impacts on climate onshore (Linacre & Geerts, 1997; Tyson & Preston Whyte, 2000). The El Niño events are associated with catastrophic droughts in South Africa, with La Nina

associated with higher rainfall and floods (Tyson & Preston-Whyte, 2000). The two successive El Niño events 2014/15 and 2015/16 produced an extreme climate anomaly over southern Africa.

Table 4.1: The ranks for selected droughts and floods over Limpopo Province, South Africa

Rank	Years	ENSO Events	Rank	Years	ENSO Events
4	2006/07	El Niño	1	1999/00	La Nina
6	2000/01	El Niño	3	2005/06	La Nina

4.3 Temperature

4.3.1 Mean Spatial Pattern

Figure 4.5 below shows that the mean spatial pattern of maximum temperature is highly variable over the study region, showing that the area receives high values during the summer season. The annual cycles (Figure 4.6) for Limpopo Province show that the region is cooler (minimum temperature) in the winter season June-July, with the temperature rising to >33°C from October to January (Chikoore, 2016). The maximum temperature (Tmax) for Limpopo Province shows temporal and spatial variability. Tmax anomalies over the study area (Limpopo Province) appear to be associated highly with the drought and floods seasons. The interannual maximum temperature variability and maximum temperature anomalies show a rising trend, over the region. With observations (Figure 4.7 and Figure 4.8) from the region support that of Kruger and Shingle, (2004), by showing a piece of strong evidence about the warming trend over southern Africa.

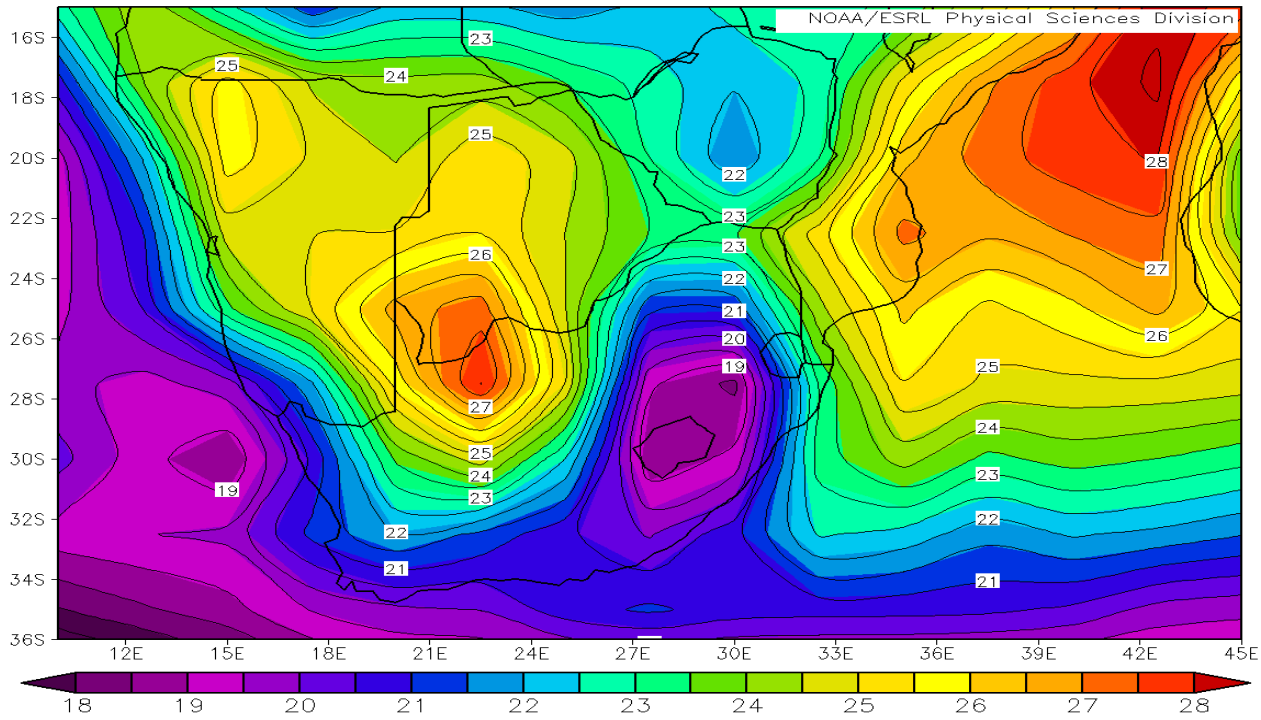

Figure 4.5: Showing mean summer (DJF) spatial distribution of air temperatures over Southern Africa

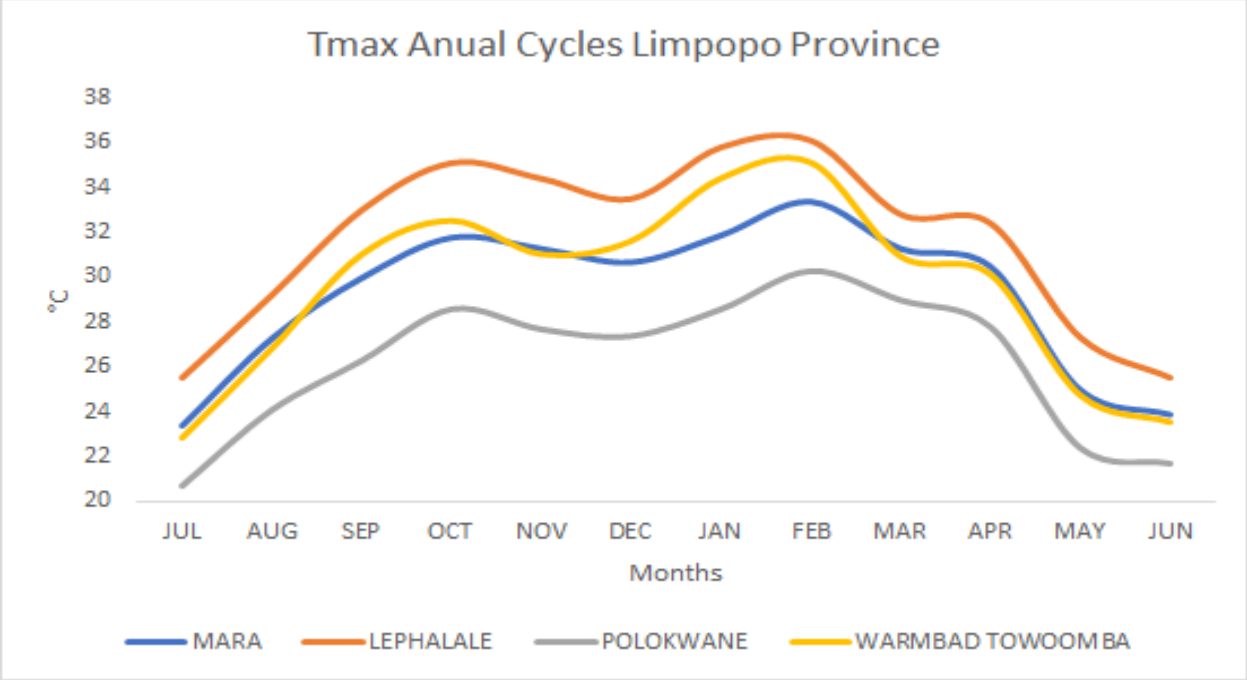

Figure 4.6: Annual cycles of maximum temperature over Limpopo Province based on South African Weather Service (SAWS) data

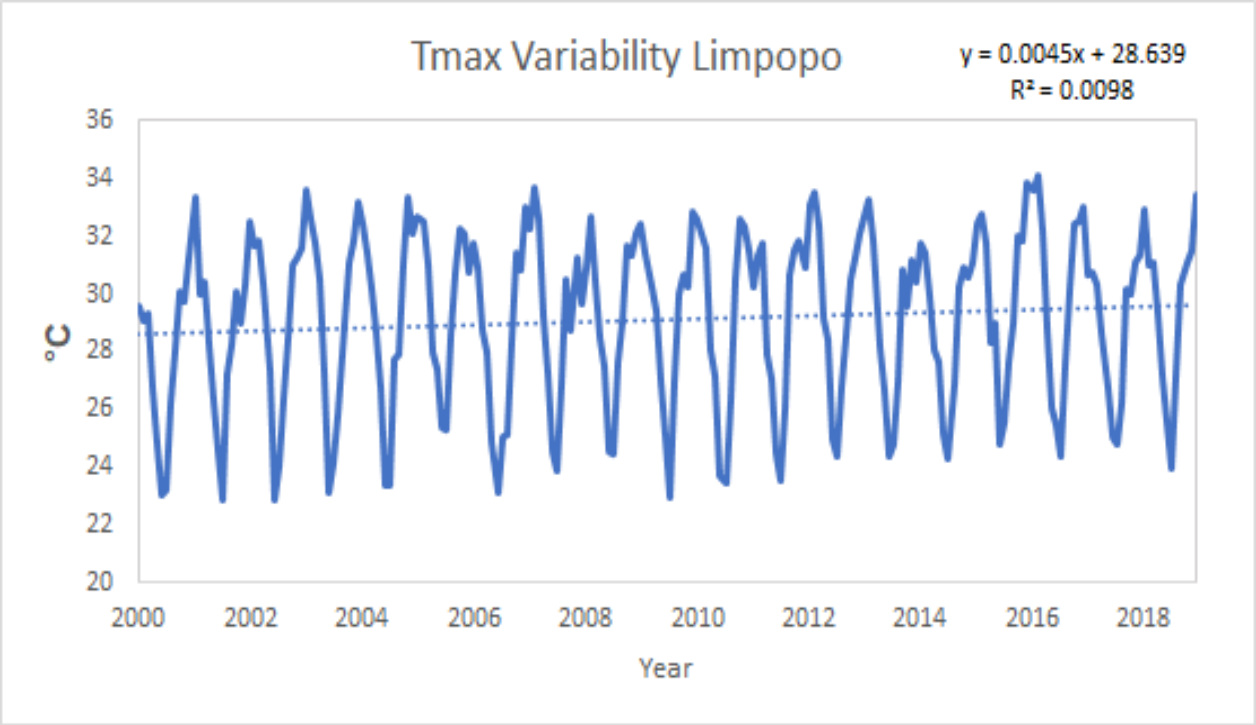

Figure 4.7: Interannual summer maximum temperature variability over Limpopo Province

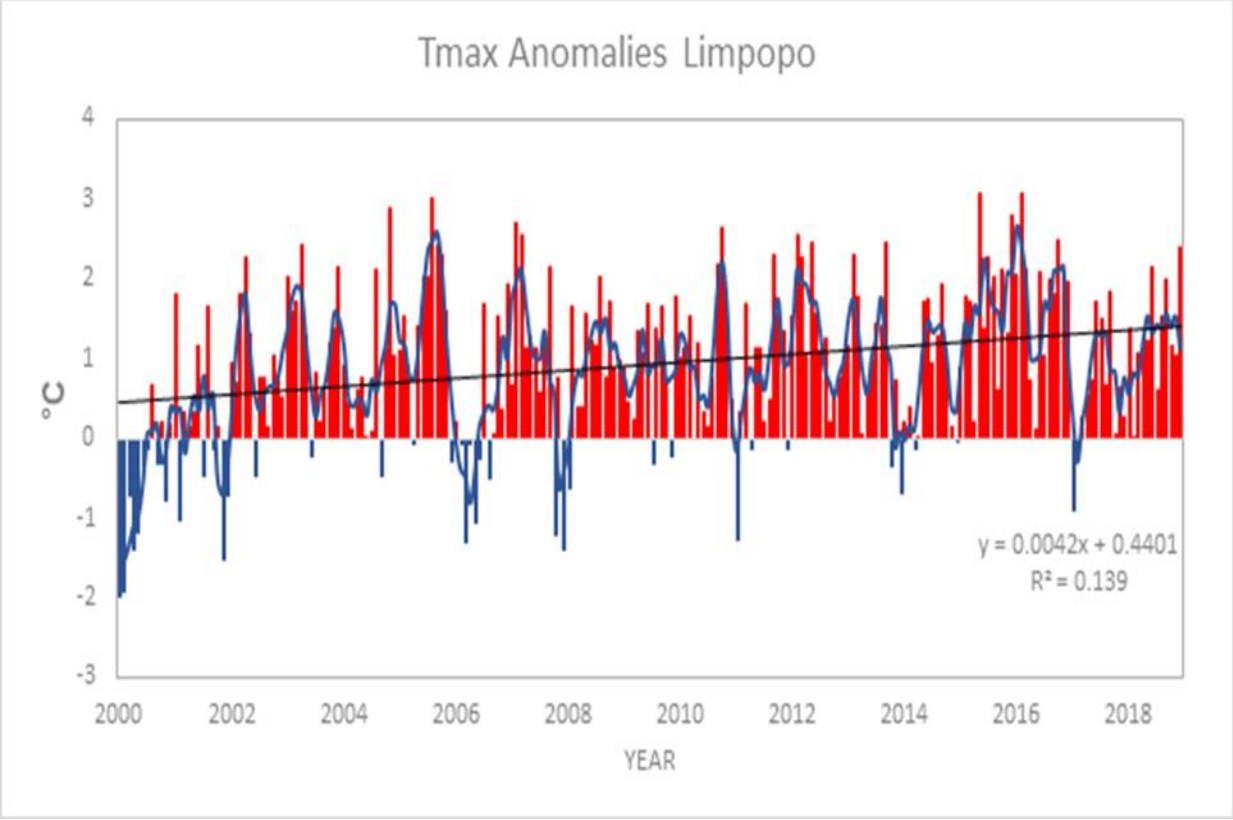

Figure 4.8: Maximum temperatures anomalies over Limpopo Province for the period 2000-2017

4.4 Extent and characteristics of extreme weather events using the Standardized Precipitation Evapotranspiration Index (SPEI)

To establish the nature and characteristics of meteorological drought and floods over Limpopo Province, SPEI time series were analysed using monthly values of rainfall, minimum temperature (Tmin) and maximum temperature (Tmax) data from (4) four different weather stations (Mara, Lephalale, Polokwane and Warmbad stations). SPEI index was used to characterise the nature and intensity of extreme weather events, namely; drought and floods. All meteorological station data were acquired from the South African Weather Service (SAWS) for 2000 to 2017 2000 - 2017 period. The trends of SPEI values at 1 (SPEI-1), 3 (SPEI-3), 6 (SPEI-6), and 12 (SPEI-12)-month timescales were calculated and retrieved from R-Studio. SPEI values were used to identifies the period of wet seasons and dry seasons.

Figure 4.9; Figure 4.10; Figure 4.11; and Figure 4.12 illustrate the existence of a strong seasonal and interannual variability in both dry and wet conditions in Limpopo Province. The SPEI indices managed to detect the severity, intensity, and duration of all drought episodes and wet episodes experienced between 2000 and 2017. The intensity of extremely dry conditions and extreme wet conditions differ in different stations and different climatic conditions. Due to the escarpment barrier (Soutpansberg mountain), climate variability exists in Limpopo Province with the eastern side of the escarpment receiving higher annual rainfall than the western part (Chikoore, 2016). As a result, to variation to climatic conditions, the onset and end period of fine or drought conditions and wet conditions differ according to stations.

The SPEI results display the general trends of fluctuation between dry and wet periods from one month to twelve months in Limpopo Province. The 1-month SPEI from (Figure 4.9; Figure 4.10; Figure 4.11; and Figure 4.12) displays the monthly trend patterns of wet and dry conditions over the region. The SPEI results reveal that dry periods start from May to October and wet cycles start from November to April, thus creating normal dry winter period and wet summer period respectively (Mpandeli, *et al*., 2015). The monthly wet cycles are frequent during the first period of the study. However, this could be attributed to a succession of tropical cyclones making landfall in southern Africa. Monthly dry cycles are frequent in the last period of the study, being attributed to less amount of precipitation received, leading to successive drought conditions 2014/15 and 2015/16 seasons. In SPEI 1, the moisture differences between months cannot be attributed to making the trend between positive and negative SPEI values.

Figure 4.9; Figure 4.10; Figure 4.11; and Figure 4.12 show SPEI 3-time scale with moisture deficits over the 3-month intervals, representing the mid-season moisture conditions from 2000 to 2017. For clear mid-season analysis, SPEI 3 displaying the 3-month cycle was calculated. The 3-month cycle shows more wet seasons during the first decade (2000 to 2010) and dry season in the last decade (2011 to 2017). During the vegetation growing season, 3 months SPEI is suitable for monitoring soil moisture and rainfall conditions (Rouault & Richard, 2003). As per the SPEI 6 results, fluctuations from wet to dry season were observed (Figure 4.9; Figure 4.10; Figure 4.11; and Figure 4.12). The 6-month SPEI reflects the medium seasonal distribution over the 6-month period to show the moisture conditions throughout each season.

Table 4.2: Table of SPEI 6, Extreme weather events classification over Limpopo Province

Extreme Weather Severity Category	Category			
	Lephalale Station	Mara Station	Warmbad Station	Polokwane Station
1999/00	Severely Wet	Extremely Wet	Severely Wet	Severely Wet
2001/02	Severely Wet	Moderately Wet	Moderately Wet	Severely Wet
2002/03	Severe Drought	Moderate Drought	Moderate Drought	Severe Drought
2004/05	Severe Drought	Mild Drought	Moderate Drought	Severe Drought
2005/06	Extremely Wet	Moderately Wet	Extremely Wet	Moderately Wet
2007/08	Severe Drought	Moderate Drought	Severe Drought	Severe Drought
2008/09	Moderately Wet	Moderately Wet	Moderately Wet	Extremely Wet
2009/10	Severe Drought	Moderate Drought	Severe Drought	Moderate Drought
2010/11	Severely Wet	Extremely Wet	Severely Wet	Severely Wet
2011/12	Severe Drought	Extreme Drought	Severe Drought	Severe Drought
2012/13	Severely Wet	Moderately Wet	Moderately Wet	Mildly Wet
2013/14	Severely Wet	Moderately Wet	Moderately Wet	Moderately Wet
2014/15	Moderate Drought	Severe Drought	Severe Drought	Severe Drought
2015/16	Moderate Drought	Severe Drought	Severe Drought	Severe Drought

In 1999/00 the region experienced a severely wet season with the influence of landfall tropical cyclones (TCs) making landfall in February 2000 (Chikoore *et al.*, 2015). The season 2005/06 came with severely wet conditions over Limpopo Province. The 2002/03 season brought severe drought conditions and moderate conditions in two stations each. For 2014/15 and 2015/16 seasons, drought seasons were recorded as the two most drought prolonged periods and consecutive warming temperatures which were severe for more than 20 months over Mara (Figure 2.7 and Figure 2.8), Warmbad and Polokwane stations and moderate in Lephalale station. This can be seen from SPEI 12 of each station (Rouault & Richard, 2003).

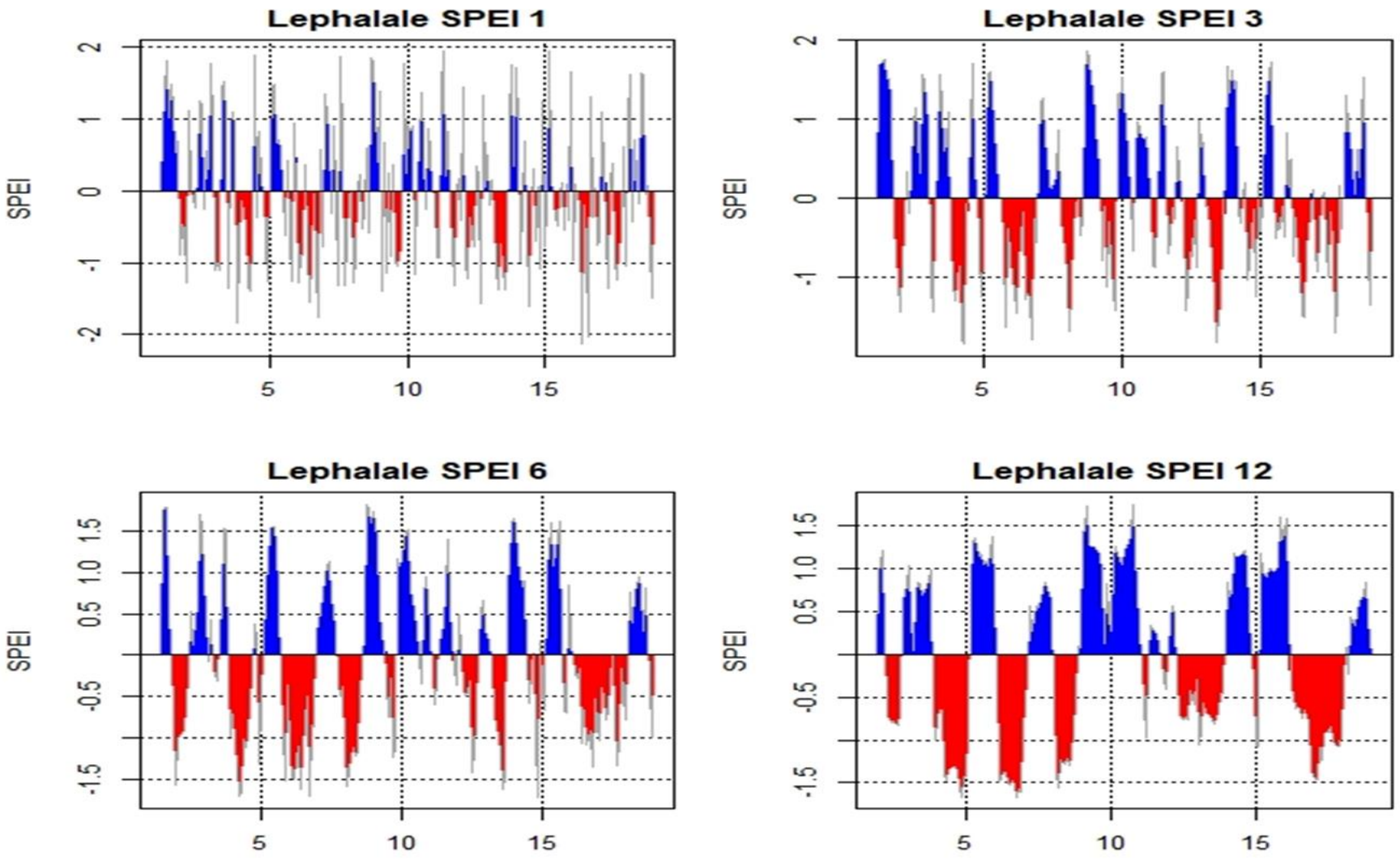

Figure 4.9: Lephalale Weather Station SPEI (SPEI 1, SPEI 3, SPEI 6 and SPEI 12)

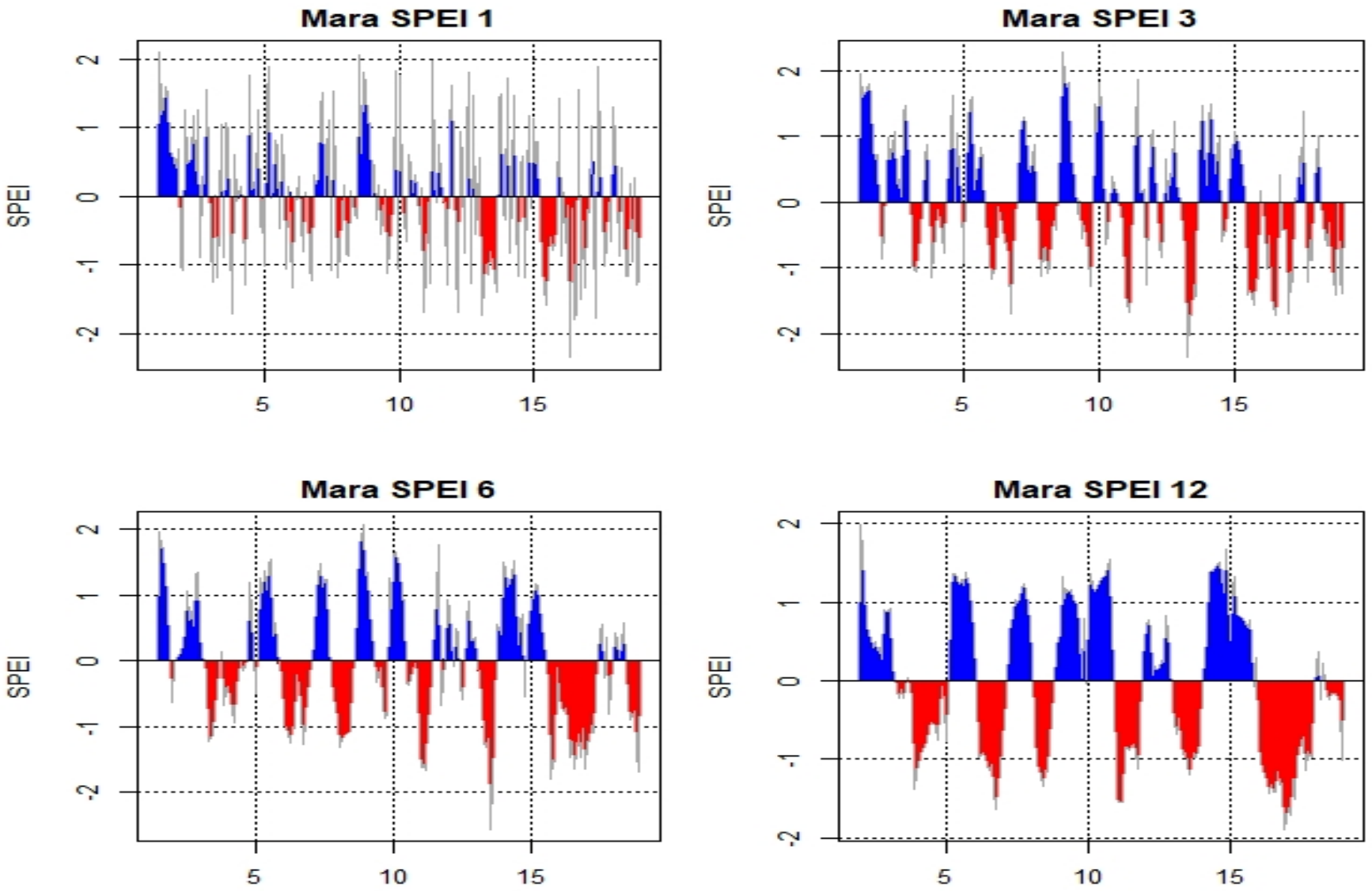

Figure 4.10: Mara Weather Station SPEI (SPEI 1, SPEI 3, SPEI 6 and SPEI 12)

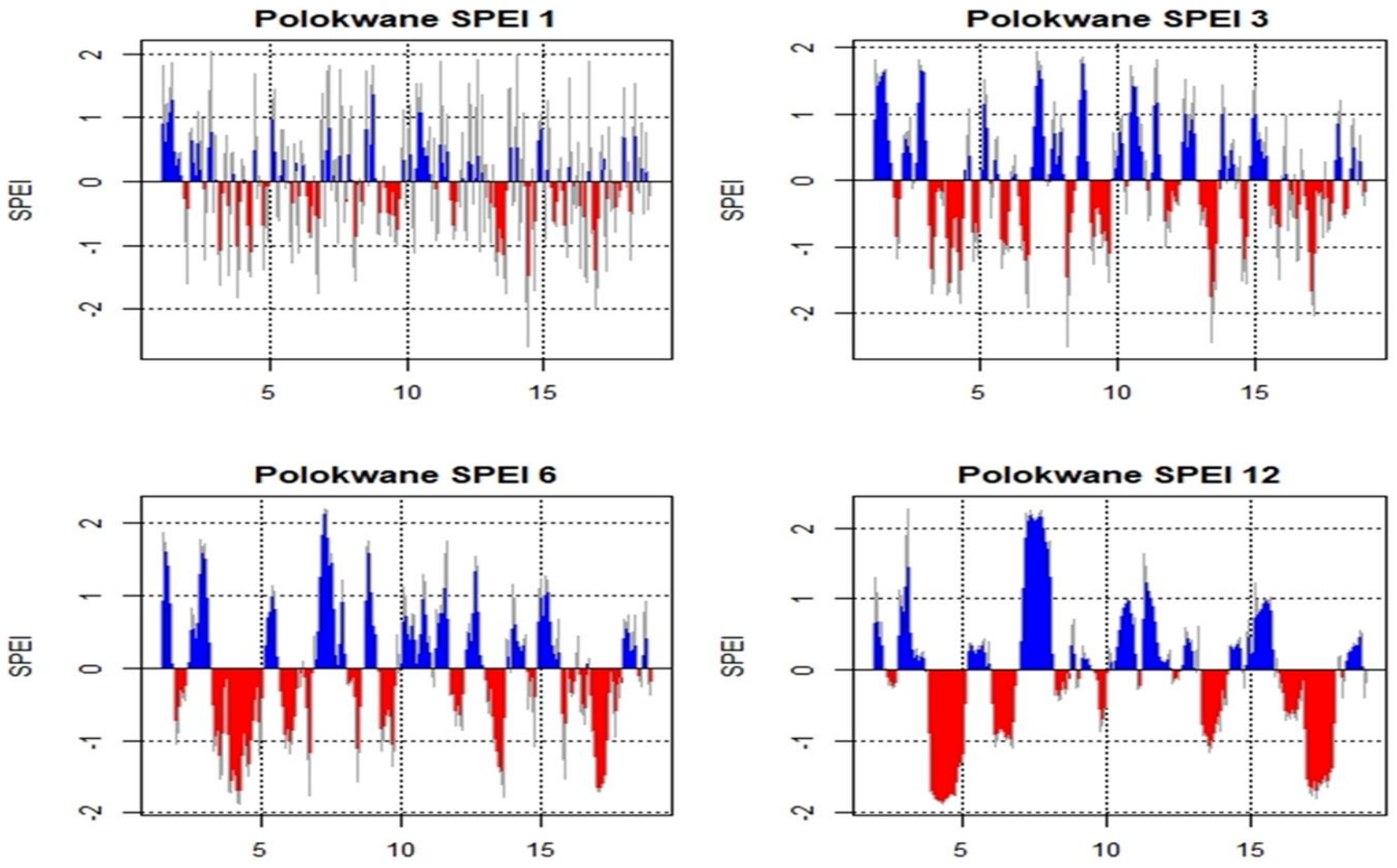

Figure 4.11: Polokwane Weather Station SPEI (SPEI 1, SPEI 3, SPEI 6 and SPEI 12)

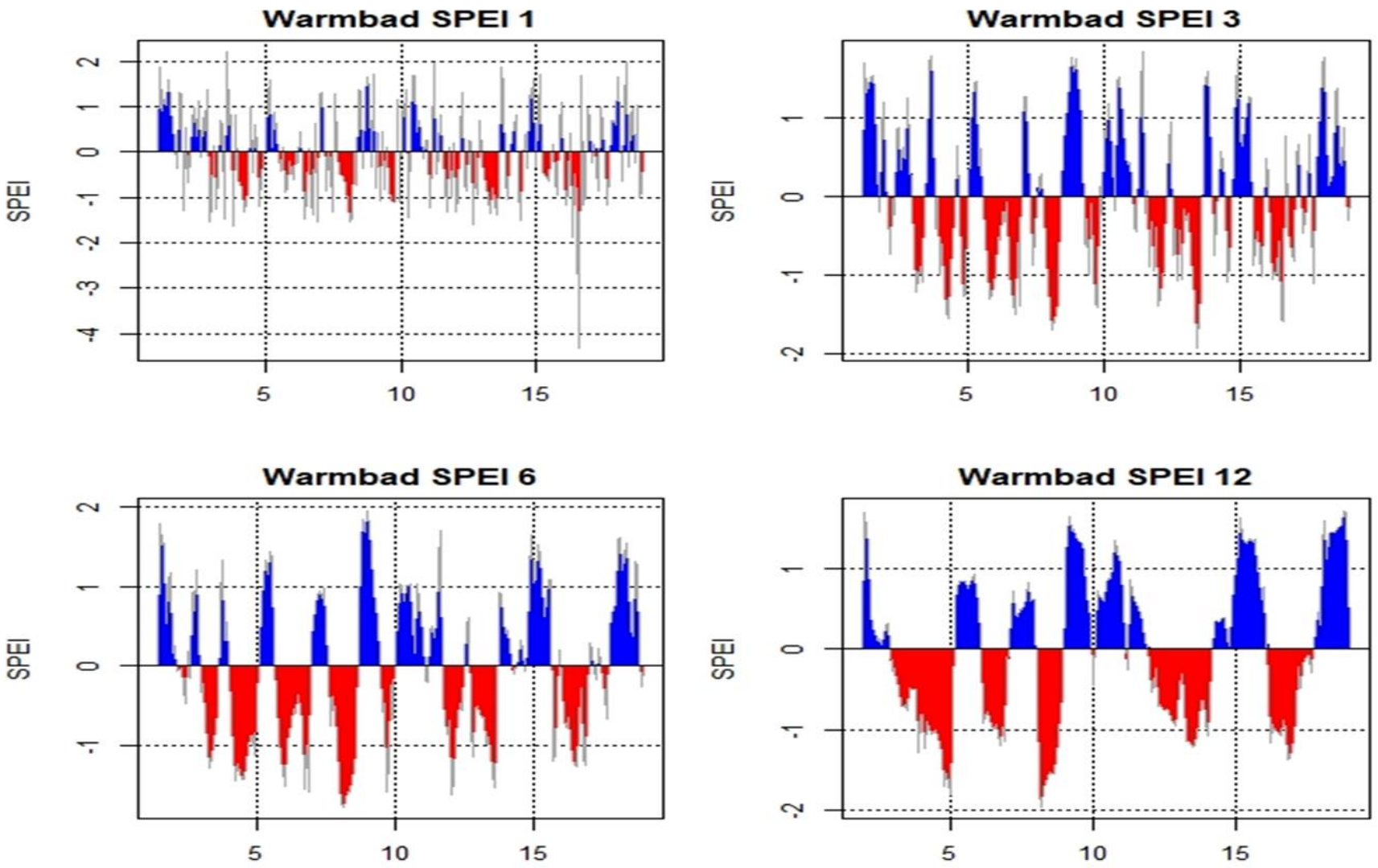

Figure 4.12: Warmbad Weather Station SPEI (SPEI 1, SPEI 3, SPEI 6 and SPEI 12)

- **Frequency of Extremes in Limpopo Province**

The climatic conditions over Limpopo Province are highly variable with rainfall starting in late October and peaking in January-February months, making it the wet season thus droughts and floods are also expected (Mpandeli, 2015). To characterise extreme weather events over Limpopo province, SPEI 6 was used to categorise floods and drought according to four different weather stations over Limpopo Province. To compose extreme frequency occurrence table over Limpopo province, all periods of extreme wet and dry conditions that fell in each category of SPEI were considered. Table 4.3 shows extreme weather frequency occurrence over Limpopo province for a period of 18 years. Due to climate variability over southern Africa, the study area is subjected to different climatic weather conditions (Chikoore, 2016).

The results show that Limpopo province experienced extremely wet conditions of 0.5% frequency over Lephalale and Warmbad stations meanwhile Mara and Polokwane frequency was 0.9% respectively. Mild seasons conditions such as wet or drought are frequent over the province, with occurrence frequency of above 30% over Lephalale, Mara, Warmbad, and Polokwane Stations (Table 4.3). Extreme and severe drought seasons are most frequent over Limpopo Province, with the province more vulnerable to extreme weather events (Tshiala *et al.*, 2011). The results show that the number of drought seasons is almost like the wet seasons (Table 4.3). Over the region, fine conditions or drought seasons are most likely associated with low precipitation trend meanwhile, wet conditions are noted during the high precipitation trend.

Table 4.3: Extreme weather frequency over Limpopo Province

Level	Extreme Weather Severity Category	Frequency Occurence (%)			
		Lephalale Station	Mara Station	Warmbad Station	Polokwane Station
≥ 2.0	Extremely Wet	0.5	0.9	0.5	0.9
1.5 to 1.99	Severely Wet	10.4	5.7	7.6	6.6
1.0 to 1.49	Moderately Wet	8.1	13.3	9	8.5
0 to 0.99	Mildly Wet	30.8	30.3	31.3	32.2
0 to -0.99	Mild Drought	31.3	31.8	35.1	35.5
-1.0 to -1.49	Moderate Drought	14.7	12.8	10.4	8.5
-1.5 to -1.9	Severe Drought	4.3	4.7	6.2	7.6
≤ -2.0	Extreme Drought	0	0.5	0	0

4.5 Correlation of GPCP Precipitation and Temperature with ENSO Southern Oscillation (El Niño and La Niña)

The fluctuation of sea surface temperature (SSTs) in the Pacific Ocean results in the occurrence of floods and droughts over Limpopo Province. Figure 4.13a displays the correlation of ONI and GPCP precipitation for the 2000-2017 period in Limpopo Province. ONI and GPCP precipitations show a negative correlation (r = -0.627) which is anticipated if the two variables are correlated, while negative degrees correspond to La Niña years and show that there is high variability between precipitation and ONI whilst positive degrees correspond to El Niño years, showing years of low rainfall. In general, the correlation between ONI and GPCP precipitation implies that an increase in the sea surface temperatures anomalies is associated with a decline precipitation anomaly. During the period of 2015/16, SST was over 2.5 leading to a decline in precipitation pattern to below 40mm/month.

From the correlation, ENSO cycles dominated by El Niño (Positive phase) were associated with more areas affected by below-average precipitation (meteorological drought) meanwhile negative phases (La Niña) are most likely to be associated with the area affected by above-average precipitation (floods) events. Table 3.1 shows years of El Niño (2002/03, 2004/05, 2006/07, 2009/10, 2014/15, and 2015/16) and La Niña (1999/00, 2000/01, 2005/06, 2007/08, 2008/09, 2010/11, 2011/12, and 2016/17).

ONI and GPCP precipitation correlation show that ENSO cycles coincide with the summer rainfall season and the two variables are inversely correlated over southern Africa (Figure 4.13a). The correlations identify the relationship between ENSO cycles and GPCP precipitation, with La Niña episodes associated with above-average precipitation as a decline in SST anomalies, result in an increased rainfall anomaly and El Niño episodes associated with bellow average precipitation. Figure 4.13a features period of wet years 1999/00 (218 mm/month), 2005/06 (136 mm/month), and dry years 2015/16 (50 mm/month), and 2002/03 (55 mm/month).

Correlation of the Southern Oscillation Index (SOI) and GPCP precipitation (Figure 4.13b) shows a positive correlation coefficient and the findings from ONI and GPCP precipitation correlation in the region. SOI and GPCP precipitation show a positive correlation (r = 0.428) which is anticipated if two variables are positively correlated, with positive degrees correlating with wet years (La Niña) and negative degrees correspond to dry years (El Niño). The correlation between SOI and GPCP precipitation implies that, an increase in the SLP anomalies and lead on an increase in GPCP precipitation anomalies. From the correlation, ENSO cycles dominated by Positive phase (Wet

years) were associated with more areas affected by above-average precipitation (floods) meanwhile negative phase (Dry years) are most likely to be associated with the area affected by below-average precipitation (drought) events. Figure 4.13b features wet years 1999/00 (7.8 mm/day), 2005/06 (5 mm/day), and dry years 2015/16 (1.5 mm/day), and 2002/03 (2 mm/day.

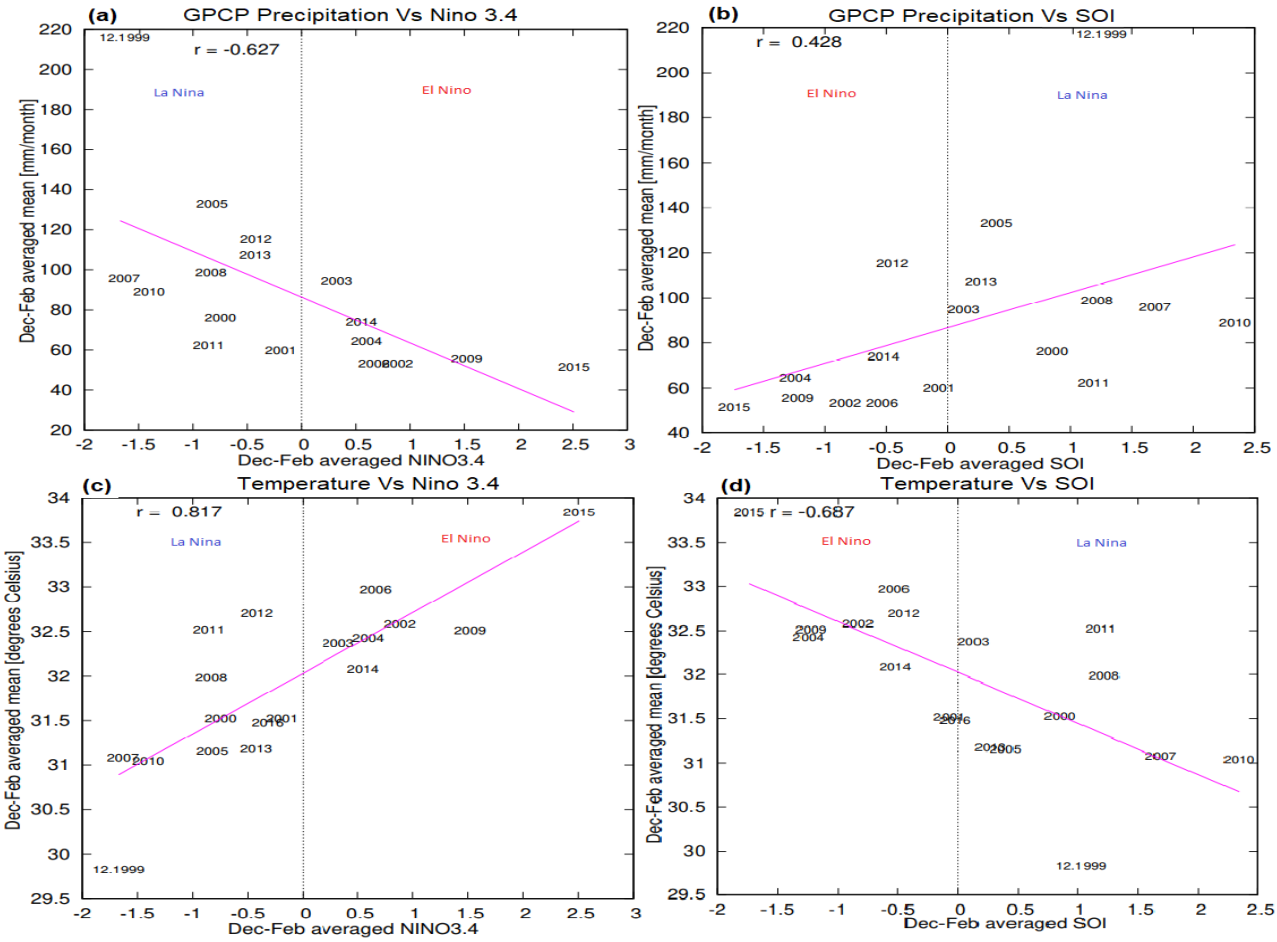

Figure 4.13: ONI/SOI vs GPCP Precipitation and ONI/SOI vs Temperature correlation in Limpopo Province

The correlation of ONI and temperature (Figure 4.13c) and SOI and temperature (Figure 4.13d) shows the relation between dry years and wet years with temperature. Temperature and ONI/SOI correlation shows the link between El Niño and La Niña episodes with temperature. The correlation shows that La Niña years were associated with lower temperature whilst El Niño years were associated with high temperature. Thus, during the period of high SST anomalies, an increase in temperatures is also observed. Whilst during the period of anomalously high low temperatures are observed. Figure 4.13c and Figure 4.13d show that the year 2014/15 was the

hottest year with a maximum temperature of about 33.8 °C, while 1999/00 was the year recorded the lowest temperature of about 29.8°C the period.

4.6 GPCP Precipitation Composite (Summer) of La Niña and El Niño Events

Based on the Niño 3.4 SST index and Southern Oscillation Index (SOI) observed, a composite of El Niño events and La Niña events over southern Africa region is constructed using GPCP precipitation by selecting years with Sea Surface Temperature (SST) index that exceeds 0.5 (less than -0.5) or SLP with +1 (less than -1) with SOI. Figure 4.14a and 4.14b displays the observed composite for the period 2000-2017 and is an average of 6 El Niño events and 8 La Niña events. Figure 2.7 and Figure 2.8 displaying the temporal evolution of the difference between El Niño composite and La Niña composite during the summer season (DJF).

The La Niña composite was based on the selection of years for which the SOI exceeds +1 or ONI less than -0.5 minus years with -1 or +0.5 ONI during the summer season (DJF) for 2000-2017 period. Similarly, the El Niño composite was based on the selection of years for which the SOI was less than -1 or exceeds +0.5 with ONI during summer (DJF) for the period 2000-2017. In the ENSO composite, Figure 4.14a illustrates the La Niña composites (Cool) which were extracted from El Niño (Warm) composites to illustrate the difference between El Niño and La Niña events. The ENSO composites illustrate high variability between El Niño (Dry years) and La Niña (Wet years) events, indicating that the area is highly vulnerable to extreme weather events.

The composite presents the GPCP precipitation for the wet years that were selected from Niño 3.4 and SOI to display the condition during high rainfall in DJF summer season (Figure 2.7 and Figure 2.8). During the wet periods (La Niña) in DJF, the region indicates extreme wet conditions with the western part receiving less rainfall (0.6) and the eastern part receiving much of the rainfall of about 1.2mm/day. Figure 4.14a and Figure 4.14b show that the ENSO cycle corresponds with the summer rainfall of the southern Africa region. The ENSO composite suggests that the Limpopo region is vulnerable to floods events, with the region receiving a positive departure from 1.2mm/day to 1.4mm/day.

Similarly, to Figure 4.14a, Figure 4.14b illustrate anomalous dry years (El Niño) composites using GPCP precipitation for the years selected from ONI and SOI to display summer month (DJF) during dry years. During dry years composite, a strong negative departure of rainfall over the Limpopo region with values ranging between -0.8mm/day to -1.4mm/day were observed. From

the dry years composite, it appears that the eastern part receives the least mean rainfall with the lowest negative departure than the western part. From the ENSO composites, it appears that Limpopo province is prone to extreme events which are droughts and floods. The region can be dry to the extent of negative departure of about -1.4 and receive the highest rainfall anomalies with a positive departure of about 1.2.

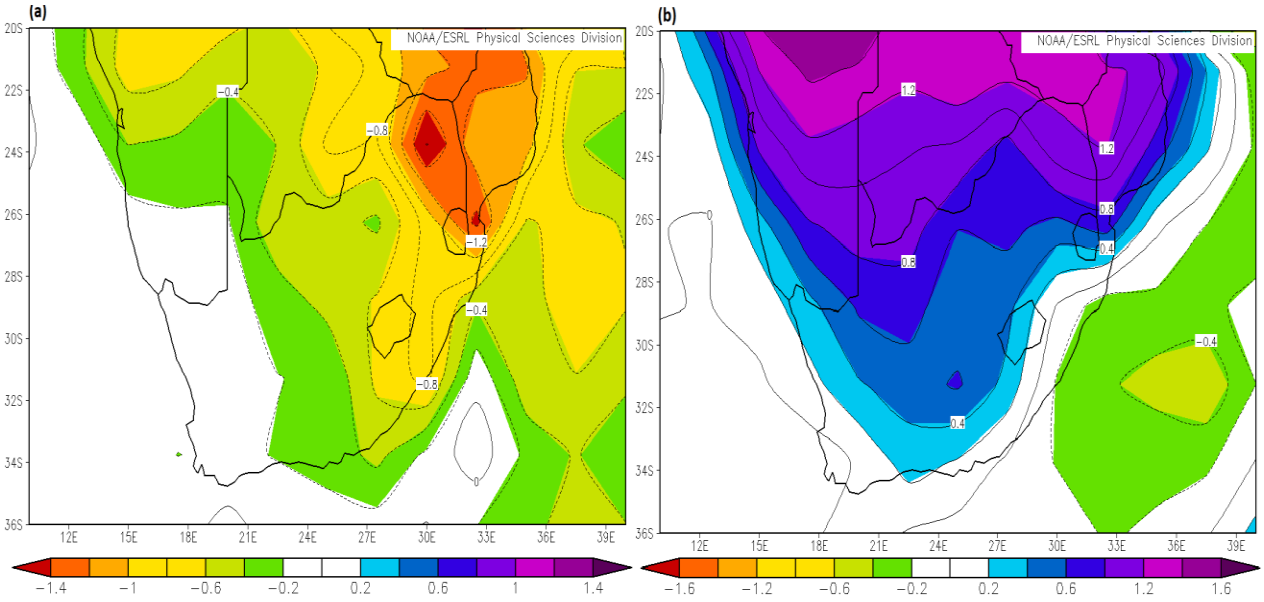

Figure 4.14 a+b: Composite mean GPCP precipitation anomaly (mm/day) for summer (December-February), for strongest events 2000-2017 for southern Africa during drought (a) and wet years (b)

4.7 Case Studies of extreme events over Limpopo Province

Case studies were considered for extreme events i.e. wet years with copious heavy rainfall and droughts that have brought a devastating impact in Limpopo Provinces. The cases investigate various variable and their influence on extreme cases in Limpopo Province. Variables considered for the study include GPCP precipitation, geopotential height, outgoing longwave radiation, maximum temperature, and vector winds.

4.7.1 Case 1: 1999/2000 DJF over Limpopo Province

The case investigates the anomalous heavy rainfall over Southeast Africa that resulted in devastating impacts in Limpopo Province during the summer season DJF of 1999/00. The extremely heavy rainfall was created by the succession of tropical cyclones (Chikoore *et al.*, 2015), producing copious rainfall and lasted for several days. The 2000 TCs season was active

with several landfalls affecting southern Africa. This includes the TC Eline which formed in February and traversed over southern Africa bringing flooding to the Limpopo River Valley (Dyson & van Heerden, 2001; Reason & Kiebel, 2004; Chikoore *et al.*, 2015).

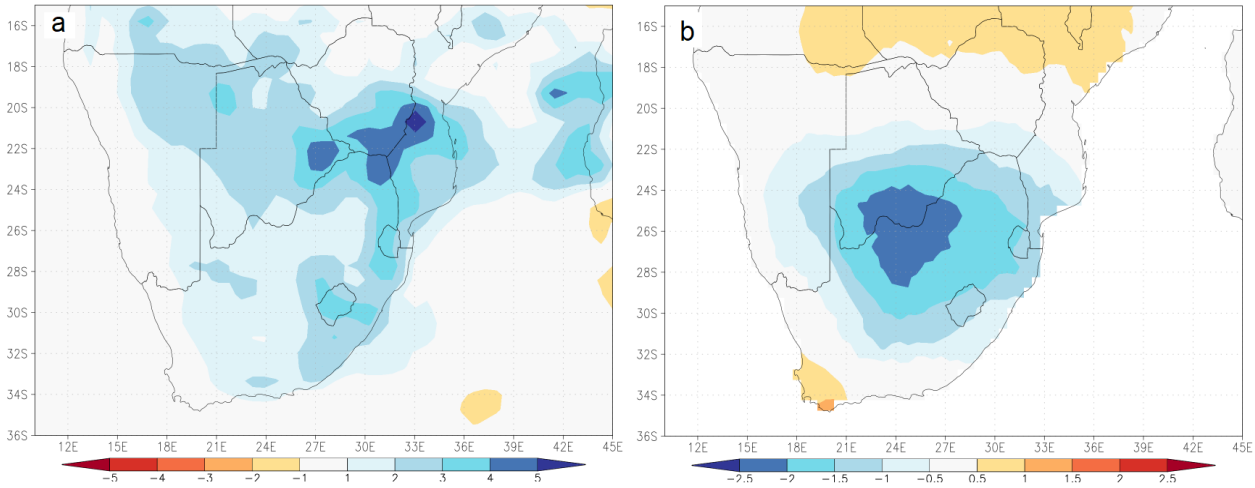

Figure 4.15a+b: Summer (DJF) rainfall (a) and maximum temperature (b) over southern Africa during 1999/00 wet condition.

The anomalous wet season in 1999/00 was influenced by the La Niña episode which was categorized as strong with the intensity value of about -1.5mm/day that peaked in December-January-February 1999 (Figure 2.7 and Figure 2.8). The condition started in July-August-September 1999. The event was influenced by the tropical cyclone Eline formed in the South West Indian Ocean and traversed southern Africa, bringing devastating impacts to the region (Reason, 2004 & Chikoore *et al.*, 2015). The TC Eline propagated on the north of South Africa and Zimbabwe resulting in copious heavy rainfall over the interior part.

Deep convection that has persisted over Limpopo Province in this period, has resulted in heavy rainfall (flood conditions) >4mm/day (Figure 4,14a). The resultant of the heavy rainfall is more TCs making landfall in 2000 (Reason, 2004 & Chikoore *et al.*, 2015), influencing the heavy rainfall received over Limpopo Province. Due to heavy rainfall, below normal geopotential height >-9 (Figure 4.19a), indicating enhanced convection. The strong negative anomaly of OLR was observed with values ranging between -15 to -20 meaning the amount of radiation reduced by cloud cover which is associated with wet seasons (Figure 5.20a). During this period, negative values of OLR, as well as geopotential height (Figure 4.19a), were observed in the northern part of southern Africa, covering largely Limpopo Province. The weather conditions and weather systems during the period were related to La Niña. Vector winds played an important role in

triggering flooding in southern Africa by transporting moisture inland, making heavy rainfall (Tyson & Preston, 2000; Chikoore, 2016).

4.7.2 Case 2: 2002/2003 DJF over Limpopo Province

During 2002/03 summer, negative precipitation departures over Limpopo Province were observed, indicating low rainfall conditions or drought. The regions' fine condition or drought is influenced by El Niño's condition impacting east of southern Africa, including Limpopo province (Figure 2.7 and Figure 2.8). The El Niño 2002/03 was categorised as moderate with an intensity value of about 1.3 that have peaked in October-November-December 2002. The condition started in June-July-August 2002 and lasted for a period of 10 months. The event follows a neutral condition with values close to -0.3.

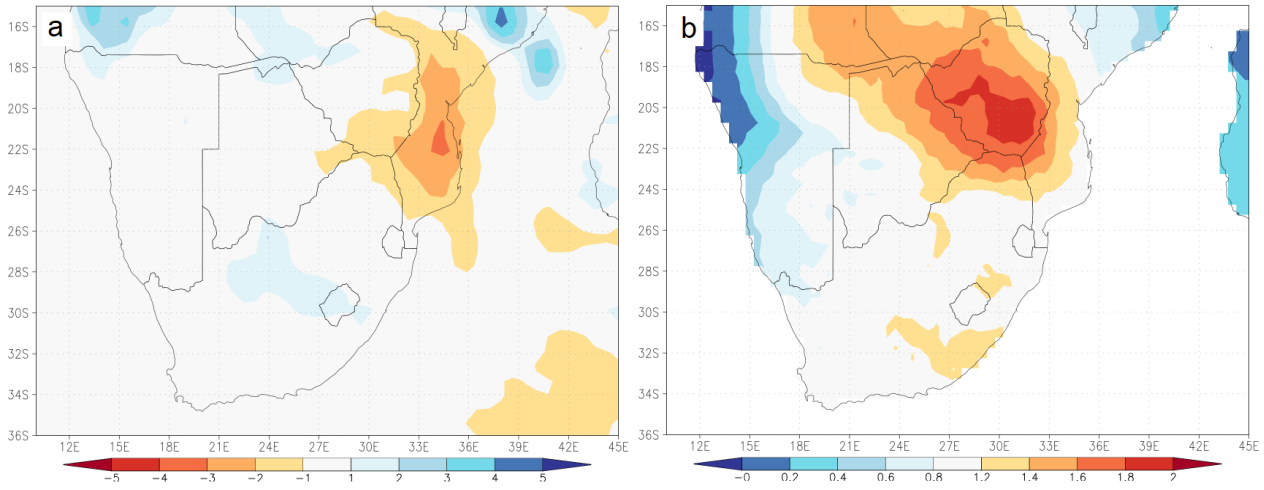

Figure 4.16 a+b: Summer (DJF) rainfall (a) and maximum temperature (b) over Southern Africa during the 2002/03 drought condition.

The composite mean displaying a strong positive summer geopotential height in meter at 500 hPa over Limpopo Province (Figure 4.19 (b)). Positive geopotential heights are characterised with drought conditions and warmer atmospheres (Chikoore, 2016). Strong positive geopotential anomalies are found in the middle of southern Africa, with anomalies values ranging between +3 to +6; Same with geopotential height, positive OLR indicates drought conditions. In 2002/03, the composite anomalies of OLR for drought season displayed a strong positive OLR > 8 Wm^{-2} (Figure 4.20b). The 2002/03 drought condition affected the southeast side of southern Africa.

Strong positive maximum temperature (Figure 4.16b) over the northern part of southern Africa, has been found to have a strong relationship with the occurrence of drought in southern Africa (Chikoore, 2016). The positive maximum temperature was observed during 2002/03 from

December to February. The wind vector anomaly of the 2002/03 summer (DJF) drought period shows the westerly vector wind anomaly over southern Africa, bringing greater impacts on the eastern part (Figure 4.21b). ENSO-induced drought conditions in southern Africa is associated with the westerly wind vector anomaly (Chikoore, 2016). Based on Figure 2.7 and Figure 2.8, the case of the 2002/03 drought condition shows that it's an ENSO-induced drought condition.

4.7.3 Case 3: 2005/2006 DJF over Limpopo Province

During this case, heavy rainfall and severe storms were experienced over southern Africa (Figure 4.17a), resulting in floods conditions in some parts of the region including Limpopo Province. La Niña for 2005/06 was categorised as weak with an intensity value of about -0.8 anomaly that has peaked in December-January-February 2005 (Figure 2.7 and Figure 2.8). The condition started in November-December-January 2005 and lasted for a period of 5 months.

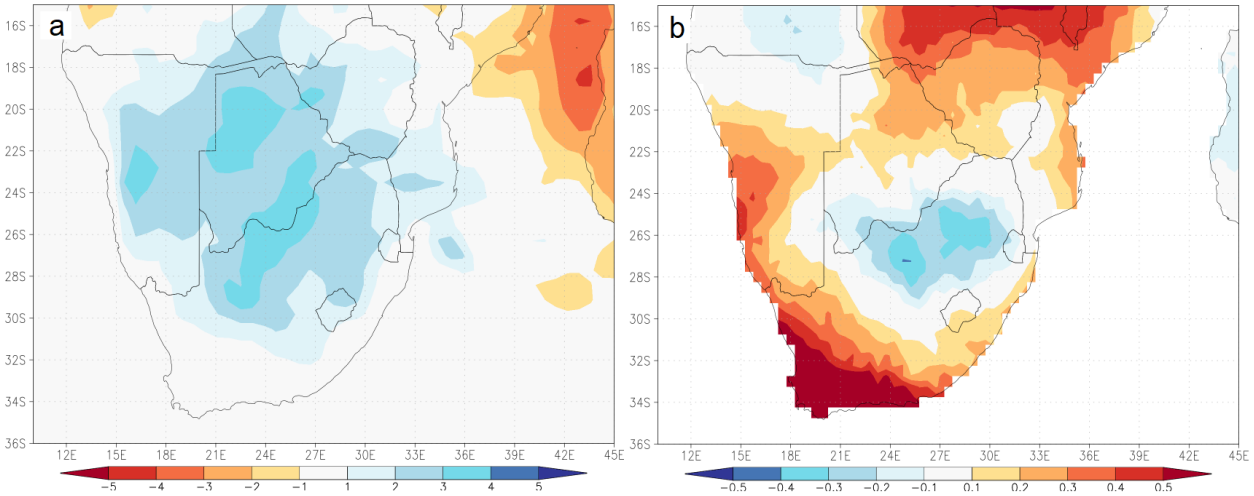

Figure 4.17 a+b: Summer (DJF) rainfall (a) and maximum temperature (b) over Southern Africa during 2005/06 wet condition.

Figure 4.17(a) shows GPCP precipitation of summer rainfall over southern Africa including Limpopo Province, during 2005/06 floods. The absolute rainfall rate over the region is between 1 mm/day to 3 mm/day. The composite mean of geopotential height shows a negative anomaly in the western part of southern Africa between -2 to -4 (Figure 4.19c). Negative geopotential height is associated with a cooler temperature and usually characterised with heavy rainfalls (Chikoore, 2016). During the 2002/03 flood period (DJF), the region experienced negative temperature anomalies with absolute values ranging between (-0.1 to -0.4) over the interior (Figure 4.17b).

The strong negative anomaly of OLR in the interior (<-12 Wm^{-2}; Figure 4.20c) is associated with floods season in southern Africa. Low OLR indicates the presence of clouds and precipitation while high OLR (Figure 4.20c) indicates deep convection clouds in the upper level. During the heavy rainfall in southern Africa including Limpopo Province, the region was dominated by negative OLR. The heavy rainfall during 2005/06 was associated with easterly wind vector anomaly, which had a significant role in transporting moisture which results in heavy rainfall leading to flooding (Figure 4.21c). Figure 4.21c displays a vector wind anomaly at 500 hPa levels from December to February.

4.7.4 Case 4: 2015/2016 DJF over Limpopo Province

During the 2015/16 summer (DJF) extreme negative GPCP precipitation departures (-0.5 mm/day to -2.5 mm/day) was observed in southern Africa, resulting in the region experiencing the worst prolonged drought since 1991/92 extreme drought impacting the whole region including Limpopo province (Baudion, 2017). Figure 4.18 (a) illustrates the absolute amount of rainfall received between December 2015 and February 2016 in southern Africa. During this period, rainfall was below -1.5 mm/day across the northeast of South Africa including Limpopo Province, Mozambique, and Zimbabwe. Figure 4.18a highlights that the 2015/16 season was the driest in the past 17 years.

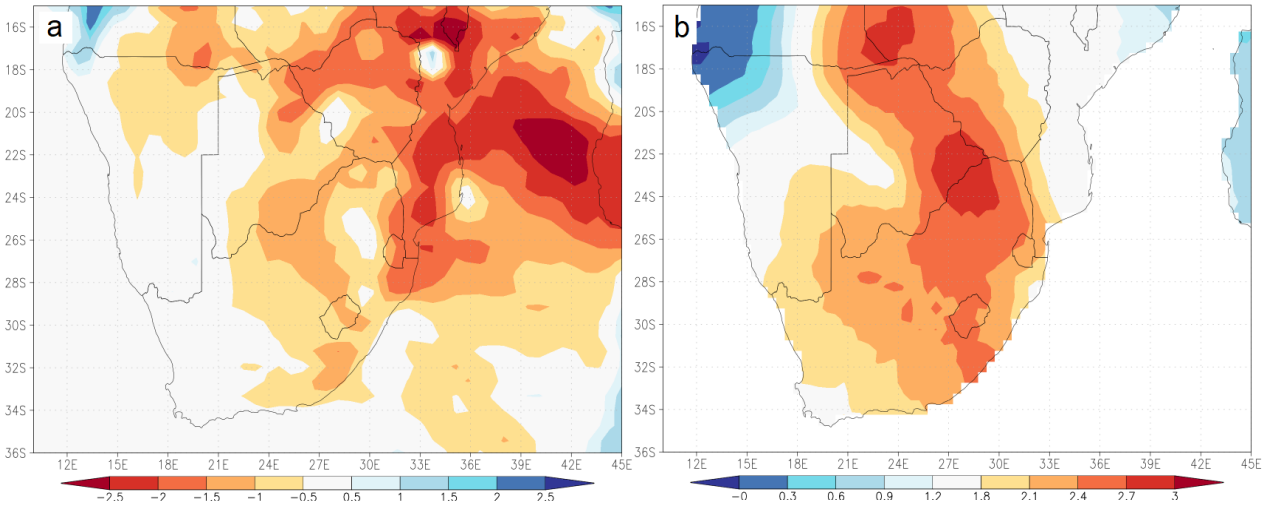

Figure 4.18 a+b: Summer (DJF) rainfall (a) and maximum temperature (b) over Southern Africa during the 2015/16 drought condition.

The severe drought condition related to a strong El Niño 2015/16 events across southern Africa peaked at 2.6 in November-December-January (Figure 2.7 and Figure 2.8). The El Niño event prior to 2015/16 drought conditions follows weak 2014/15 El Niño events. El Niño 2014/15 and 2015/16 were the two most prolonged drought periods and consecutive warmings events that

have influenced the climate over southern Africa for a period of 27 months without interruption during the time frame 2000-2017 (Figure 2.7 and Figure 2.8). This resulted in higher than normal temperatures and longer fine or dry season than in the past 17 years in the southern Africa region.

The composite mean displaying strong positive geopotential height in the meter at 500 hPa over southern Africa (Figure 4.21d), with the region dominated by positive geopotential heights which are characterised with drought conditions and warmer atmospheres (Chikoore, 2016). A positive geopotential height was observed in southern Africa from December 2015 to February 2016. During the period, the region experienced very warm temperatures ranging from 1.8 to 3 across southern Africa (Figure 4.18b).

In 2015/16, high OLR was observed over the north east of South Africa i.e. Limpopo Province (Figure 4.20d). High OLR indicates the absence of deep cloud in the upper level, resulting in fine or dry conditions. The region is dominated by positive OLR from 0 to 6. Figure 4.21d shows vector wind blowing from west to the east transporting the moisture offshore from December 2015 to February 2016. During the season of dry or fine condition, an El Niño was identified (Figure 2.7 and Figure 2.8).

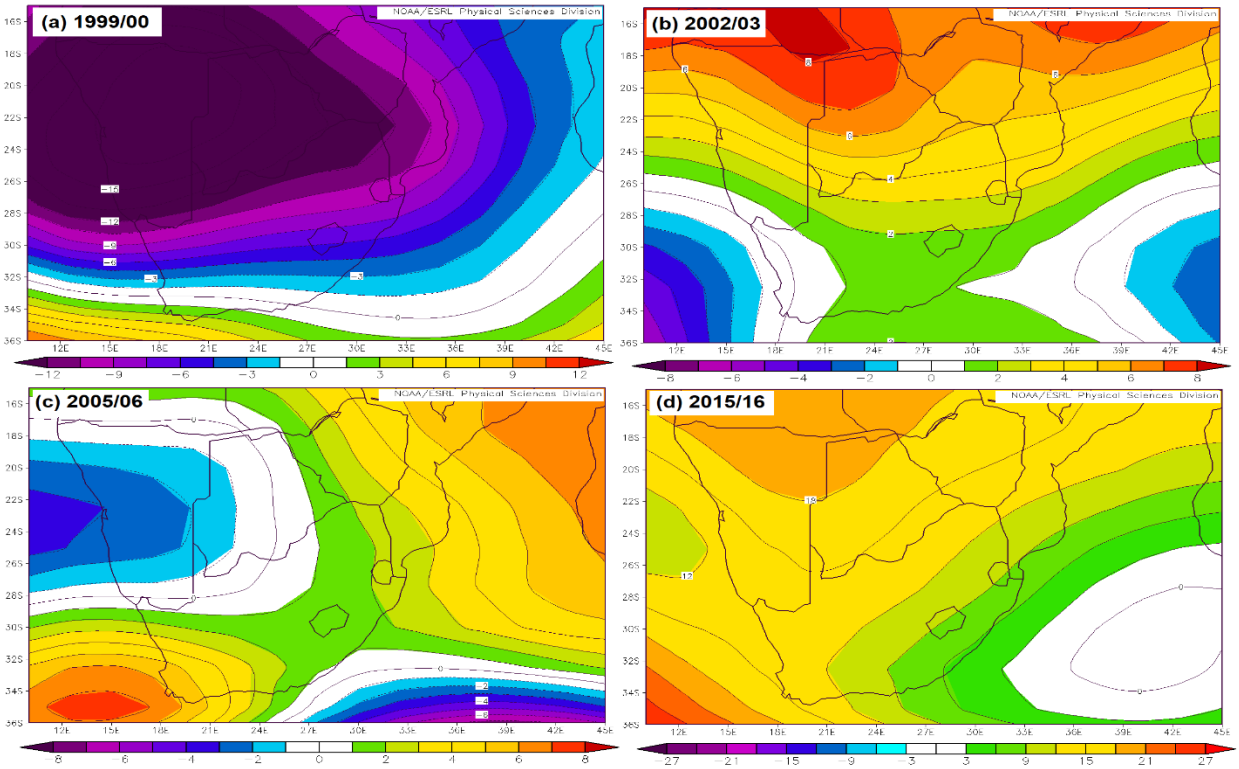

Figure 4.19: Mean composite of summer (DJF) geopotential height at 500-hPa over Southern Africa, during extreme weather events.

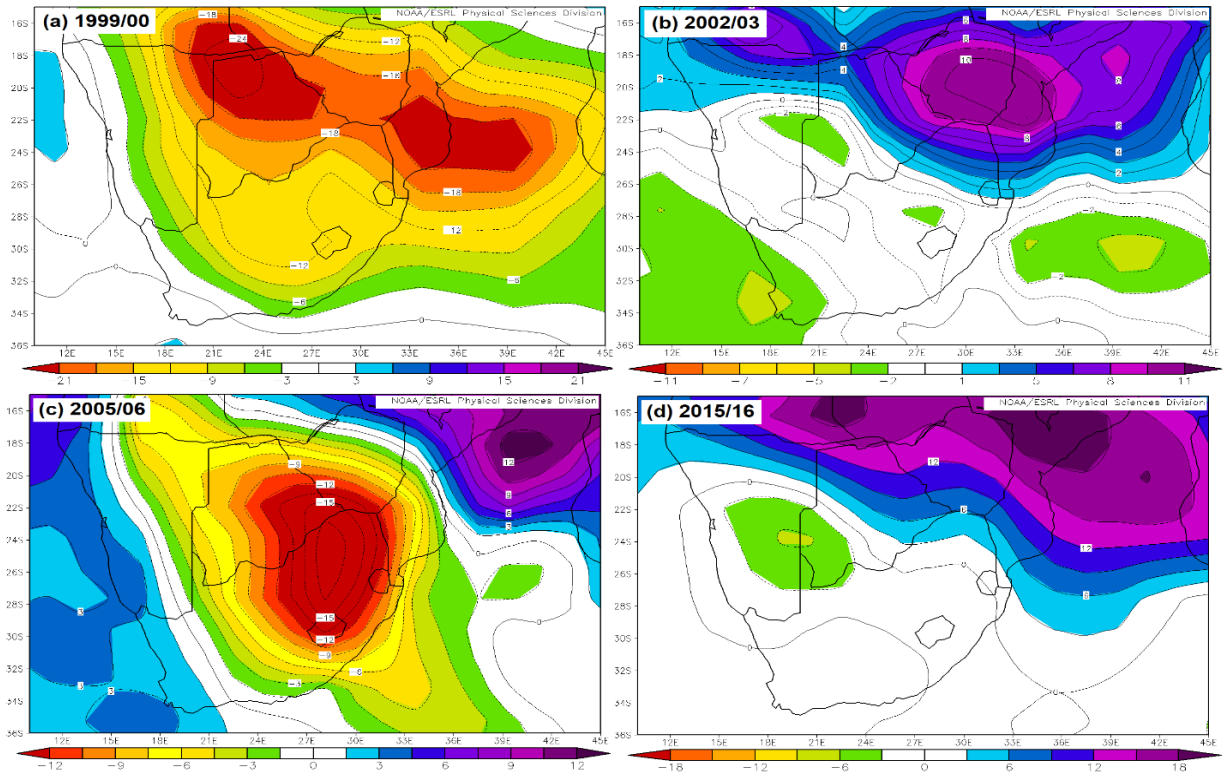

Figure 4.20: Mean composite of summer (DJF) OLR at 200-hPa over Southern Africa, during extreme weather events.

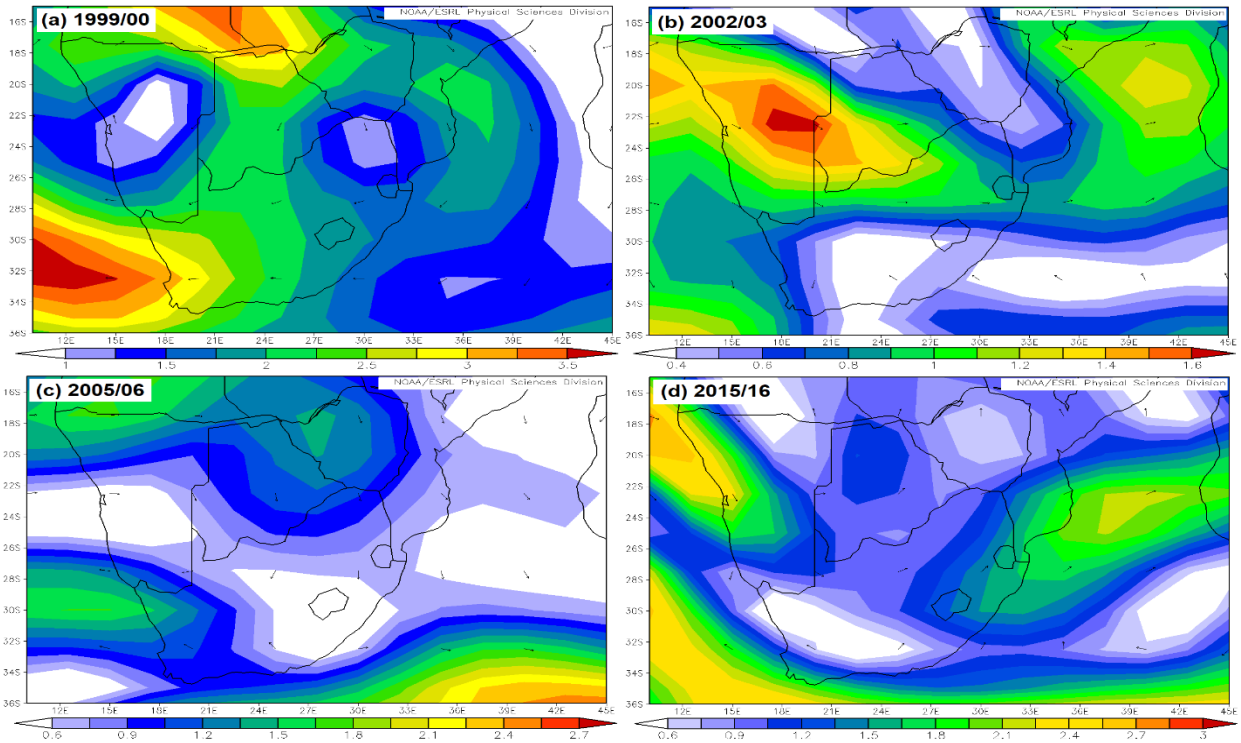

Figure 4.21: Composite mean of summer (DJF) vector winds 500-hPa over Southern Africa, during extreme weather events.

4.8 Summary

In this section, the spatial and temporal variation of climate condition over Limpopo Province were investigated. Over the region, extreme weather events are distinct and recurring features. The precipitation and temperature over Limpopo Province for a period of 17 years were displayed and interpreted. The region receives most of its rainfall during the austral summer and is associated with a cool temperature, with rainfall, reach its peak from December, January, and February. Most of the droughts and wet conditions over the region are from mild to extremes in frequency. Copious heavy rainfall over the region occurred in the first period of the study influenced by TCs whereas prolonged dry season occurred during the summer season of 2003, 2007, and the successive dry period of 2014/15 and 2015/16 seasons. From the section, it is revealed that El Niño and La Nina have a direct relationship with precipitation and temperature over Limpopo Province.

CHAPTER 5: VEGETATION CHANGE, RESPONSE, AND SENSITIVITY TO EXTREME WEATHER EVENTS

5.1 Introduction

This chapter highlights the complex nature of extreme weather events i.e. meteorological drought and floods, and the impacts they present for early warning and effective monitoring. Satellite remote sensing offers a unique way of monitoring drought and floods activities because it provides synoptic, repeat coverage of spatially continuous spectral measurements collected (Hua *et al.*, 2019). The Moderate Resolution Imaging Spectroradiometer (MODIS) satellite data were used to characterise changes in the vegetation over time. Limpopo Province is a region sensitive to climate change due to its vulnerability to extreme weather events (Tshiala *et al*., 2011). Vegetation sensitivity can be measured through the response of vegetation patterns to climate variability in this region. Time series analysis of Normalised Difference Vegetation Index, Enhanced Vegetation Index and Land Surface Water Index imagery are effective tools to study the land cover changes and vegetation response to climatic variations.

Vegetation Index (VI) provides information which is primarily related to vegetation health, that enables a more comprehensive view of extreme weather condition such as meteorological drought and floods (Huete *et al.*, 2002). Vegetation product (MODIS/Terra vegetation Indices, MOD13Q1, version-6) and land cover product (MCD12Q1, version-6, Terra), was downloaded from Level-1 and Atmosphere Archive and Distribution System (LAADS) Distributed Active Archive Center (DAAC) from the tile (h20 v11). MOD13Q1 data is provided after every 16 days at 250-meter spatial resolution since February 2000, whilst MCD12Q1data is an annual data at 500-meter spatial resolution since 2001. Raster calculator is used for pre-processing MOD13Q1 data (NDVI and EVI) with a scale factor of 0.0001.

5.2 Land cover extent and rate of change over Limpopo Province

The MODIS MCD12Q1 Terra was used to display land use/ land covers over Limpopo Province from 2001 to 2017. The satellite helped with the identification of Land Use and Land Cover (LULC) for the region. Land cover is a fundamental variable required when studying the ecological and morphological changes occurring in the environment and earth's ecosystems (Congalton, *et al*., 2014). The MODIS MCD12Q1 land cover product is produced using the supervised classification of the reflectance data. The MCD12Q1 International Geosphere-Biosphere Program (IGBP) classification which classifies each land cover into 17 classes at 500 m and has been reported to have overall land cover classification accuracy of 75% (Friedl *et al.*, 2010) was used. The

MCD12Q1 500 m IGBP supervised classification were followed by Land Cover Type QC data layer to assess and select good training class and of high confidence.

5.2.1 Extent and distribution of Land Cover over Limpopo Province

The chapter provides the extent and spatial distribution of land covers over Limpopo Province for 2001, 2010, and 2017. The MODIS MCD12Q1 supervised classification of the International Geosphere-Biosphere Program (IGBP) identifies 17 (Table 5.2) land cover classes (0-16) which include 11 natural vegetation classes, 3 developed and mosaicked land classes and three non-vegetated land classes (Friedl *et al.*, 2010). From the established land covers, urban/ built-up land is difficult to classify reliably, due to a variety of land cover types and land uses that can also be mixed spatially even at Landsat 30 m scale (Lu *et al.*, 2008; Griffiths *et al*, 2010).

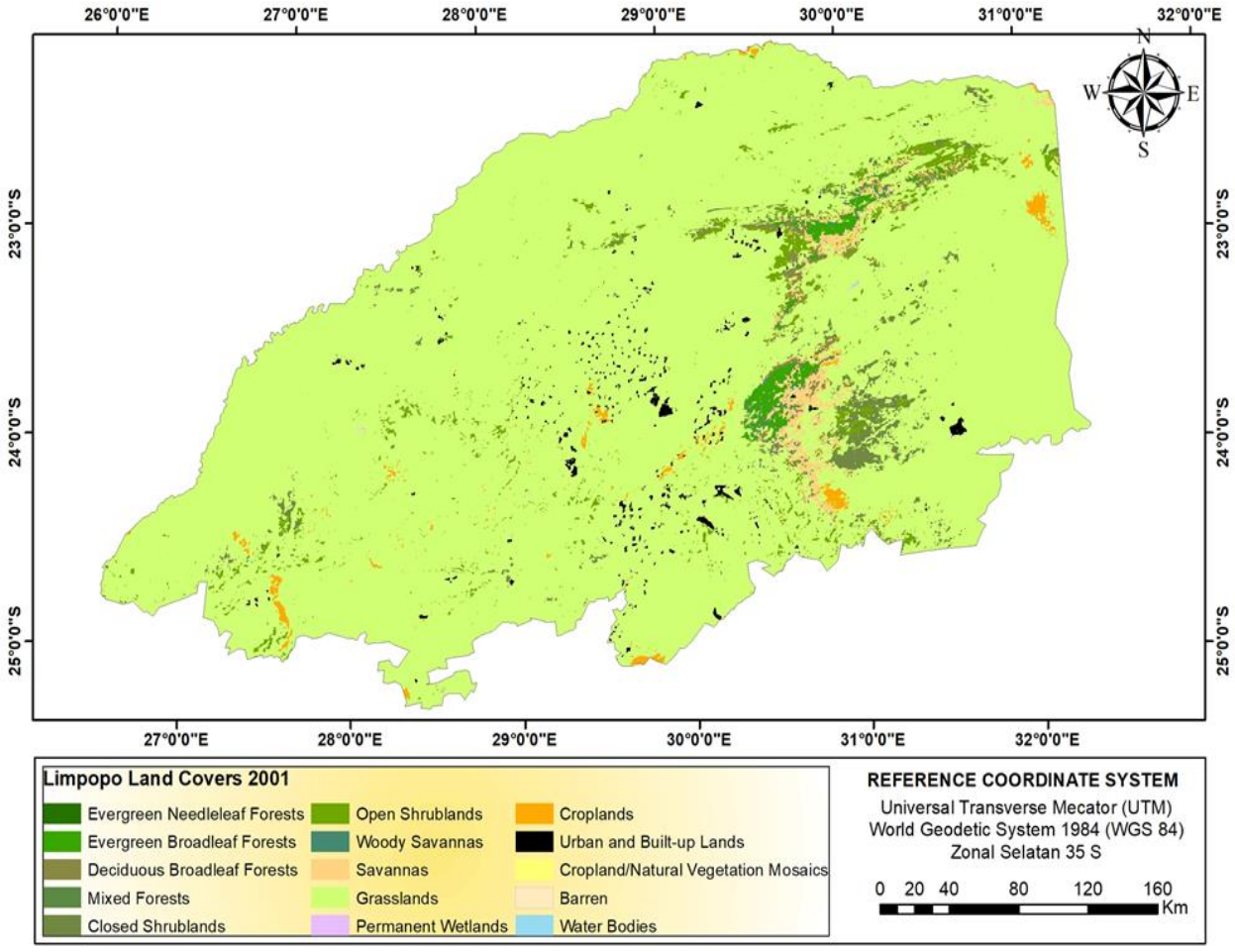

Figure 5.1: Map showing 2001 annual IGBP vegetation land covers over Limpopo Province, South Africa

The MCD12Q1 IGBP classification at 500 m spatial resolution is used to show the land cover classes over Limpopo Province. Figure 5.1 shows the annual IGBP land cover classification map

dated 2001. Figure 5.1, Figure 5.2 and Figure 5.3 provide distributions about land cover classes over Limpopo Province. The region is composed of arid and semi-arid climatic conditions (Mpandeli, *et al*., 2015), with growth of vegetation in arid and semi-arid areas which depends on the topography and rainfall (WenBin *et al*., 2011). When describing the spatial distribution of annual rainfall over Limpopo Province (Figure 1.4), it shows a significant variation of rainfall due to the escarpment i.e. Soutpansberg mountain (Chikoore, 2016). Figure 1.3 is the topographic map of Limpopo Province. The terrain affects the distribution of warm and moist air onshore, therefore making the precipitation distribution very uneven, which affects vegetation distribution (WenBin., *et al.*, 2011). Across the province, dense vegetation cover such as Evergreen Needleleaf Forests, Evergreen Broadleaf Forests, Deciduous Broadleaf Forests, and Mixed forests are located along the area of high elevation, with grassland and another small vegetation cover at a lower elevation.

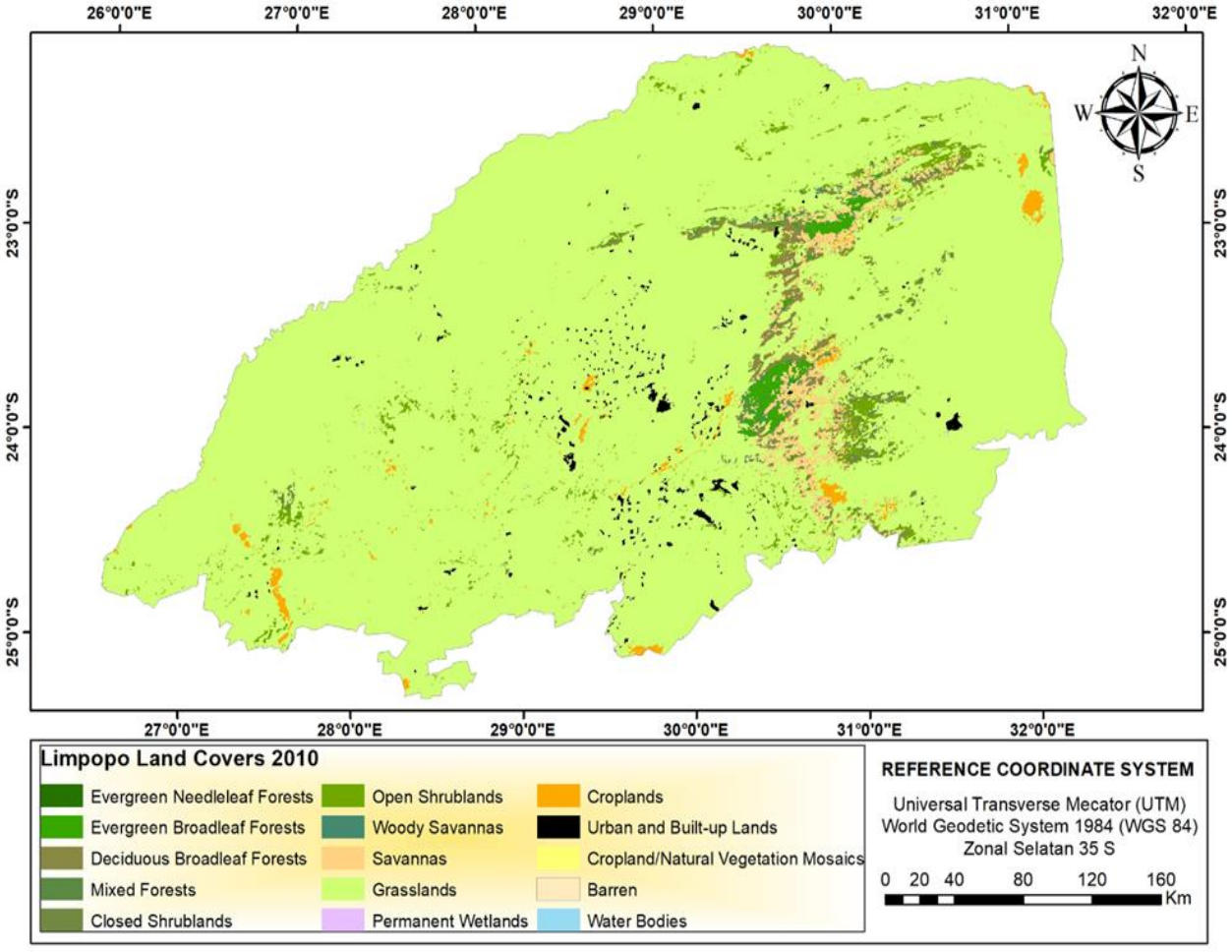

Figure 5.2: Map showing 2010 annual IGBP vegetation land covers over Limpopo Province, South Africa

The northwest of the province is composed of the low elevation, where the altitude ranges between 0-8% above the ocean level. Among these lower terrains, the major land cover class i.e. grassland land covers and occupies an area of about 110546 km^2. The far eastern part with altitude ranges from 25%, the area is dominated by dense vegetation covers such as Evergreen Needleleaf Forests, Evergreen Broadleaf Forests, Deciduous Broadleaf Forests, and Mixed forests respectively. Therefore, there is a spatial variation of the annual vegetation condition distribution (Figure 1.2) over Limpopo Province, with more intense vegetation conditions over the eastern part and low to poor vegetation conditions on the north western part. Dense vegetation such as a forest is located mainly in the rainy areas with an altitude greater than 25% (Figure 1.3 and Figure 1.4).

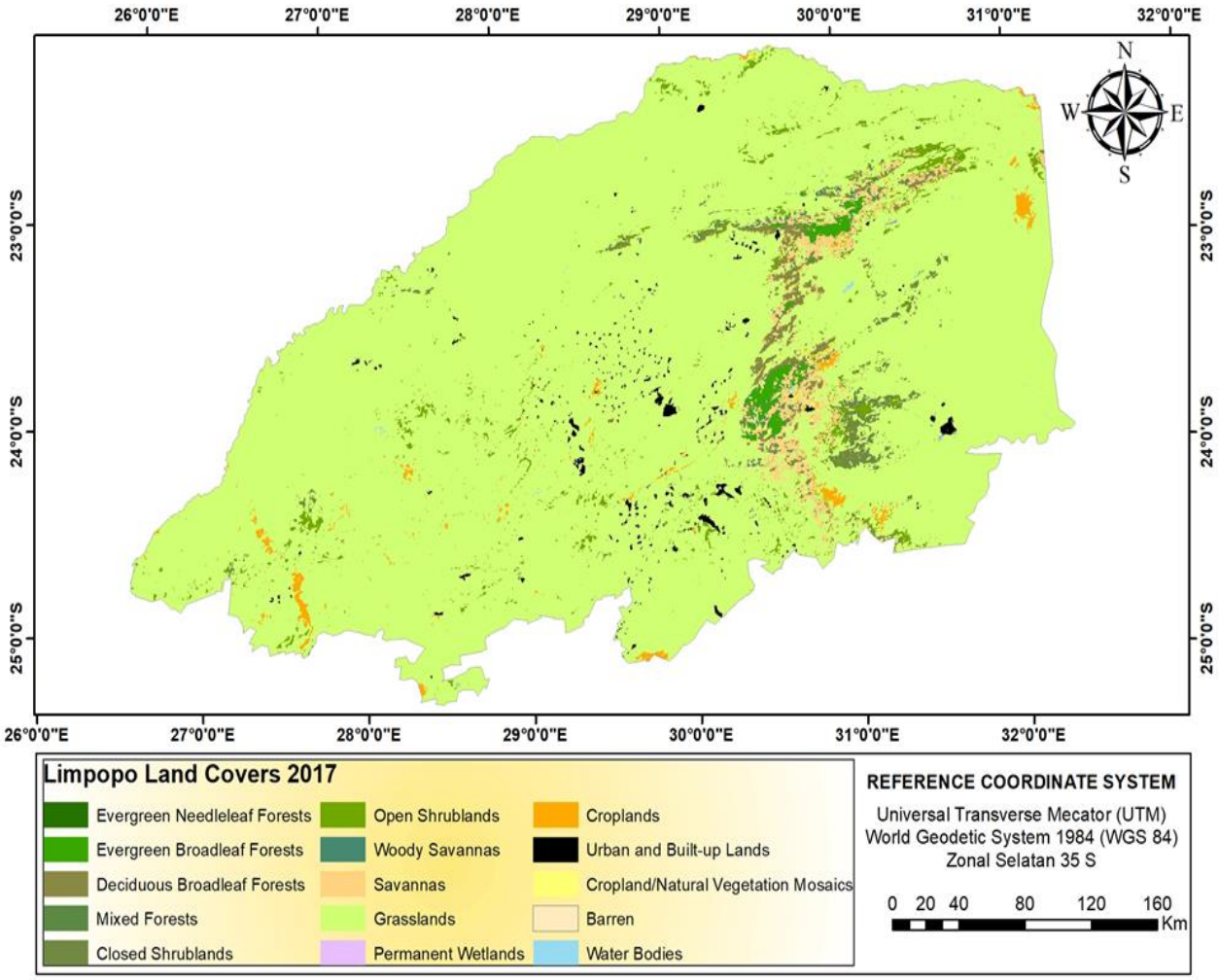

Figure 5.3: Map showing 2017 annual IGBP vegetation land covers over Limpopo Province, South Africa

5.2.2 Spatiotemporal Distribution of Land Covers

The statistical analysis and plotting were conducted using Microsoft Excel, displaying fifteen land covers classified over Limpopo Province. The deviation of area coverage in Km^2 of different land covers of MODIS MCD12Q1 annual IGBP classification was used to create the table and plot the spatiotemporal distribution of land cover types in Limpopo Province. To understand changes of the land covers, spectral profiles reflecting land covers were generated for 2001, 2010, and 2017.

Table 5.1: The spatial extent of annual IGBP land covers classes (Area_Km2) for 2001, 2010, and 2017 in Limpopo Province.

Class	Class Name	Area_Km^2		
		Land Cover_2001	Land Cover_2010	Land Cover_2017
1	Evergreen Needleleaf Forests	3	5	3
2	Evergreen Broadleaf Forests	956	885	797
4	Deciduous Broadleaf Forests	633	1500	1302
5	Mixed Forests	66	138	118
6	Closed Shrublands	1683	753	1017
7	Open Shrublands	2916	2443	2486
8	Woody Savannas	401	397	400
9	Savannas	1915	2589	2679
10	Grasslands	110564	110138	109958
11	Permanent Wetlands	20	15	6
12	Croplands	904	1124	1078
13	Urban and Built-up Lands	862	919	960
14	Cropland/Natural Vegetation Mosaics	2	17	28
16	Barren	9	13	8
17	Water Bodies	5	4	97

Table 5.1 presents the spatiotemporal distribution of the annual IGBP classification scheme for the period 2001, 2010, and 2017 (Area – Km^2). From Table 5.1 above, changes in land cover were detected using change assessment through comparing the areas of identified land covers and generating bar graphs (Figure 5.4). The IGBP classification shows that the region is dominated by grassland land cover with area coverage of about 110564 km^2 (2001), 110138 Km^2 (2010), and 109958 Km^2 (2017) respectively. Globally, exponential increase of urbanization results in the reduction of areas of natural vegetation (Hussein *et al.*, 2017). Table 5.1 shows a dynamic vegetation change throughout the study area. From the spatiotemporal distribution, the foremost visual difference is the reduction in coverage (Area-Km^2) of Grasslands vegetation land

cover and increase in Urban and Built-up land. However, the spatial distribution of other land covers has remained relatively similar with no significant difference.

Based on the observation, it can be assumed that a decline in the permanent wetlands, grasslands, and Evergreen Broadleaf Forests has been transitioned into build-up and other land. In rural areas, agriculture has expanded slightly, possibly to support population growth impacting and reducing permanent wetland (Hussein *et al.*, 2017). Urbanization and population can alter distribution of vegetation and abundances (Gregg *et al.*, 2003). Moreover, the main causes of land cover changes are attributed to pressure due to human activities (Duadze 2004) with high rate of deforestation across the world, also with the effects of climate variability leading people into converting permanent wetland into agricultural area due to raising temperatures. This can be supported by increasing area coverage of cropland from a class of 2001 to 2017. The spatiotemporal distribution of land covers is illustrated in Figure 5.4 below, with grassland being the most dominant land cover throughout the study area. Despite changes from some land covers, others remained unchanged.

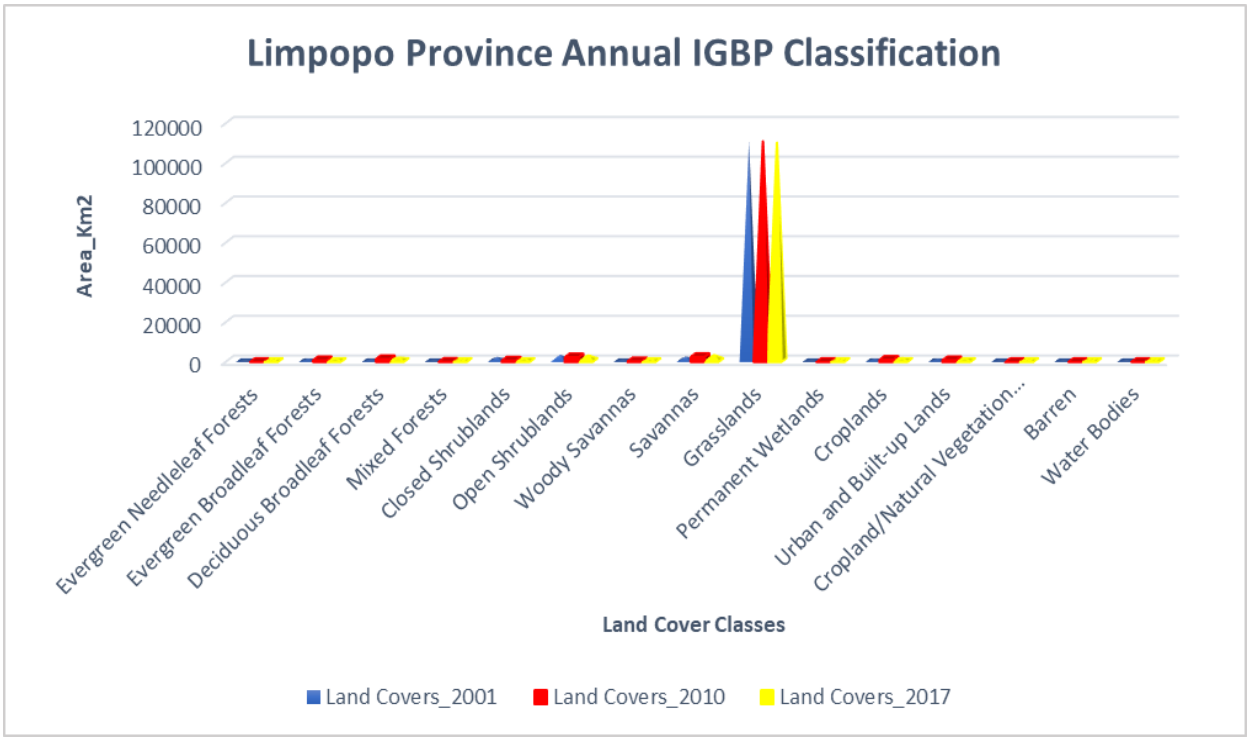

Figure 5.4: The annual IGBP spatiotemporal classification over Limpopo Province

5.2.3 Land Use/ Land Cover Change

To detect and quantify land use/ land cover change, post classification change detection was employed over Limpopo Province using MODIS MCD12Q1 imagery for 2017 and 2001. The IGBP supervised classification was employed identifying land use/ land covers over the region. From Figure 5.5 below, post classification change detection is presented illustrating three class categories, with limegreen representing no change, dark green representing significant gain, and red representing significant loss. Due to the transformation of land use/ land cover over Limpopo Province, the region witnessed 2% of significant loss or change, 95% of no change and 3% of significant gain.

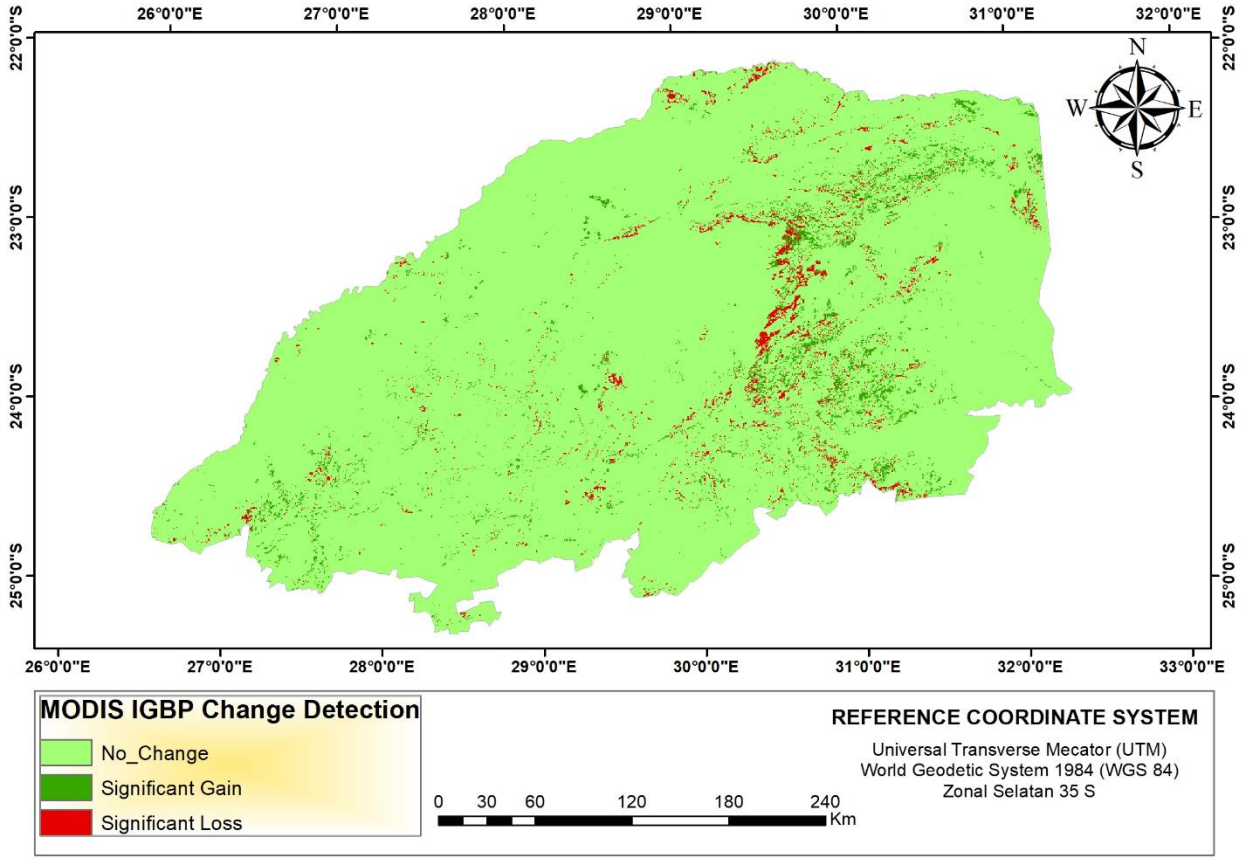

Figure 5.5: Temporal analysis of MODIS MCD12Q1 IGBP change detection over Limpopo Province

As presented in Table 5.1, much change was observed in Evergreen Broadleaf forest, Grassland and Permanent wetlands constituting 2% of significant loss, with 3% constituted by area of significant gain or increase such as urban and built up, deciduous broadleaf forest, mixed forest cropland, water bodies and savannas (Table 5.2). From Figure 5.5, the region consists of large

area of no change 95%. The post classification change detection corresponds to the spatiotemporal distribution of land covers (see section 5.2.2). Table 5.2 represents changes in land use/ land covers over Limpopo Province.

Table 5.2: Percentage of Post classification change detection over Limpopo Province.

Change Detection	Count	Change Percentage
Significant Loss	11824	2
No Change	536774	95
Significant Gain	14825	3

5.2.4 Land Use/ Land Cover Classification Quality Confidence

MODIS land cover quality confidence (QC) were derived to provide an insight into classification performance. Quality assurance (QC) does not measure the level of accuracy but rather indications of quality in the classification (Zhang and Roy, 2017). The maximum possible confidence was 9 and the minimum was 0. Figure 5.6 shows the classification confidence images for the land cover of 2001, 2010, and 2017. The spatial distribution of confidence map shows area of higher confidence performance occurring over water bodies, as water displays different spectral reflectance than other classes (Sheng *et al.*, 2016). Apparently, low classification confidence is over natural vegetation and developed mosaic lands reflecting the diversity of vegetation types with spectral and temporal signatures (Cheng *et al.*, 2007 and Yan and Roy, 2015).

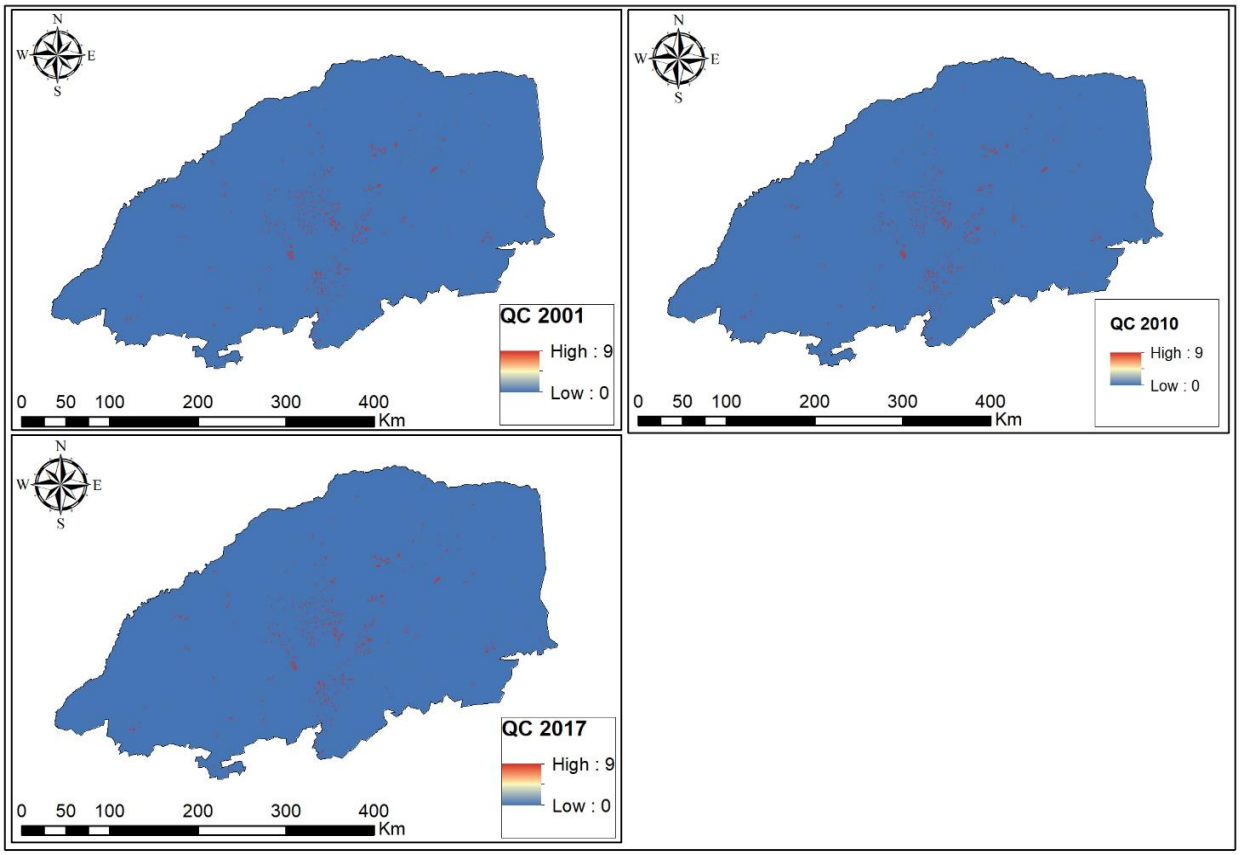

Figure 5.6: classification confidence (highest confidence 9 shown in red) for the IGBP land cover classifications.

Based on the IGBP land cover classification, 1520 training points were created from google earth to quantify the level of accuracy for the land cover class of 2017. Table 5.2 shows the report of accuracy assessment in terms of the classification confusion matrix, commission, omission, producer's and user's accuracy that quantifies the level of agreement between the classification. Considering both producer's and user's accuracy, the water bodies class (0) has the greatest classification accuracy compared to other land cover classes due to different spectral signatures (Sheng *et al.*, 2016). The producer's accuracy helps to quantify training data given per land cover class whether they are classified correctly (Story & Congalton, 1986). Mixed forest had the lowest level of user's accuracy (<50%) as compared to other land covers. The reason for this could be due to changes in land cover on the surface as IGBP classifies annually, as quantified by the user's accuracy. The user's accuracy was used to quantify classes in the classification that were not present on the surface (Story & Congalton, 1986).

The overall classification accuracy shows that the classification is reliable and acceptable for further analysis showing an overall accuracy of 73% with a kappa coefficient of 71%. Water

bodies, barren lands, urban and built-up, evergreen needleleaf forests, evergreen broadleaf forest and woody savannah show high reliable accuracy. The IGBP overall land cover classification accuracy follows that of Friedl *et al.*, (2010), with an overall accuracy of over 75% accuracy. The disparities in user's and producer's accuracy indicate a tendency to overestimate the number of land cover class. From the confusion matrix (Table 5.2), land cover types with high producer's accuracy than the user's accuracy indicate over mapping (Yang *et al.*, 2017). Considering both the user's and producer's accuracy the water class (0) has the greatest accuracy.

Low producer's accuracy simply indicates the level of misclassified classes, with classes being on the ground but not committed to the class (Yang *et al.*, 2017). Class with low producer's accuracy such as closed shrubland, savanna and woody savanna (49.1%, 53.6%; and 60%respectively), as highlighted by the confusion matrix were misclassified into different class type i.e. closed shrubland class are misclassified into cropland and mixed forest; savanna being misclassified into mixed forest and closed shrublands, and woody savanna being misclassified into grassland. Permanent wetlands represent a class with a land cover consisting of configurations of water and trees or herbaceous cover; thus, covered with different classes which is easily misclassified into the mixed forest, grassland, and forests (Yang *et al.*, 2017). This explains the misclassification of permanent wetlands with mixed forest, water bodies and forests. Relatively high user's accuracy and producer's accuracy for the land cover classes were found to explain the over mapping of classes (Yang *et al.*, 2017).

Table 5.3: IGBP classification confusion matrix, commission, omission, producer's accuracy, and user's accuracy.

MCD12Q1 IGBP Land Covers	1. Evergreen Needleleaf Forests	2. Evergreen Broadleaf Forests	4. Deciduous Broadleaf Forests	5. Mixed Forests	6. Closed Shrublands	7. Open Shrublands	8. Woody Savannas	9. Savannas	10. Grasslands	11. Permanent Wetlands	12. Croplands	13. Urban and Built-up Lands	14. Cropland/Natural Vegetation Mosaics	16. Barren	0. Water Bodies	Ground Total	Comision	Omision	Producer's Accuracy	User's Accuracy
Evergreen Needleleaf Forests	72	3	9	0	0	0	0	0	0	0	0	0	0	0	0	84	14.3	7.5	90.0	85.7
Evergreen Broadleaf Forests	0	65	0	0	4	0	0	0	0	2	0	0	0	0	0	71	8.5	17.5	81.3	91.5
Deciduous Broadleaf Forests	0	0	75	22	0	0	0	9	0	0	0	0	0	0	0	106	29.2	36.4	68.2	70.8
Mixed Forests	6	9	17	67	13	20	0	20	0	12	5	0	13	0	0	182	63.2	46.4	60.9	36.8
Closed Shrublands	0	0	0	0	54	0	0	13	7	0	17	0	0	0	0	91	40.7	50.9	49.1	59.3
Open Shrublands	0	0	14	0	27	78	0	0	0	0	0	0	0	0	0	119	34.5	29.1	70.9	65.5
Woody Savannas	0	0	0	0	0	0	66	9	0	0	0	0	0	0	0	75	12.0	40.0	60.0	88.0
Savannas	0	0	0	9	0	5	10	59	12	0	0	0	0	0	0	95	37.9	46.4	53.6	62.1
Grasslands	0	0	0	0	0	0	16	0	172	0	0	0	0	0	0	188	8.5	21.8	78.2	91.5
Permanent Wetlands	0	0	0	0	0	0	10	0	0	63	0	0	0	0	3	76	17.1	23.8	78.8	82.9
Croplands	0	0	0	13	12	7	8	0	18	0	58	14	9	0	0	139	58.3	27.5	72.5	41.7
Urban and Built-up Lands	0	0	0	0	0	0	0	0	0	0	0	70	0	10	0	80	12.5	27.5	87.5	87.5
Cropland/Natural Vegetation Mosaics	0	0	0	7	0	0	0	0	11	0	0	0	63	4	0	85	25.9	27.5	78.8	74.1
Barren	0	0	0	0	0	0	0	0	0	0	0	8	0	66	0	74	10.8	17.5	82.5	89.2
Water Bodies	0	2	0	0	0	0	0	0	0	5	0	0	0	0	77	84	8.3	3.8	96.3	91.7
Total	80	80	110	110	110	110	110	110	220	80	80	80	80	80	80	1520				

5.3 Vegetation Response and Sensitivity to extreme weather events

Climate variabilities such as drought and floods have been recognized as the key influences of vegetation dynamics and response resulting in the global change of the ecosystem (Fu & Li, 2010). Due to residual moisture stored in the soil, vegetation tends to show lagged response to extreme weather events as a result of the delayed vegetation response to developing rainfall (Thenkabail *et al.*, 2004). As the precipitation deficit lasts for a longer period (Drought), it often results in the reduction of photosynthetic activity and subsequently reduced vegetation conditions (Maselli *et al.*, 2009). Such a reduction in vegetation conditions can be monitored by remotely sensed data such as vegetation indices. The opposite goes with extreme wet conditions, it results in the increase of photosynthetic activity and an increase in the vegetation conditions. In this case, MODIS MOD13Q1 Terra vegetation product at 16 days was used to determine the vegetation response and sensitivity to extreme climate in Limpopo Province. From the study, vegetation sensitivity was accomplished by placing more weight on the NIR reflectance components of the EVI equation (Huete *et al.*, 1997). To describe the different responses of NDVI and EVI to different weather conditions (water content conditions), the relationship between NDVI, EVI, and LSWI was studied.

5.3.1. Normalized Difference Vegetation Index (NDVI)

In the arid environments, vegetation conditions and dynamics are controlled to a large degree by abiotic factors such as moisture availability either directly as rainfall or temperature (Collins, *et al.*, 2014; Reynolds, *et al*, 2004). The MODIS MOD13Q1 250 m spatial resolution NDVI was used to the visualized distribution of vegetation health conditions during dry seasons and wet seasons over Limpopo Province. NDVI is widely used to study drought and floods (Dutta, *et al.*, 2015). The short term NDVI for different rainfed seasons/ summer seasons (DJF) was used to study the floods and drought conditions.

Figure 5.7 presents the NDVI during the wet season of the year 2000. The 2000 wet season was influenced by the successive landfall of the tropical cyclone, with TC Eline resulting in heavy rainfall bringing floods condition over Limpopo Province (Chikoore, *et al.*, 2015). Due to the availability of MOD13Q1 satellite data, two consecutive months February and March were chosen to study the distinct characteristics of their NDVI. Due to vegetation indices response of to rainfall, one more month is added to the summer month of each case (Zhang *et al*., 2013). The vegetation indices show a lag time between occurrence of extreme and vegetation response.

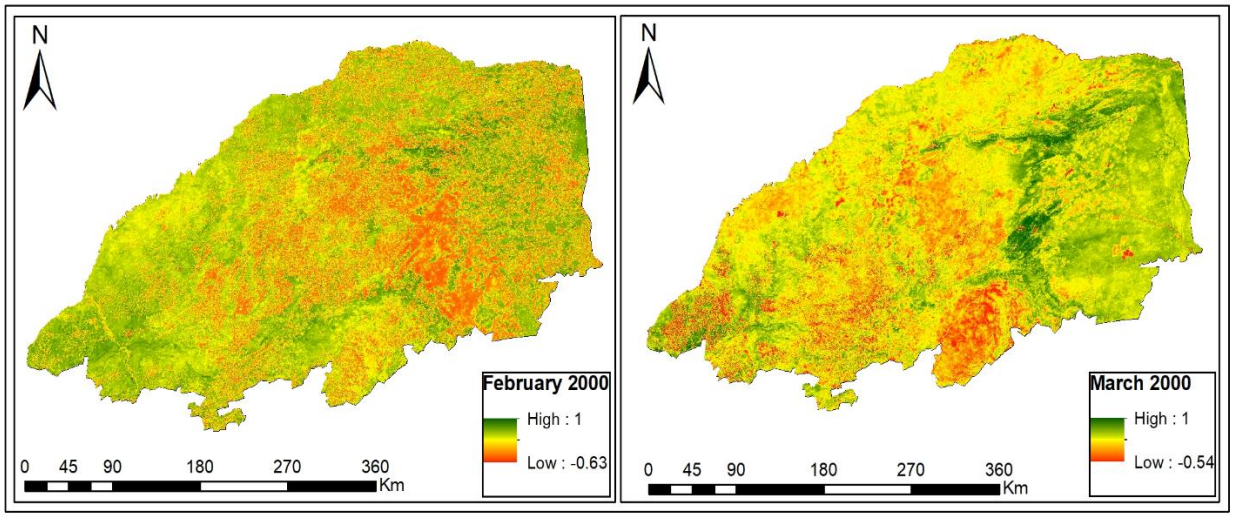

Figure 5.7: Spatial distribution of the NDVI over Limpopo Province during the wet condition of 1999/00

Under the influence of climate variability such as extreme drought and copious heavy rainfall (floods), vegetation growth, mainly the grassland, croplands and shrubland are significantly affected by these extreme climate changes (Wu *et al.*, 2015), resulting in changing the function of vegetation ecosystem and even cause damages (Brotherton & Joyce, 2015). The seasonal rainfall (DJF) across the country varied substantially during the 1999/00 summer season, with the north eastern side receiving over 5 mm/ day and the western side about >1 mm/ day (Figure 4.15(a)).

Figure 5.7 displays the MCD13Q1 NDVI for two consecutive months of 2000, it shows healthy vegetation conditions with values ranging between -0.63 to +1 for February and -0.54 to +1 for March. The NDVI for both months February and March show healthy vegetation conditions over Limpopo Province. Higher NDVI values represent healthy vegetation condition while lower values represent poor vegetation conditions. The two consecutive months i.e. February and March show very high NDVI values; and are probably due to vegetation's response to intense heavy rainfall. From the study analysis, 1999/00 were identified as a wet year with absolute precipitation values ranging between 2mm/day to 5mm/day over Limpopo Province.

During the 2000 period, Limpopo Province shows a large LSWI (Figure 5.19) increase, with values ranging from as high as 0.94 mm (February) and 0.84 mm (March). Increased LSWI values reduce evaporation rate of soil moisture, resulting in vegetation under healthy conditions due to low moisture stress (Chandrasekar, *et al.*, 2010). Under the circumstances, the vegetation over the

region displayed a very healthy condition with values ranging between +0.63 to +1 (February) and -0.54 to +1 (March).

Due to heavy rainfall over the region in 2000, vegetation showed great variability with the mean NDVI value (Figure 5.15) showing significant variation. In February 2000, the region experienced heavy rainfall influenced by TC Eline. The NDVI image for March compared to February to visualize the spatiotemporal variation of vegetation conditions. After the wet season, March generally has higher NDVI values, showing vegetation response lag by a month. The mean NDVI values for March were 0.62 higher compared to 0.42 for February. The NDVI shows high values due to heavy rainfall (Hussein *et al.*, 2017).

Figure 5.8 shows the spatial distribution of NDVI images for four consecutive months (December, January, February, and March) of 2002/03 over Limpopo Province during a drought condition.

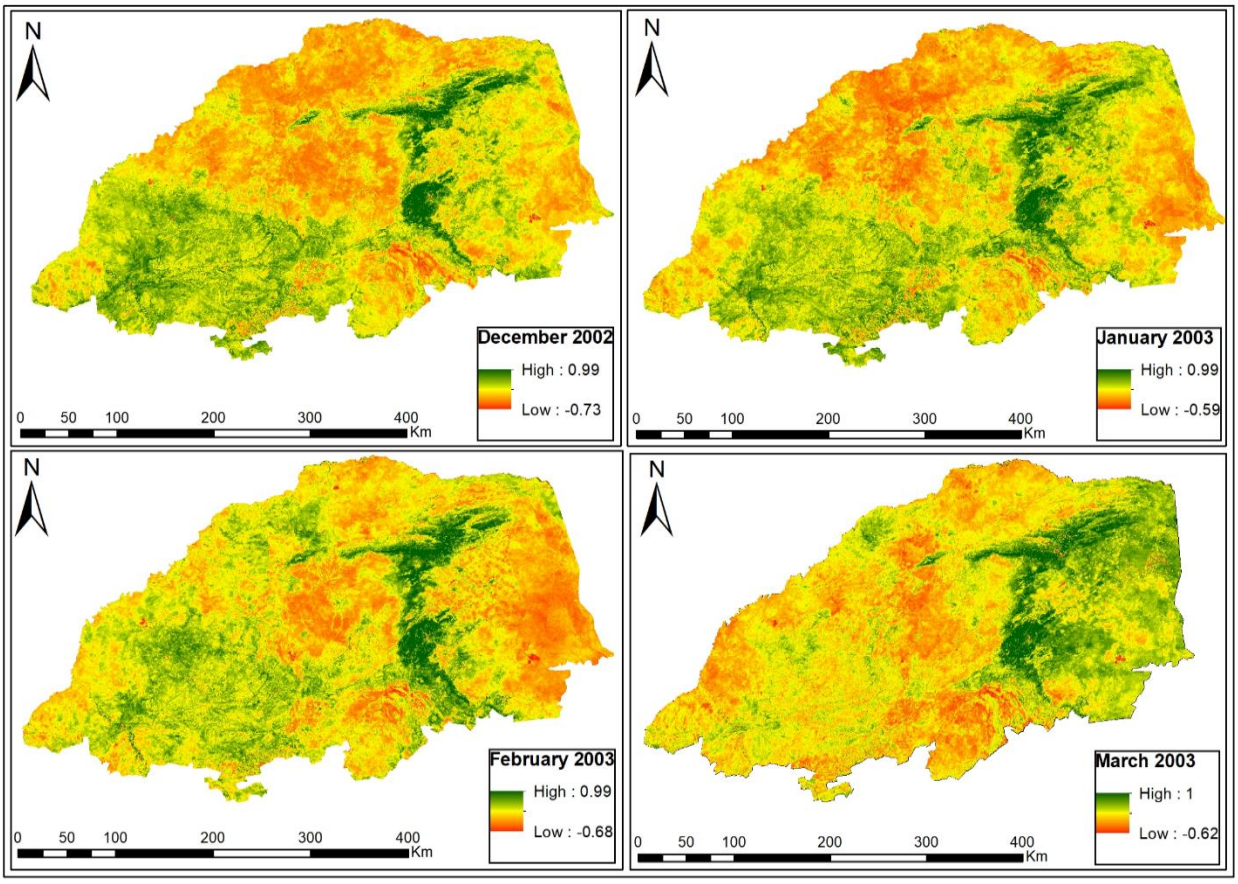

Figure 5.8: Spatial distribution of the NDVI over Limpopo Province during the drought condition of 2002/03

The study area is composed of areas of different elevation (Figure 1.3) with an area of higher elevation associated with precipitation (Chikoore, 2016), which is enough for vegetation growth, thus making the area compatible to different vegetation cover dominated by forests and mixed forests, namely Evergreen Needleleaf Forests, Evergreen Broadleaf Forest and, Deciduous Broadleaf Forests which are resistant to dry conditions (Li *et al.*, 2018).

Figure 5.8 displays the 2002/03 drought condition which spared across Limpopo Province and resulted in the reduction of vegetation health conditions (NDVI). During the period, the region received below normal rainfall with negative despatcher between -1 mm/day to -3 mm/day (Figure 4.15 (a)). The 2002/03 drought condition was observed mostly on the north eastern side of the country, Limpopo Province. Low precipitation in the arid area and excessive temperature increases the evaporation rate, resulting in the reduction of water deficit in the atmosphere and soil which prohibits vegetation growth (Li, *et al.*, 2018). In southern Africa, vegetation responds poorly and is vulnerable to excessive raising temperatures (Ziervogel *et al.*, 2014; Lawal *et al.*, 2019). As a result of low rainfall, the region was subjected to increasing maximum temperatures ranging between +1.2 to >2 (Figure 4.15 (c)). Rising temperatures result in increased evaporation of moisture from the soil and lead to vegetation being subjected to severe moisture stress (Chandrasekar *et al.*, 2010).

The impact of drought conditions is a gradual process that accumulates as the condition persists over a period (Lei & Duan, 2011). From Figure 5.3 the spatial analysis of NDVI response to the 2002/03 drought condition, due to poor vegetation health condition it can be concluded that vegetation on the western side of the province, mostly grassland, is sensitive to drought condition, while in the forest, it shows they are not really affected. As a result of low precipitation over the region, vegetation responded poorly with values ranging between -0.73 to +0.99 (December), -0.59 to +1 (January), -0.68 to +0.99 (February) and -0.62 to +1 (March). During the period, the LSWI (Figure 5.20) over Limpopo Province was very low with values ranging between -0.51 to +0.53 (December), -0.35 to +0.47 (January), -0.33 to +0.52 (February) and -0.35 to +0.52 (March). The shortage of water resources on soil or environment (LSWI) is the limiting factor for vegetation growth in the arid areas (Li, *et al.*, 2018). The 2002/03 drought case was followed by the 2005/06 wet condition over Limpopo province.

Figure 5.9 shows NDVI from four consecutive months of 2005/06 summer season. It can be observed that, during the year 2005/06 summer season (DJF), the region was subjected to heavy rainfall (Figure 5.16 (a), with rainfall ranging between 1 mm/day to 3 mm/day. Heavy rainfall over Limpopo Province resulted in an increase of LSWI values. Increased moisture content (LSWI)

due to heavy rainfall (Figure 5.21), resulted in vegetation being in a healthy condition. As observed, Figure 4.17(b) shows the absolute maximum temperature over the region during the summer season (DJF) of 2005/06, with temperature ranging between -0.1 and -0.2. Low temperature indicates low evaporation of soil moisture and reduction of vegetation stress (Chandrasekar, *et al.*, 2010).

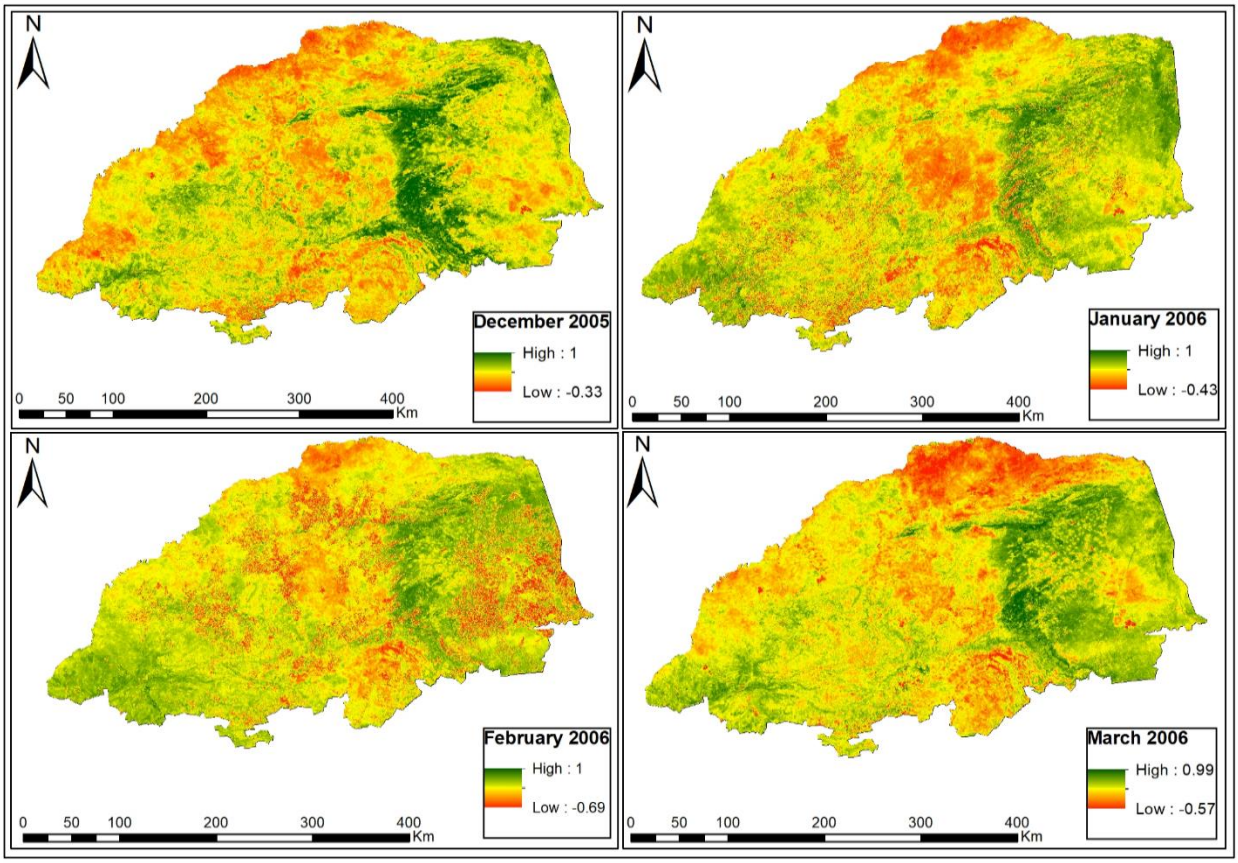

Figure 5.9: Spatial distribution of the NDVI over Limpopo Province during the wet condition of 2005/06

In the high rainfall season of 2005/06 (Figure 5.16 (a) it can be observed that the NDVI for four consecutive months responded very well, with values ranging between -0.11 to +0.95 (December), -0.20 to +1 (January), -0.20 to +1 (February) and -0.19 to +0.92 (March) respectively. The NDVI and LSWI show a strong correlation r = 0.73, and in the LSWI values and lead to an increase in the NDVI values. The LSWI during the 2005/06 period responded very well (r = 0.83) with the rainfall, as values, increased spontaneously ranging between -0.38 mm to +0.58 mm (December), -0.37 mm to +0.62 mm (January), -0.28 mm to +0.91 mm (February) and -0.33 mm to +0.66 mm (March). From the analysis, it can be observed that vegetation grows well in wet and unstressed conditions. However, the response of vegetation to weather conditions (rainfall or

temperature) depends on the vegetation type present in the region, and the availability of water content in the background soil (Chandrasekar, *et al.*, 2010).

Figure 5.10 displays the characteristics of four consecutive NDVI months during the dry summer season of 2015/16. Distribution of drought conditions over Limpopo Province as detected is shown by SPEI (Figure 4,9; Figure 4.10; Figure 4.11 and Figure 4.12) and GPCP Precipitation (Figure 4.18 (a)). During the year, it can be observed that the region was subjected to extreme drought conditions with GPCP precipitation departures ranging from -1 mm/day to -2 mm/day. Fine condition or drought over the region, influenced the temperatures to be above normal, with maximum temperatures over the region ranging between 1.8 $°C$ and 3$°C$ thus increasing the rate of evaporation of soil moisture (Chandrasekar *et al.*, 2010) leading to low LSWI values correlation between LSWI and Temperature.

The condition prior to the 2015/16 drought was a weak El Niño drought 2014/15 which affected most of the eastern side of southern Africa (Chikoore 2016). Due to high temperature and low moisture content from the soil, the NDVI showed the lowest values in four consecutive months, ranging from -0.93 to 0.99 (December), -0.75 to 0.99 (January), -0.68 to 0.99 (February), and -0.60 to 0.94 (March). Low NDVI values follow very low LSWI values over Limpopo Province, showing a weak correlation between NDVI and GPCP precipitation (r= 0.31), with values ranging between -0.38 mm to 0.46 mm (December), -0.48 mm to 0.48 mm (January), -0.58 mm to 0.50 mm (February), and -0.41 mm to 0.61 mm (March).

During the period, Limpopo Province was subjected to very low NDVI and LSWI values for all four consecutive months, except for area covered with Evergreen Needleleaf forest, Evergreen Broadleaf forest and Deciduous broadleaf forest, where the NDVI and LSWI values were high, with area dominated by grassland land cover observing low NDVI and LSWI (Viana and Alvalá, 2011). The results show that due to severe moisture stress, vegetation growth or health is poor, with NDVI values over the region dominated by low values. This can be supported by the LSWI values for four consecutive months.

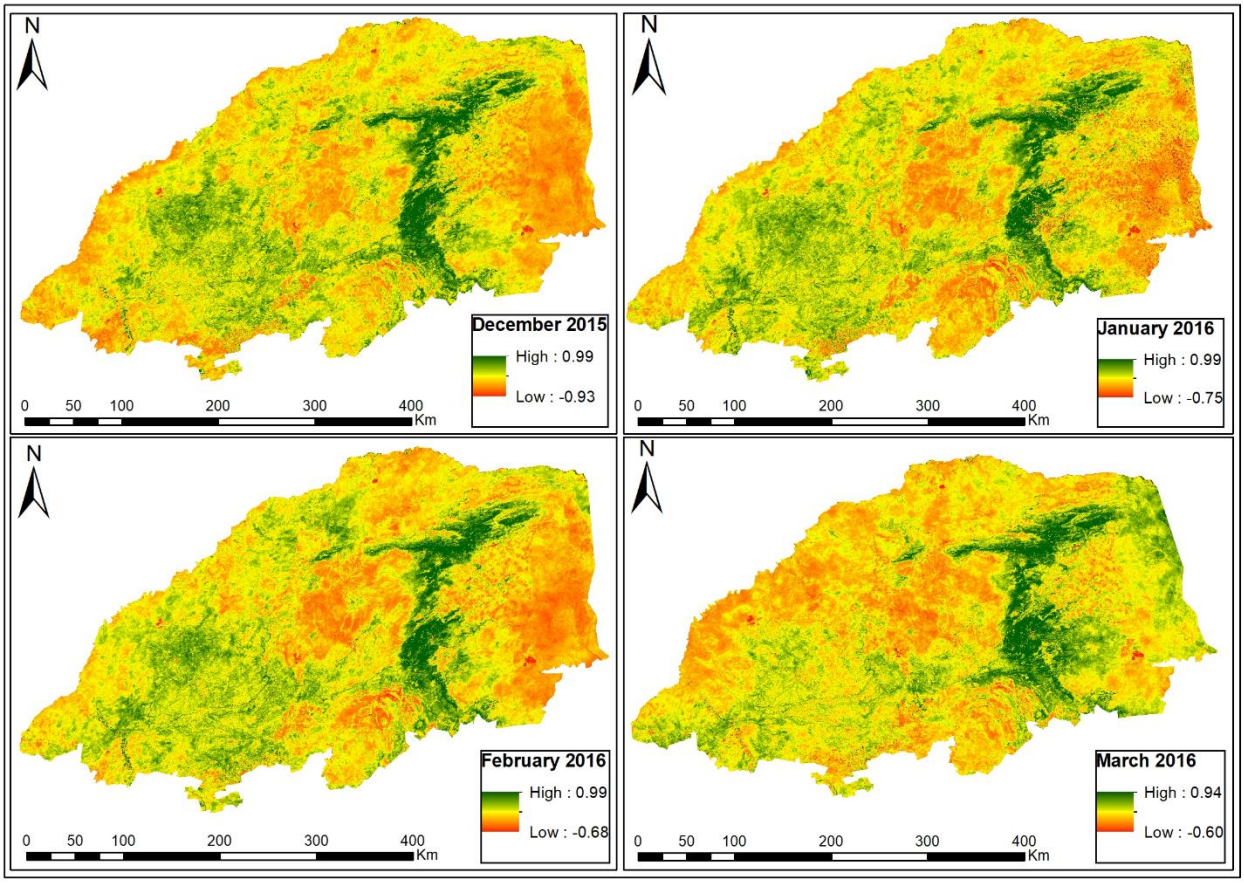

Figure 5.10: Spatial distribution of the NDVI over Limpopo Province during the drought condition of 2015/16

5.3.2. Enhanced Vegetation Index (EVI)

Similar to the NDVI, the EVI is used to monitor vegetation conditions specifically vegetation sensitivity over Limpopo Province by showing characteristics of vegetation response and sensitivity to extreme weather events. Thus, EVI has been considered for the study as a modified VIs with improved vegetation monitoring capabilities and improved sensitivity to higher biomass regions with the reduction of atmospheric influences (Huete *et al.*, 1999). The EVI helps to reduce the effects of environmental factors i.e. atmospheric conditions and soil background, contributing to noise of VIs calibration in hilly areas (Holben & Justice, 1981; Matsushita *et al.*, 2007). Therefore, reduction of atmospheric influences improves the sensitivity of EVI to vegetation signals as compared to NDVI (Huete *et al.*, 2002). Thus, this section displays MODIS MOD13Q1 EVI for cases during extreme weather events.

Figure 5.11 shows the distribution of two consecutive months of the wet period of 2000 namely, February and March. In the study area, due to copious heavy rainfall caused by TCs Eline,

vegetation condition was good with values ranging between -0.2 to +1 (February) and -0.2 to +1 (March).

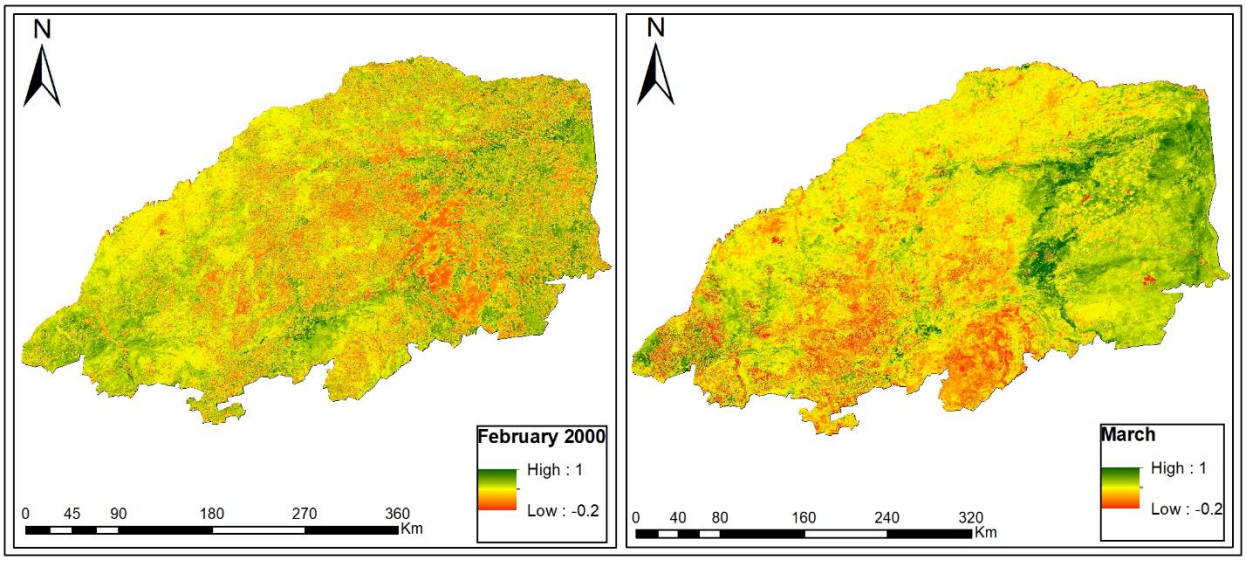

Figure 5.11: Spatial distribution of the EVI over Limpopo Province during the wet condition of 1999/00

Figure 5.11 shows the spatial distribution of EVI over Limpopo Province during the wet season of 1999/00. Similarly, the spatial distribution of EVI shows the same patterns with NDVI of 2000, but with lower values. Although it can be clearly seen that the NDVI and EVI spatial distribution patterns are similar, the reflectance of NDVI and EVI show great variation. According to Matsushita *et al.*, (2007), the spatial variation of the reflectance is mainly due to the topographic effects.

As the result of copious heavy rainfall, an increase of water content in the soil (soil moisture) was observed thus represented by high LSWI values ranging from -0.79mm to 0.94mm for February and -0.81mm to 0.84mm for March respectively, showing positive correlation (r = 0.83). Heavy rainfall with high LSWI values is associated with low temperature which indicates low evaporation of soil moisture and reduced vegetation stress (Chandrasekar *et al.*, 2010). During two consecutive months of 2000 wet period, both LSWI and EVI had similar spatial distribution.

The spatial distribution of both consecutive months is mainly dominated by normal vegetation conditions, with the high condition found in the area of higher elevation and forests like vegetation (Chandrasekar *et al.*, 2010). The analysis of LSWI shows high values during the period, meaning that the moisture condition over the region was high due to a low evaporation rate. Moreover,

more than half of the province was characterised by good vegetation conditions, as a result of heavy rainfall.

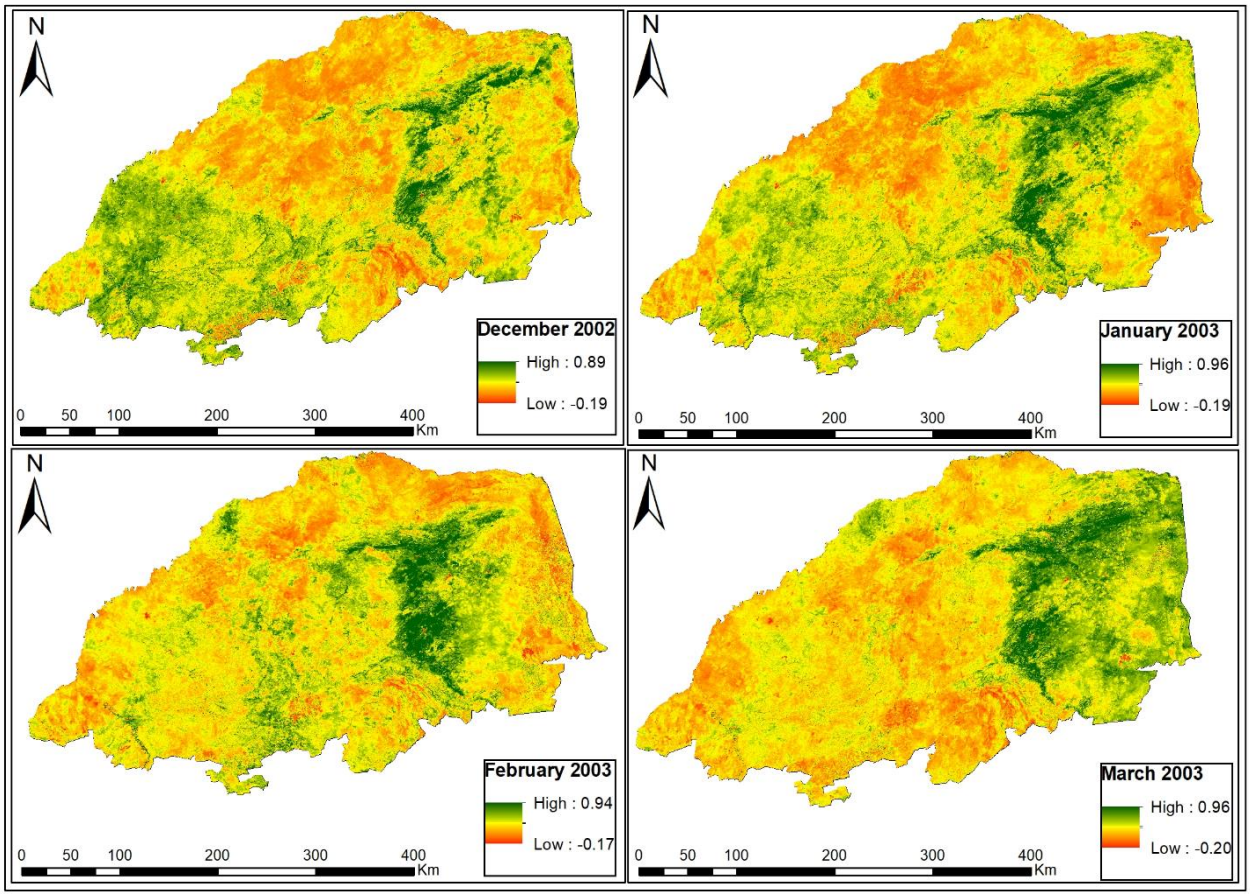

Figure 5.12: Spatial distribution of the EVI over Limpopo Province during the drought condition of 2002/03

In 2002/03 Limpopo Province was affected by drought conditions (Chikoore, 2016). The analysis of drought indices (SPEI) showed that the region was subjected to severe conditions and moderate conditions in some regions. Figure 5.12 shows the spatial distribution of EVI for four consecutive months over Limpopo Province from the 2002/03 drought. Low rainfall recorded -1mm/day to -3mm/day over the province (Figure 4.16 (a)), resulted in excessive temperatures which lead to increasing evaporation rate causing a decline in the soil moisture prohibiting vegetation growth.

For EVI analysis during the drought period, the region was dominated by the vegetation of low condition (Figure 5.12). As a result of different reflectance variation between NDVI and EVI, also lead to variation between the two spatial distribution patterns, with NDVI show more reflectance

than the EVI (Matsushita *et al.*, 2007). Due to drought condition, resulting in poor vegetation condition with values ranging between -0.19 to 0.89 (December), -0.2 to 0.96 (January), -0.17 to 0.95 (February), and -0.2 to 0.96 (March) respectively.

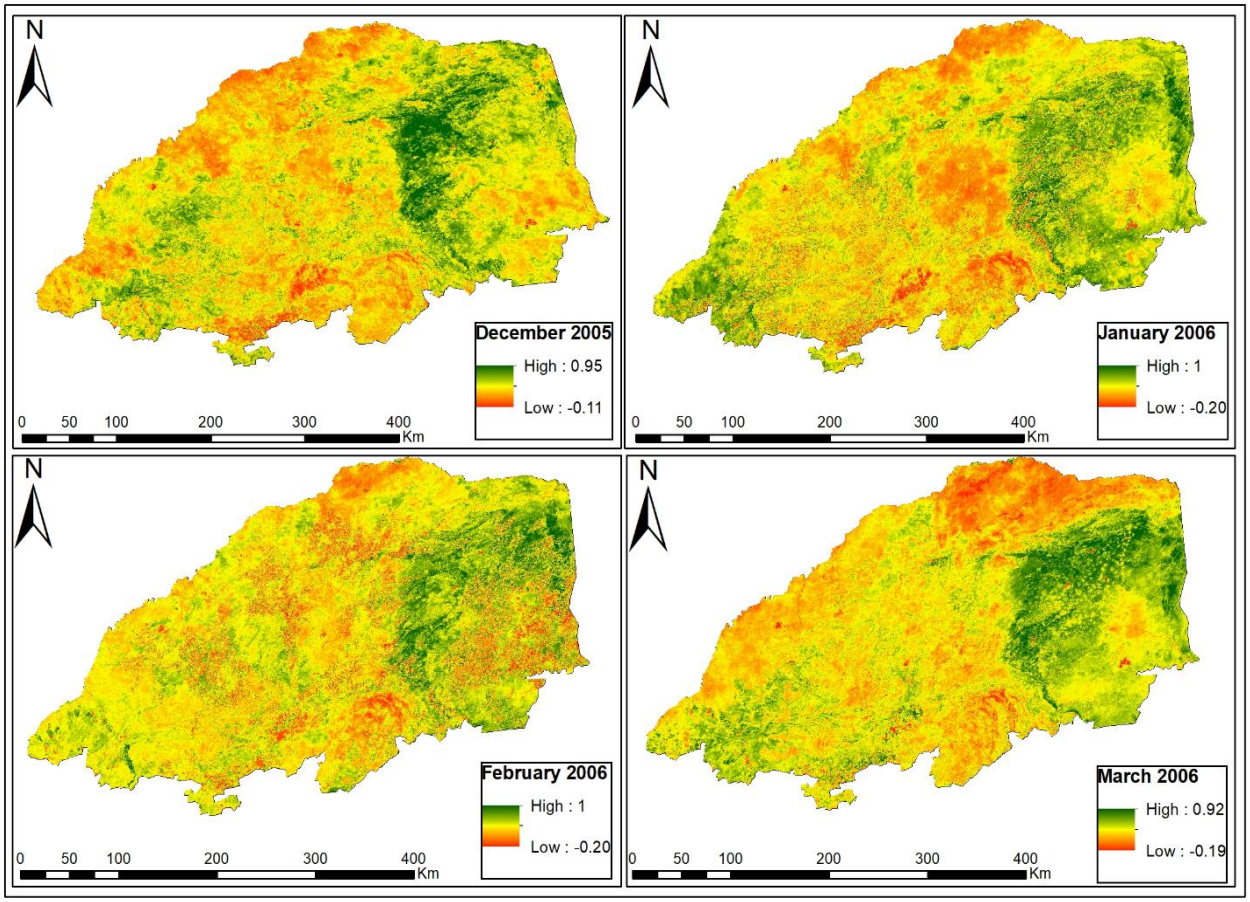

Figure 5.13: Spatial distribution of the EVI over Limpopo Province during the wet condition of 2005/06

Following the drought case of 2002/03, is the wet period of the 2005/06 summer season. Figure 5.13 illustrates four consecutive months of EVI during wet seasons. It can be observed that during the period vegetation responded well with values ranging between -0.11 to +0.95 (December), -0.20 to +1 (January), -0.20 to +1 (February), and -0.19 to +0.92 (March) respectively. Figure 5.13 shows the characteristics of EVI during the wet summer season of 2005/06.

During the 2005/06 wet period, the four consecutive images of EVI show less reflectance as compared to the NDVI images (Figure 5.7), suggesting that the vegetation responds well with EVI than NDVI without the influence of atmospheric aerosols (Huete *et al.*, 2002). It can be observed that during the period, vegetation condition (Figure 5.13) responded positively with LSWI values

(Figure 5.23) over the region ranging from -0.38 mm to +0.52 mm for December, -0.37 mm to +0.62 mm for January, -0.28 mm to +0.91 mm for February, and -0.33 mm to +0.66 mm for March and are positively correlated with correlation coefficients (r = 0.73, and p =0.002906).

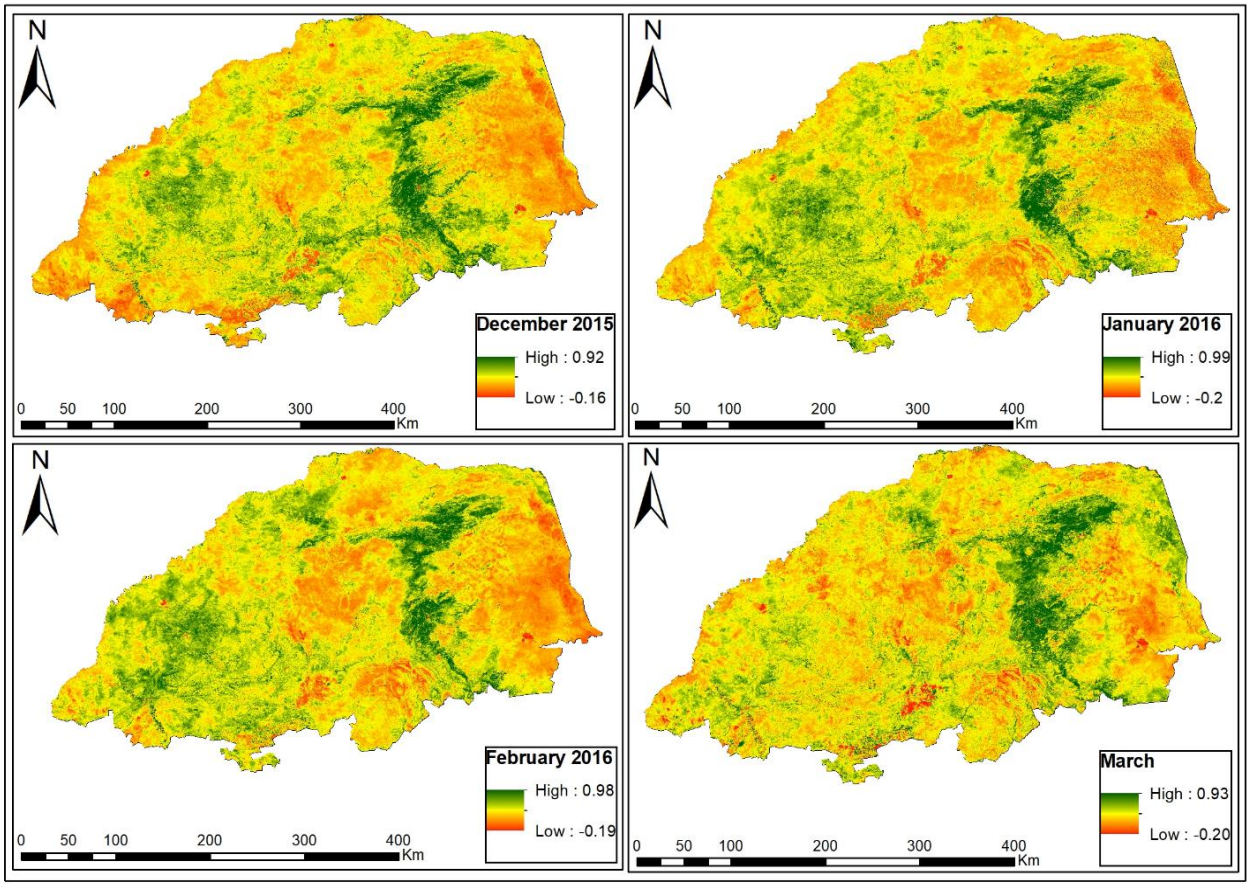

Figure 5.14: Spatial distribution of the EVI over Limpopo Province during the drought condition of 2015/16

Drought conditions are considered to be among the most far-reaching natural disasters affecting the world (Edenhofer, 2015). During the 2015/16 summer period, Limpopo Province received below normal rainfall resulting in the worst prolonged drought condition impacting the whole region and some neighboring countries (Baudion, 2017). Due to excessive temperatures and low precipitation over the region, it resulted in an increased evaporation rate leading to a reduction of water content from the soil (soil moisture) affecting the vegetation condition over the area (Li, *et al.*, 2018). Reduced water content is demonstrated by low LSWI values ranging from -0.38 mm to 0.46 mm (December), -0.48 mm to 0.48 mm (January), -0.58 mm to 0.50 mm (February), and -0.41 mm to 0.61 mm (March). As a result of excessive temperature and increased evaporation, this has impacted the vegetation condition severely with values ranging between -0.16 to +0.92

(December), -0.2 to +1 (January), -0.19 to +0.99 (February), and -0.2 to +0.93 (March) respectively.

Due to improved sensitivity to atmospheric aerosols and topographic effects, EVI serve as the best-improved indices to study vegetation sensitivity without limitations (Huete *et al.*, 2002). The EVI images for four consecutive months show vegetation conditions with low reflectance NDVI indices. stop

5.4 Monitoring Vegetation Spatiotemporal Dynamics

To understand the vegetation sensitivity to extreme weather events i.e. wet condition and drought condition, using MODIS MOD13Q1 and MOD09A1, the section presents time series of line graphs using the mean values of VIs (NDVI, EVI, and LSWI) for each year of an extreme case for the period 2000- 2017. From the time series generated, it reveals the spatial pattern and temporal variation in the vegetation indices in Limpopo Province on the Seasonal time scale. The time series generated to allow the comparison of vegetation conditions between seasons of drought and wet conditions, to examine the temporal trend between VIs. Due to extreme weather events i.e. drought or wet conditions, vegetation is widely affected, with impacts varied spatially and temporally (Huang *et al.*, 2014).

5.4.1 NDVI and EVI

Figure 5.15 and Figure 5.16 present the time series of mean NDVI and EVI values for four consecutive months in different cases of extreme weather events during summer seasons for the period 2000-2017. The presented time series showed that vegetation had greater variability of the mean spatial values during the presented months namely December, January, February, and March. March had a significantly higher mean and showed a greater variability of the VI levels compared to other months. After the wet season, the mean NDVI and EVI value increases for months with March generally possessing higher VI values, showing that vegetation legged by a month (Hussein *et al.*, 2017).

The difference of the mean NDVI and EVI values between December- March during an extreme weather event could be based on seasonal vegetation growth variability (Hussein *et al.*, 2017). Due to the availability of MODIS MOS13Q1 satellite data, the cases of 1999/00 extreme weather events are studied using two consecutive months i.e. February and March. In February 2000 mean NDVI values were about 0.45 and 0.32 (EVI) followed by a gradual increase to about 0.62 for NDVI and 0.42 for (EVI) in March, with a similar trend during another wet season of 2005/06

represented by mean NDVI and EVI values peaking in March with values of about 0.60 for NDVI and 0.40 for EVI. The NDVI and EVI show that after the heavy rainfall, VI reached the highest level after one month, depending on the conditions of the area (Hussein *et al.*, 2017). During the wet seasons, March had the highest vegetation growth compared to other months (Figure 5.15 and Figure 5.16).

In the summer season of 2002/03 and 2015/16, the region experienced drought conditions, with the NDVI and EVI during this season showing the lowest values. In December 2002 the NDVI (0.42) and EVI (0.23) values were very lower due to low rainfall over the region (Hussein *et al.*, 2017). Lower NDVI and EVI values represent poor vegetation conditions. However, both months for NDVI and EVI showed a gradual increase in the mean values. During the dry period, the NDVI and EVI images for four consecutive months are presented from Figure 5.5 to Figure 5.12 and compared to show the spatial variation of vegetation conditions.

Both VI (NDVI and EVI) during the period showed lower values, with EVI displaying the lowest values (Figure 5.15 and Figure 5.16). This is because of the additional band (blue) for EVI which improves its monitoring capabilities and improved sensitivity to higher biomass region with the reduction of atmospheric influences such as aerosols (Huete *et al.*, 1999). In December 2002 NDVI values were 0.42 and peaked at 0.47 in March. Similarly, the patterns repeat in the 2015/16 season with NDVI mean of 0.42 in December and 0.45 in March. A decline in the mean NDVI values could be attributed to a lack of rainfall. This simply shows that during the period, the region had very poor vegetation conditions.

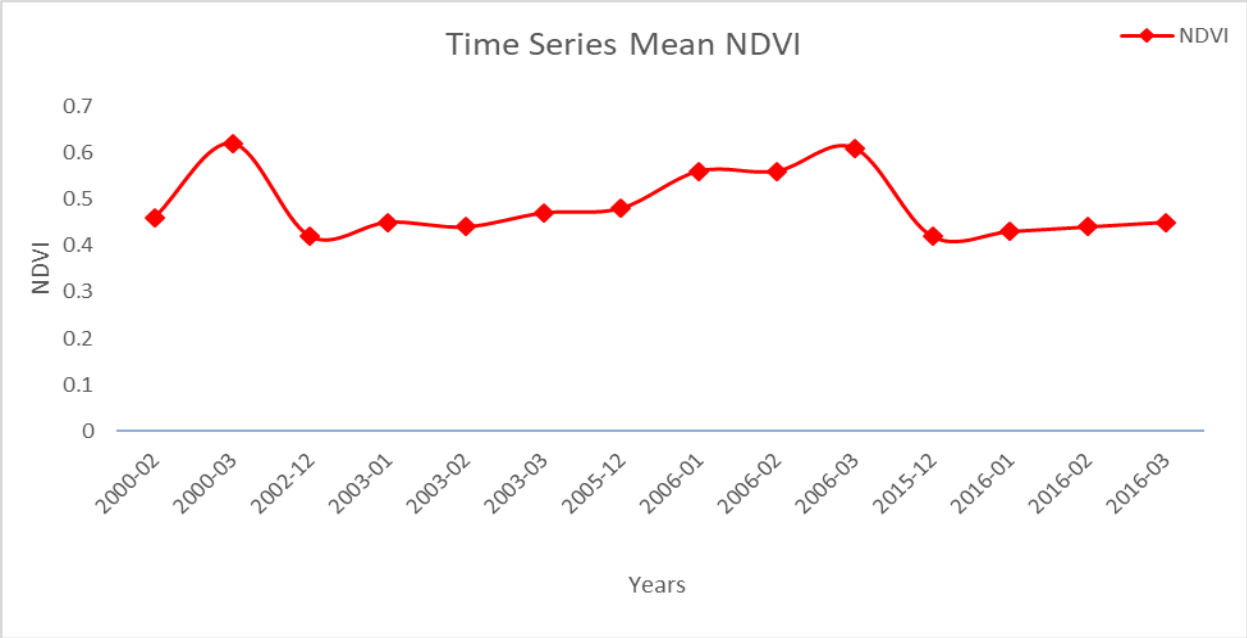

Figure 5.15: Time series showing mean NDVI values over Limpopo Province during droughts and floods conditions.

The results show that the vegetation was sensitive to the severe drought conditions with the area along the high elevation and covered by forests being less sensitive (Huang *et al.*, 2014) and sensitive to high rainfall (Hussein *et al.*, 2017). The study used NDVI and EVI images for during 1999/00, 2002/03, 2005/06 and 2015/16 summer season is compared to visualise the spatiotemporal variation of vegetation in different climatic conditions. In 1999/00 and 2005/06 the region experienced copious heavy rainfall, with the dry spell (drought condition) experienced in 2002/03 and 2015/16 season respectively. Both VI shows differences in vegetation growth between December, January, February, and March.

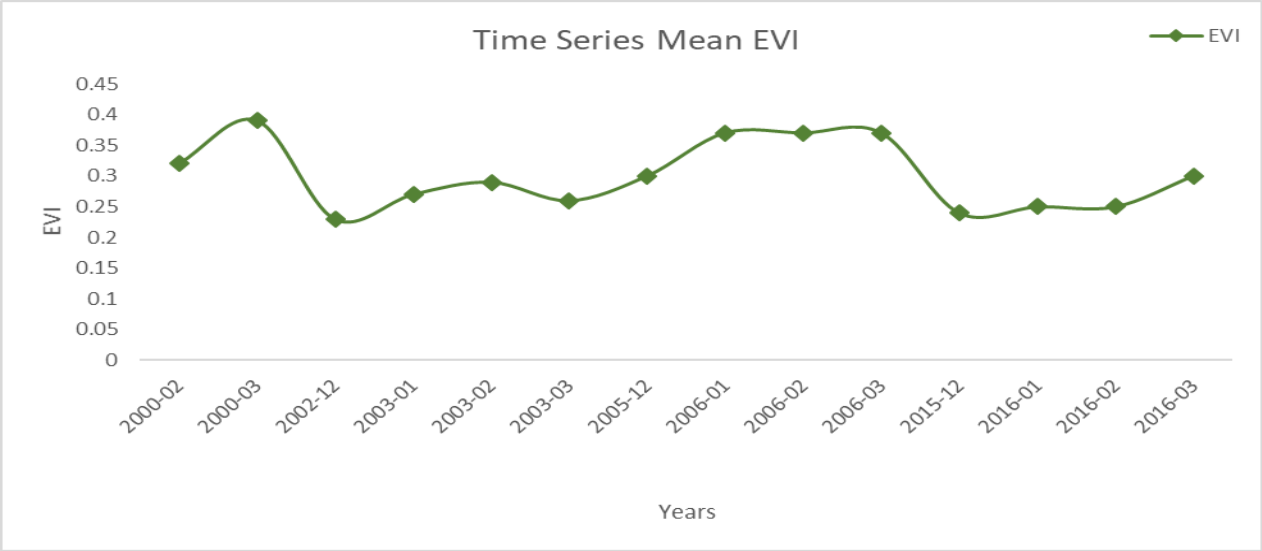

Figure 5. 16: Time series showing mean NDVI values over Limpopo Province during droughts and floods conditions.

5.4.2 Land Surface Water Index (LSWI)

Figure 5.17 presents the mean time series of LSWI over Limpopo Province during years of extreme cases. During the wet period, the duration of LSWI is observed to be LSWI > 0 and was positive throughout the season. As such, LSWI < 0 is designated as a dry or drought condition (Bajgain *et al.*, 2015). As illustrated by Figure 5.17, LSWI values never fell below zero in the wet summer season (1999/00 and 2005/06). Based on the time series, when VI (NDVI and EVI) are lower the LSWI < 0 and are associated with the drought conditions, whereas VIs and LSWI >0 was higher during the wet condition or non-drought condition (Bajgain *et al.*, 2015). The LSWI is strongly correlated with VI (NDVI and EVI) with 0.97 against both NDVI and EVI at a 95 percent confidence interval.

In February 2000, Limpopo Province was subjected to copious heavy rainfall influenced by numerous TCs with TC Eline making landfall and resulting in heavy rainfall (Figure 4.15 (a)), followed by heavy rainfall also in the summer season of 2005/06 (Figure 4.17 (a)). The wet condition was apparent in the study area as documented by higher values of NDVI, EVI, and LSWI, also with drought condition documented by lower NDVI, EVI, and LSWI. The LSWI and EVI are the most sensitive VI indicators of vegetation conditions (Bajgain *et al.*, 2015). It is also reported that LSWI responded more directly to the water stress of the vegetation (Chandrasekar *et al.*, 2010). Over the region, good vegetation conditions exhibit higher LSWI values, which generally decreases due to precipitation deficit and ultimately becomes LSWI < 0 when drought

becomes more extreme (Bajgain *et al.*, 2015), thereby supported a positive correlation between LSWI and NDVI with r = 0.73; LSWI and EVI with r = 0.87.

Due to heavy rainfall over the region in February 2000 and February 2006, higher LSWI values were recorded with 0.16mm for February 2000 and 0.14mm for February 2006. The study also had a season of low LSWI with value < 0 representing drought conditions. Drought conditions are associated with excessive temperatures and increasing evaporation rates (Ziervogel *et al.*, 2014; Lawal *et al.*, 2019). Over the region, seasons of drought conditions are characterised by lower LSWI with values ultimately becoming negative when drought becomes severe. In December 2002 and December 2015, as a result of drought conditions, LSWI mean values ultimately became negative with values ranging from -0.10 mm (2002) to -0.8 mm (2015).

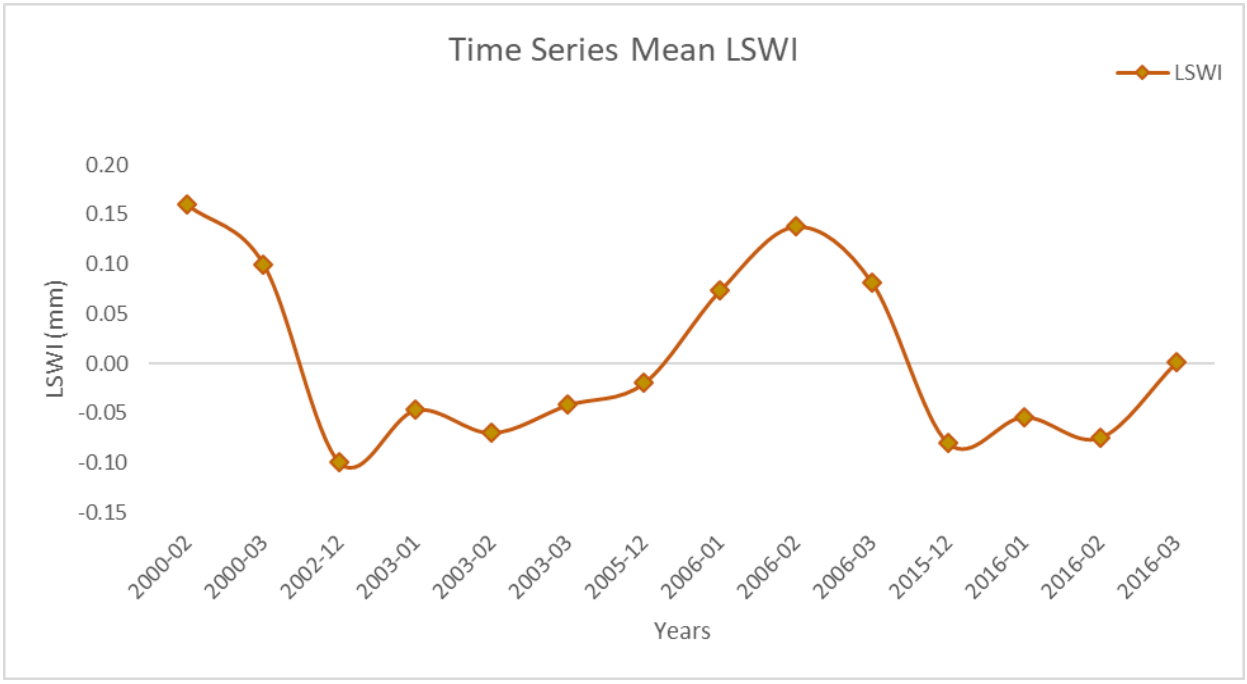

Figure 5.17: Time series showing mean NDVI values over Limpopo Province during droughts and floods conditions.

5.5 Pearson's Product-Moment Correlation Coefficient

The effects that climatic variables have on vegetation indices i.e. NDVI, EVI and LSWI may be caused by the vegetation growth phase (Piao *et al.*, 2011; Chuai *et al.*, 2013). Therefore, MODIS satellite MOD13Q1 (NDVI and EVI) and MOD09A1 Land Surface Water Index (LSWI) were used to display vegetation conditions and availability of water content from the soil in relation to climate variables i.e. GPCP precipitation and temperatures. The verified VIs mean data were analysed using Pearson product-moment correlation coefficient, measuring the strength of association

between variables. The correlation was calculated for seasons of drought conditions and flood conditions.

As displayed in Figure 5.16, both GPCP precipitation and Tmax can affect the VIs (NDVI, EVI, and LSWI); with the temperature that seems to be more significant (Figure 5.18) than that of precipitation (Chuai *et al.*, 2013). The vegetation response shows a lags time after heavy rainfall (Chuai *et al.*, 2013; Zhang *et al*., 2013), with higher values in March after heavy rainfalls in February. The effects that precipitation and temperatures have on both VIs varied according to different indices, therefore the study conducted separate correlation analysis for all VIs (NDVI, EVI, and LSWI). Figure 5.16 shows the correlation coefficients matrix, displayed in four different visualization patterns, with the blue color representing highly significant correlation and red inversely correlation.

From Figure 5.19 and Figure 5.20, the scatter plots shows the relationships between VIs and climate variables, with LSWI strongly correlating with GPCP precipitation and temperature with the correlation coefficients of (r = 0.83 and p = 0.0002 at 95 percent confidence interval 0.53 to 0.94 and the test statistics of = 5.15 for the test that correlation equal 0) for LSWI against GPCP precipitation and (r = -0.78 and p = 0.001 at 95 percent confidence interval ranging between -0.93 to -0.42 and the test statistics = -4.26 for the test that correlation equal 0) for LSWI against temperature.

The positive correlation of 0.83 between LSWI and GPCP precipitation shows that when rainfall increases, the water content from the soil also increases, whereas the negative correlation -0.78 (LSWI and temperature) shows that an increase in temperature results in reduced or decrease of water content from the soil (Bajgain *et al.*, 2015). It therefore implies a strong association between LSWI and GPCP precipitation. The LSWI were strongly correlated with GPCP precipitation (r = 0.83, and p = 0.0002 at 95 percent confidence interval ranging between 0.53 to 0.94 and the test statistics = -5.15 for the test that correlation equal 0) and highly significant whereas an inversely negative correlation was observed between LSWI and temperature (r = -0.78 and p = 0.001 at 95 percent confidence interval ranging between -0.93 to -0.42 and the test statistics = -4.26 for the test that correlation equal 0).

Due to delayed response of vegetation to precipitation, we observe a weak correlation (r = 0.31 and p = 0.28 at 95 percent confidence interval ranging between -0.27 to 0.72 and the test statistics = 1.12 for the test that correlation equal 0) less significant between NDVI and GPCP precipitation (Chuai *et al.*, 2013). Similarly, in the arid region, precipitation was proved not to be strongly

correlated/associated with NDVI changes (Weiss *et al.*, 2004). However, this is followed by a strong correlation between NDVI and temperature (r = -0.70 and p = 0.005 at 95 percent confidence interval ranging between -0.90 to 0.27 and the test statistics = -3.41 for the test that correlation equal 0) highly significant, showing than a weak decreasing GPCP precipitation and significantly increasing temperature result in a decrease of vegetation health.

Due to the low response and sensitivity of NDVI to precipitation, the land surface water index was correlated to NDVI and EVI. As shown in Figure 5.16 , strong positive correlation between LSWI and NDVI (r = 0.73 and statistical significant at p = 0.003 at 95 percent confidence interval ranging between 0.33 to 0.91 and the test statistics = 3.72 for the test that correlation equal 0); LSWI and EVI (r = 0.87 and statistical significant at p = 0.00006150 at 95 percent confidence interval ranging between 0.62 to 0.96 and the test statistics = 6.01 for the test that correlation equal 0) was observed, whereas a strong negative correlation was observed between temperature and vegetation indices i.e. NDVI (r = -0.70 and statistical significant at p = 0.005 at 95 percent confidence interval ranging between -0.90 to -0.27 and the test statistics at = -3.41 for the test that correlation equal 0) and EVI correlation (r = -0.73 and statistical significant at p = 0.003 at 95 percent confidence interval ranging between -0.91 to -0.32 and the test statistics at = -3.70 for the test that correlation equal 0) respectively.

Raising temperatures and reduced precipitation rate accelerate the evaporation rate, resulting in the reduction of water content from the soil thus prohibiting vegetation growth (Li *et al.*, 2009; and Chuai *et al.*, 2013), and resulting in a negative correlation between temperatures and vegetation indices. As discussed above, there was a significant decrease in precipitation and a rapid increase in temperature, resulting in the decrease of vegetation indices i.e. NDVI, EVI, and LSWI (Chuai *et al.*, 2013). The precipitation also decreases the temperature leading to a moderate negative correlation (r = -0.66 and p = 0.01 at 95 percent confidence interval ranging between -0.88 to -0.20 and the test statistics = -3.02 for the test that correlation equal 0). The relationship between correlated variables is presented in the scatter plots below (Figure 5.19 and Figure 5.20).

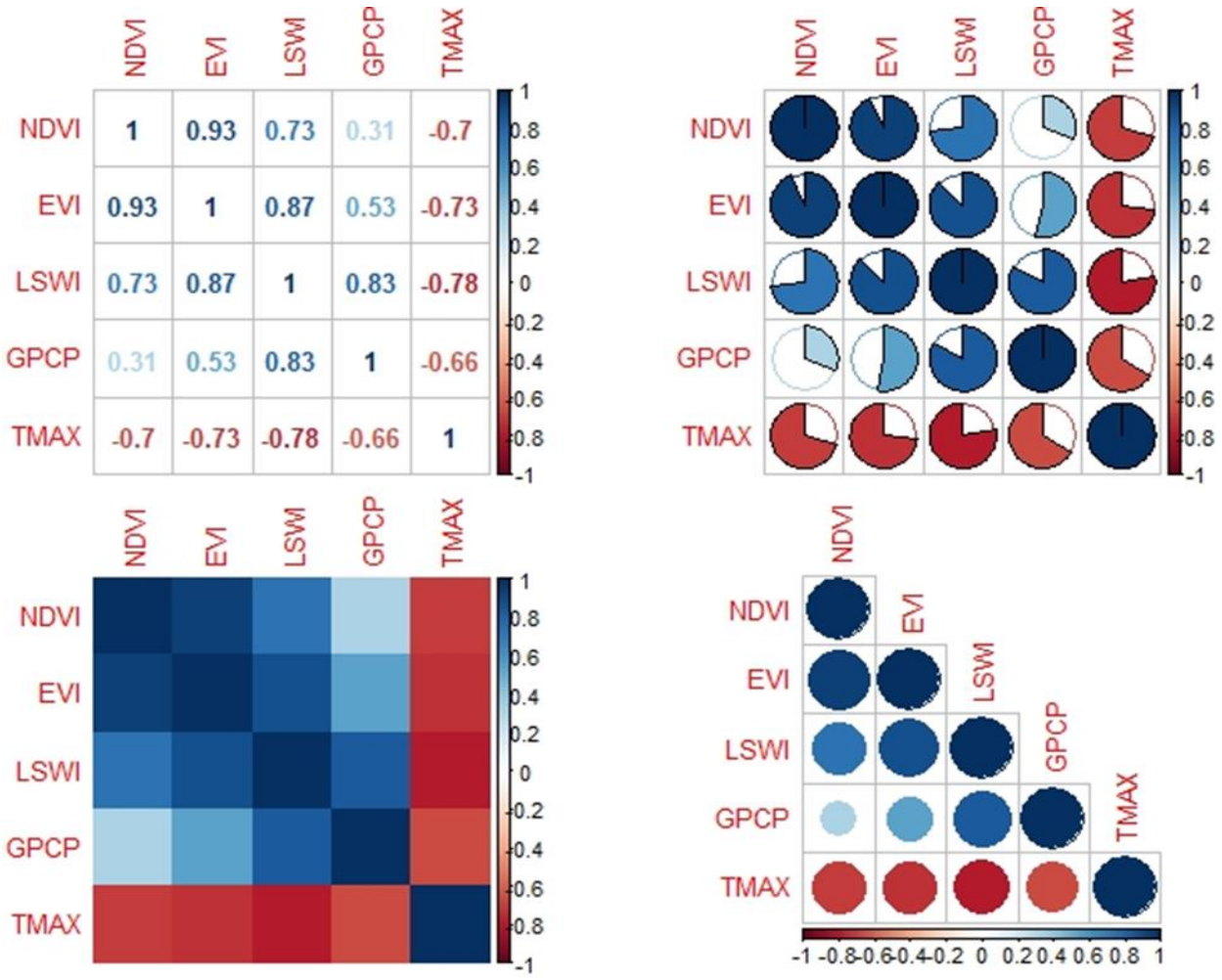

Figure 5.18: Showing Matrix table of correlation coefficients using different visualizations

The scatter plots graphically showing the association between variables are presented in Figure 5.19 and Figure 5.20). Although one variable is used against one another to determine their relationship, “relationship” doesn’t necessarily mean casualty (Hauke & Kossowski, 2011). As discussed above, the correlation between NDVI and EVI against LSWI had a strong positive correlation, with their association presented in the scatter plots (Figure 5.19 and Figure 5.20). This follows the associations that GPCP precipitation and temperature had on LSWI, as an increase in the GPCP precipitation were associated with an increase in LSWI leading to a positive association, whereas an increase in temperatures were associated with a decrease in LSWI resulting in a negative correlation.

The effects of temperature on LSWI, NDVI, and EVI were negative (-0.78; -0.70; and -0.73 respectively). however, this is due to available water content from the soil, as higher temperatures

and low rainfall are associated with low LSWI (-0.78) leading to poor vegetation conditions (Bajgain *et al.*, 2015). A positive association with a lag time effect of precipitation to vegetation indices was observed between NDVI and EVI (0.31; and 0.53 respectively). For GPCP precipitation and temperatures, the association was negative (r = -0.66 and p = 0.010652) showing that an increase in the rainfall results in temperature decrease (Chikoore, 2016). As displayed in the scatter plots, the lowest temperature is strongly associated with higher NDVI and EVI (Lin *et al.*, 1996), whereas the highest is strongly correlated with lower NDVI and EVI.

Table 5.4: P-values of correlated variables

	NDVI	EVI	LSWI	GPCP	TMAX
NDVI	NA	0.000002	0.002906	0.283859	0.005186
EVI	0.000002	NA	0.000062	0.050832	0.003258
LSWI	0.002906	0.000062	NA	0.000242	0.001105
GPCP	0.283859	0.050832	0.000242	NA	0.010652
TMAX	0.005186	0.003258	0.001105	0.010652	NA

As displayed by the scatter plots (Figure 5.19 and Figure 5.20), the level of association between variables and direction of the association is displayed. Temperatures and other variables show negative association, with an increase in temperature values, lead to a decrease of NDVI, EVI, LSWI, and GPCP (r = -0.70; r = -0.73; r = -0.78; and r = -0.66), whereas GPCP precipitation showed a positive association (correlation) with VIs except with temperature. The analysis of the correlation between temperature and vegetation indices provides a threshold range where temperatures induce vegetation growth (Hao *et al.*, 2012). The negative effects of temperature were most obvious in summer of drought conditions (2002/03, and 2015/16) where temperature was very high with absolute values of 1.2 to 1.6 (2002/03) and 1.8 to 2.7 (2015/16). Precipitation had a weak association or correlation with NDVI (r = 0.31 and not statistically significant at p = 0.283).

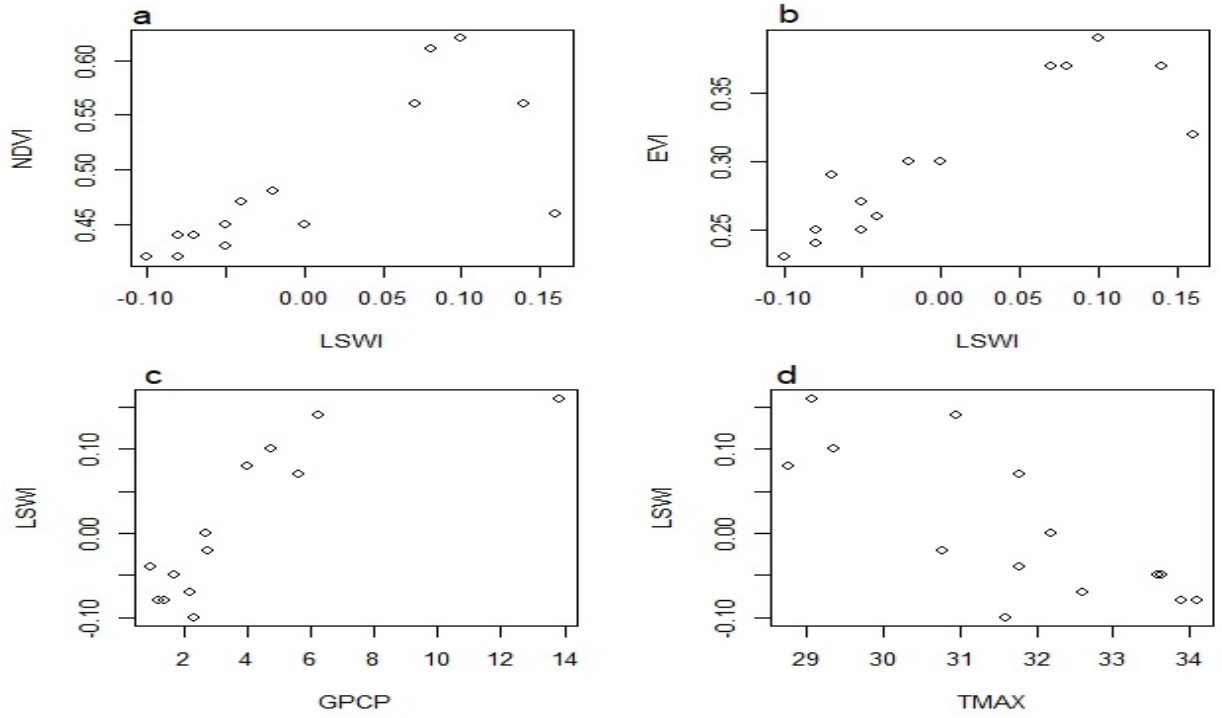

Figure 5.19 shows scatter plots showing the relationship between independent and dependent variables

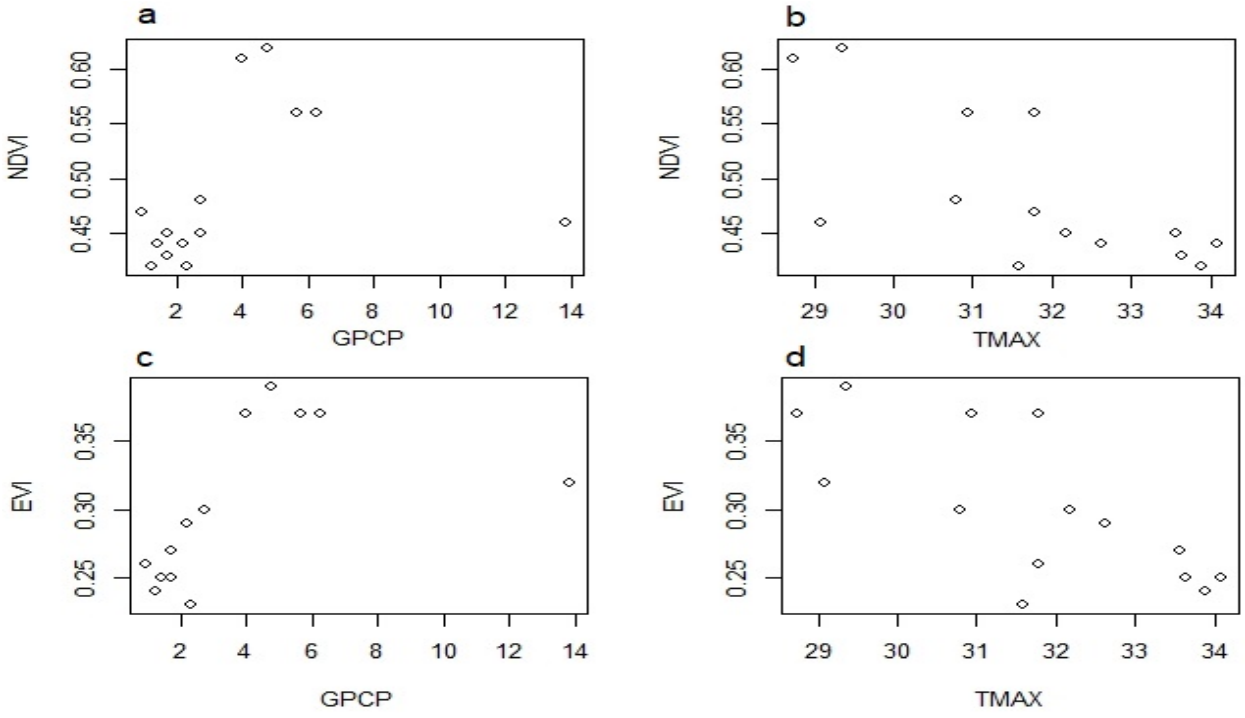

Figure 5.20: showing scatter plots showing the relationship between independent and dependent variables

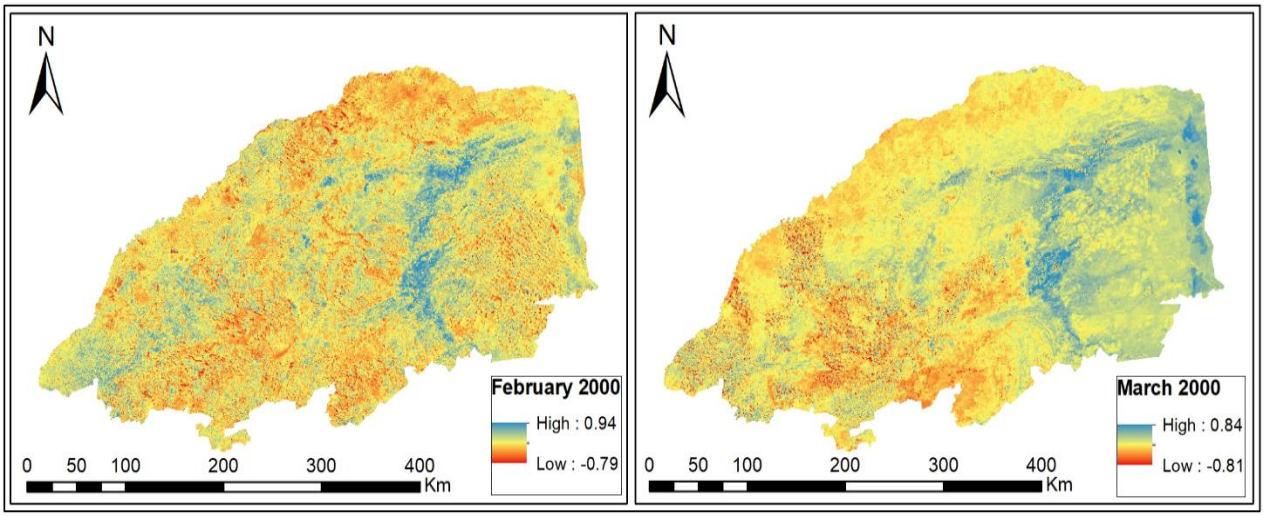

Figure 5.21: Spatial distribution of the LSWI over Limpopo Province during the wet condition of 1999/00

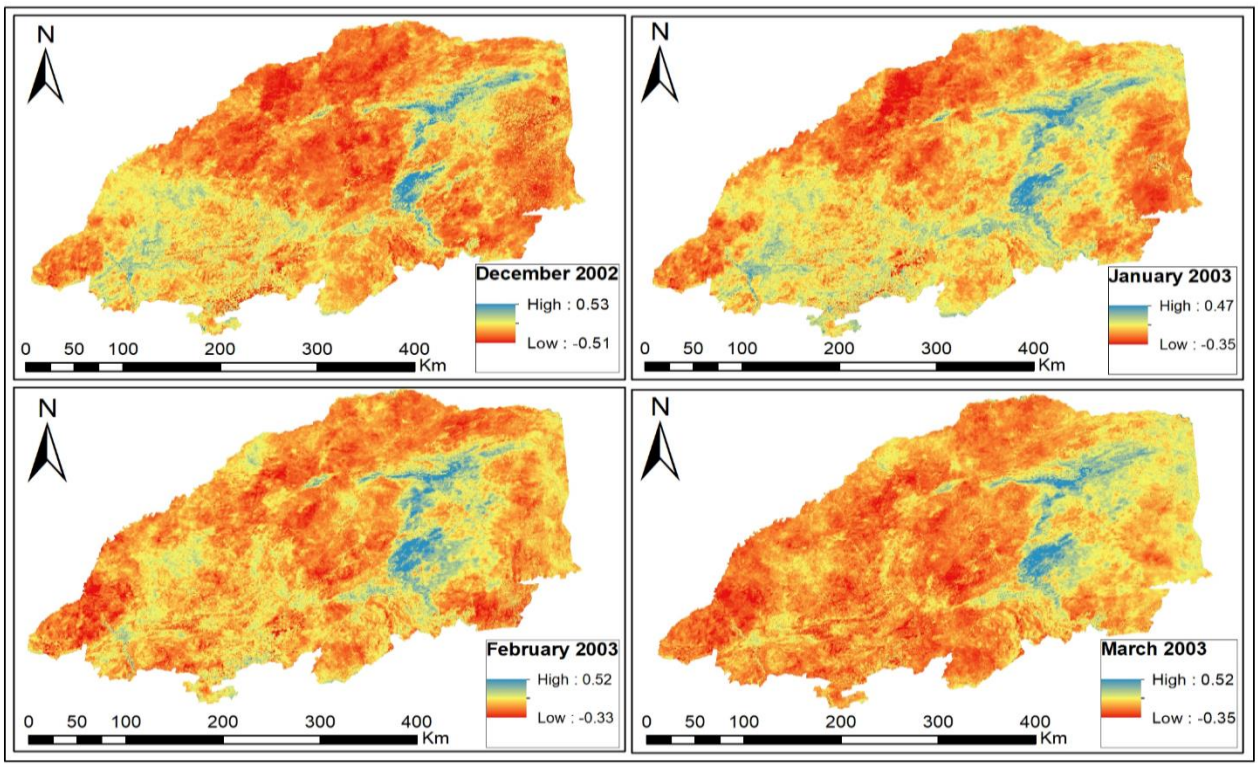

Figure 5.22: Spatial distribution of the LSWI over Limpopo Province during the drought condition of 2002/03

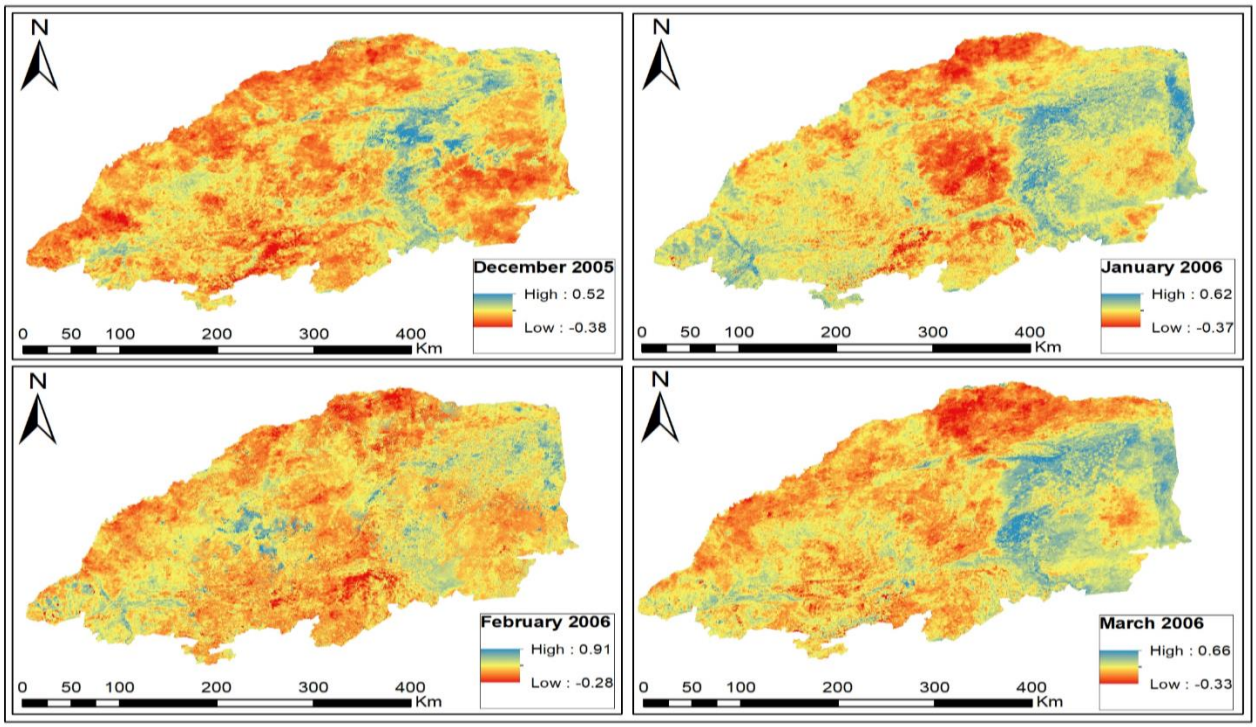

Figure 5.23: Spatial distribution of the LSWI over Limpopo Province during the wet condition of 2005/06

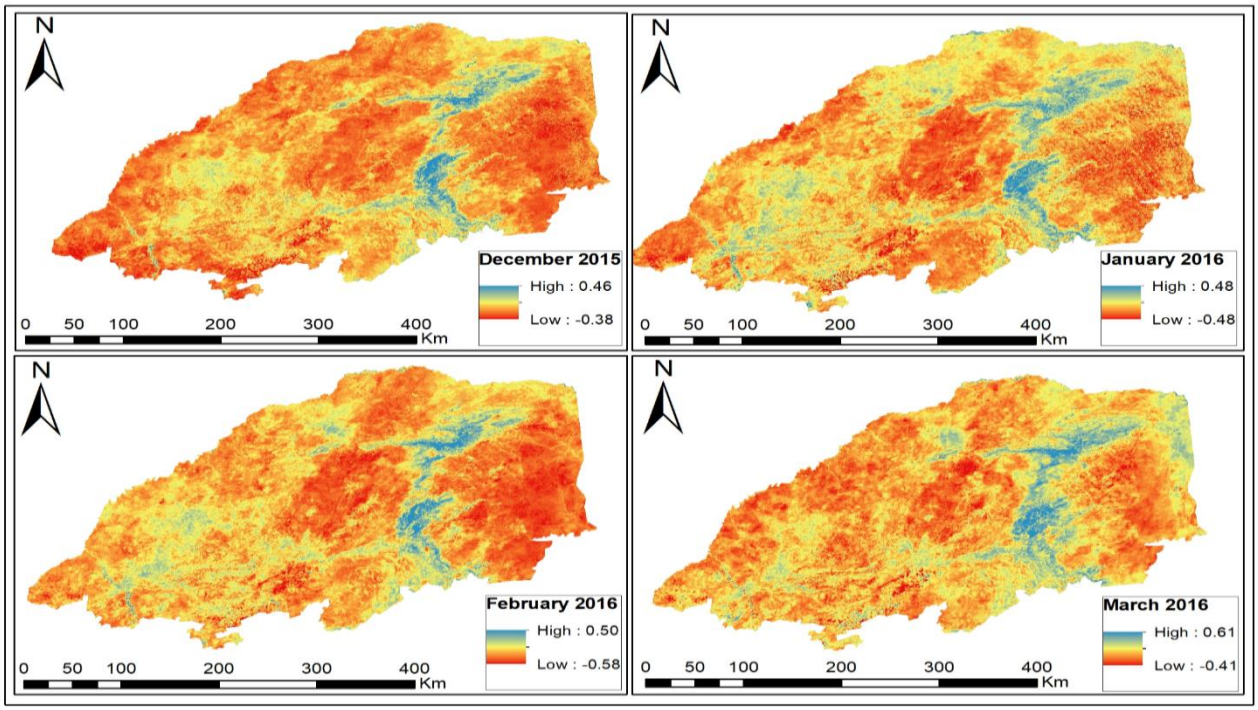

Figure 5.24: Spatial distribution of the LSWI over Limpopo Province during the drought condition of 2015/16

5.6 Summary

Understanding the spatial vegetation response and sensitivity to extreme climate is very crucial for water resource management, drought warning and disaster warning (Hua *et al.*, 2019). From the analysis, it is noted that, both VIs responded to rainfall variability in the area as vegetation in the area varies according to a different climate condition (Zoungrana *et al.*, 2015). However, differences between NDVI and EVI were noticed in accordance with their magnitude of response to rainfall variability over Limpopo Province. Figure 5.15 and Figure 5.16 show that EVI responded with lower values and reflectance over NDVI. The study employed NDVI, EVI, and LSWI observations for the assessment of vegetation response and sensitivity to climate extremes, of which NDVI was found to be relatively less sensitive to drought and wet conditions compared to EVI and LSWI. The finding corresponds to that of Bajgain *et al.*, (2015). As displayed from Figure 5.19 and Figure 5.20, the LSWI corresponds with the availability of water content such as precipitation (Figure 5.19 (c) and temperature (Figure 5.19 (d)). Figure 5.21, Figure 5.22, Figure 5.23, and Figure 5.54 displays the spatial distribution of LSWI based on the extreme cases (see section 5.4.2). stop

CHAPTER 6: CONCLUSIONS AND RECOMMENDATIONS

6.1 Introduction

Correlation analysis between vegetation indices and extreme climate variability serves as a tool probing vegetation responses and sensitivity to climate variability (Piao *et al.*, 2006). The study analysed extreme temperature and rainfall (drought and floods) changes and investigate their association with vegetation indices (NDVI, EVI, and LSWI) changes during the period 2000 – 2017 in Limpopo Province, South Africa. During the study period, four extreme weather events were identified with their characteristics and impacts on the vegetation condition over the region. The interaction between vegetation indices and climate variables is obvious, with variables strongly correlated with each other (Chuai *et al.*, 2013).

The study examined the relationship between vegetation indices namely, NDVI, EVI, and LSWI with each climatic factor identified (precipitation and temperature). The maps of each variable were stratified according to extreme weather events over the region, followed by correlation analysis. The analysis examined the relation with drought and very wet conditions across Limpopo Province. The case study describing the characteristics of each extreme events i.e. drought (2002/03 and 20145/16) and floods (1999/00 and 2005/06) were discussed.

6.2 Synthesis of key findings

Globally, climatic extremes have a greater extent impacting all ecosystems (Field *et al.*, 2014). The climate condition over Limpopo Province is highly variable, subject to different rainfall and temperature patterns (Chikoore, 2016), with the influence of the available escarpment (Soutpansberg Mountain). Such climate condition has been recognized to have a distinctive influence on the vegetation dynamic and responses of vegetation (Fu and Li, 2010). The study examined the relationship between vegetation indices and weather patterns over the region during drought years and floods years. The analysis concluded that the drought condition identified over the region confer with the findings of Chikoore, (2016).

6.2.1 Climate drivers of vegetation response

Globally, climate variables (temperature and water availability either in the form of moisture or rainfall) have been identified as the main drivers of vegetation productivity such as response and sensitivity (Seddon *et al.*, 2016). The GPCP precipitation was strongly associated with temperatures ($r = -0.66$ and $p = 0.010652$), with a decline in precipitation associated with an

increase in temperature, and LSWI ≤ 0. The findings correspond to those of Bajgain *et al.*, (2015), where LSWI plays a key role in the availability of water content. The region was subjected to the most severe floods in 1999/00 (SPEI > 1.5 to 1.99) influenced by TCs Eline impacting most of southern Africa countries, such as South Africa, Zimbabwe, and Mozambique (Chikoore *et al.*, 2015) with Limpopo Province being the most affected province in South Africa. The 1999/00 floods were followed by the 2005/06 (SPEI > 1.0 to 1.50) extreme floods. The wet conditions have been associated with available water content or moisture (LSWI > 0).

From the identified extreme weather events, also the drought conditions in 2002/03 (SPEI < -1.5 to -1.99) and 2015/16 (SPEI < -1.5 to -1.99) with 2015/16 were recorded as the most severe drought. It was observed from the interannual rainfall time series that the highest peak recorded was in 1999/00 with the absolute value of 2mm/day to 5mm/day and 2005/06 with absolute values 2mm/day to 3mm/day, also with the lowest rainfall to fine conditions recorded in 2002/03 with absolute value -1mm/day to -2mm/day and 2015/16 with absolute values between -1mm/day to -2.5mm/day in the summer seasons over Limpopo Province. However, there were other years that appeared to have common characteristics in terms of wet or dry. The interannual time series of temperatures also show a similar pattern, however with the lowest temperatures during wet years and highest during the dry year. The summer season of 1999/00 was observed to have the lowest temperature of 23°C and 2015/16 was with the highest temperature at 35°C.

6.2.2 Vegetation response

The study, involved different vegetation indices i.e. LSWI, NDVI, and EVI to study the vegetation condition in relation to extreme weather events. The negative impacts of two cases of droughts of 2002/03 and 2015/16 over Limpopo province were very apparent as documented by lower NDVI, EVI and LSWI values. Amongst examined vegetation indices, the sensitivity of vegetation to drought and floods showed different levels of response with LSWI, NDVI, and EVI respectively. The NDVI showed a lag delay of response to extreme floods as it is one month behind heavy rainfall.

From the analysis, vegetation showed variability in response to extreme drought and wet conditions. Due to heavy rainfall, vegetation showed a lag time response by one month after heavy rainfall (Thenkabail *et al.*, 2004). During heavy rainfall in 1999/00 and 2005/06 vegetation responded after a month reaching the highest peak in March with 0.62 (1999/00) and 0.60 (2005/06). The same applies to EVI findings, with the highest peak reached in March 0.42 (1999/00) and 0.40 (2005/06). The results indicate that, the vegetation shows a greening trend

during wet conditions and a decline in vegetation greening during drought conditions. The correlation analysis showed that precipitation and temperature were the limiting factors impacting vegetation response to growth and greening seasons.

6.2.3 Vegetation Sensitivity

As observed in Figure 4.3 and Figure 4.4 of the summer seasons, Limpopo Province exhibit both drought and wet conditions. Vegetation condition showed a greening trend during the wet season with r = 0.53 and r = 0.31 respectively. The study used EVI and LSWI to identify vegetation sensitivity to climate variability (Seddon *et al.*, 2016). From the analysis, the most sensitive indicators of vegetation conditions were LSWI followed by EVI and NDVI (Bajgain *et al*, 2015). The years of heavy rainfall were characterised by positive LSWI (with a positive association of 0.83) throughout the season with a decline in LSWI values associated with drought. The decline in LSWI shows that the vegetation had lost soil water content (Chaves *et al.*, 2003), therefore, giving a stronger signal of vegetation response and sensitivity than NDVI and EVI (Bajgain *et al.*, 2015).

During drought conditions, LSWI < 0 with temperature and evaporation rate increases resulting in the decline of water content from the soil. This is followed by EVI with low values showing mean values between 0.20 and 0.40 respectively. This was further supported by Chandrasekar *et al.*, (2010) that LSWI responds more directly to climate conditions than NDVI and EVI. The findings conclude that vegetation strongly relates to extreme weather events, in terms of response and sensitivity. However, the LSWI is more sensitive to vegetation conditions followed by EVI and NDVI (Bajgain *et al.*, 2015).

6.3 Conclusions

The study assessed the severity of extreme weather events namely, drought (2002/03 and 2015/16) and floods conditions (1999/00 and 2005/06) using MODIS-derived data with climate data i.e. GPCP precipitation and temperature, and examined the vegetation response and sensitivity to these extreme events using NDVI, EVI, and LSWI respectively. Therefore, it was found that NDVI, EVI, LSWI, and GPCP precipitation decreased while temperature increased during 2002/03 and 2015/16 droughts over Limpopo Province, as shown by lower values of both VIs and a negative correlation with both variables (-0.70, -0.73, -0.78, and -0.66 respectively). The condition changed during floods, as temperature decreased while variables (NDVI, EVI, LSWI, and GPCP precipitation) increased in 1999/00 and 2005/06.

The MODIS data were able to show the vegetation response and sensitivity to the extreme drought and floods over the study area. The GPCP precipitation and temperature maximum were used to detect changes in the times series to identify the trend on climate variables estimating the time and number of extreme events. The Standardized Precipitation-Evapotranspiration Index (SPEI) was also used to characterise extreme drought and floods in terms of magnitudes and severity.

The interannual and seasonal cycles over Limpopo Provinces are the first steps towards understanding the rainfall distribution and seasonal cycles. Over the region, the highest rainfall is received during the austral summer season from October to March with its peaks from December to February (Chikoore, 2016). The same implies to temperature records over Limpopo Province. The time series of GPCP precipitation and temperature detected to change the same as SPEI. Over the region, heavy rainfall is associated with low temperatures which indicate low evaporation of soil moisture and reduced vegetation stress (Chandrasekar *et al.*, 2010). Time series of GPCP Precipitation and temperature estimated floods in 1999/00 and 2005/06 and droughts in 2002/03 and 2015/16 and the SPEI showed at that time the intensity and magnitude were severe to extreme (1999/00), moderate to extreme (2005/06), moderate to severe (2002/03) and moderate to severe (2015/16) respectively. Therefore, changes in the vegetation condition were caused by extreme floods and droughts.

Based on the analysis, it can be concluded that the rainfall interannual variability and temperature interannual anomalies, SPEI 6 1999/00 and 2005/06 were found to have the most severe floods whereas 2002/03 and 2015/16 were found to have the most severe droughts throughout Limpopo Province. In 1999/00 and 2005/06 lowest temperature anomalies hit Limpopo Province; followed by increased precipitation causing more floods. However, high-temperature anomalies hit Limpopo Province; and a reduced rainfall occurred in 2002/03 and 2015/16 causing more regional drought events.

MODIS-data were employed (NDVI, EVI, and LSWI) for observations that are more detailed in characteristic features of plant conditions and plant greenness and NDVI were found to be less sensitive to extreme weather events compared to EVI and LSWI (Bajgain *et al.*, 2015). The VIs was employed as a monitoring indicator for extreme weather events, to measure the extremes by the level of severity by integrating satellite observations. Based on the extreme events i.e. droughts and floods identified, the VIs was used to measure the impacts imposed by such events. the study demonstrated a strong relationship between variables over the region.

6.4 Recommendations

The results of the study serve as a baseline data and scientific basis for better understating extreme climate and vegetation response interactions for supporting the policy designation of water resource management and planning to reduce the impacts of such extremes to ecosystems in a semi-arid environment. Based on the information about climate and vegetation relationship, localized regional trends of precipitation, temperature maximum and SPEI during drought and floods conditions, as well as characteristics of extreme weather events can be used as an early warning of the potentially extreme weather events by policymakers. Wherein vegetation indices can be used to monitor and validate the impacts that drought and floods are causing over the area.

6.4.1 Biodiversity Management

It is essential to monitor the on-going process of vegetation for sustainable biodiversity management. However, to achieve sustainable biodiversity management and assess hazard development, it is necessary for locals, policymakers, foresters, and other authorities associated with biodiversity or ecosystems to generate planning models. The findings of the study, provide detailed spatial and temporal changes and the response of vegetation greenness and explored how climate affected the vegetation health, setting a baseline data and scientific suggestions for local biodiversity or environment and natural resource management that can be used to facilitate sustainable development of the ecosystems.

As shown in Figure 5.18, a significant positive correlation between NDVI, EVI and LSWI and precipitation in the summer season was observed with a negative correlation with temperature respectively. Additionally, the context of study is covered by different types of land covers (Figure 5.1), dominated by grasslands accounting 110568 Area Km^2. The results of the study could be used as baseline data for studying and understanding the vegetation of the area for sustainable management of the ecosystems. With enough details or information about the vegetation, it can be possible to generate policies and launch programs to save ecosystems and the environment.

6.4.2 Land Use/ Land Cover Management

The findings of the study play a significant role in biodiversity officers, foresters, and policymakers in monitoring and planning programs at local and regional levels. The results entail better information on the utilization aspects, meanwhile playing an important role in biodiversity officers,

foresters, and policymakers in the formation of policies and programs required for development planning. The results of the study could provide details to the forester, community, and policymakers to understand the dynamics of land covers and their response to temperature and precipitation. Studying vegetation change also helps in identifying changes that are occurring in the ecosystems and environment.

The land covers such as wetlands, which are over-exploited as they present land cover consisting of the configuration of water, forests and herbaceous cover (Yang *et al.*, 2017), misused and covered into croplands. Therefore, the study will help policymakers, community member i.e. farmers and foresters into development strategies that will help conserve biodiversity through proper land use management. This could be achieved by proper land use and land cover planning by decision-makers, and foresters. Vegetation analysis could also prove to be useful in monitoring and assigning proper land use and land covers. Satellite remote sensing or vegetation analysis could also be used to identify poor land cover planning.

6.5 Recommendations for Future Work

The study outlined the impacts of extreme weather events on vegetation, as well as changes in the characteristics of drought and floods over Limpopo Province. The frequency of extreme weather events has changed, becoming more frequent in the past impacting vegetation over the region. Therefore, the study recommends an annual assessment of the extreme impacts on vegetation over time, such as a time series analysis (TSA) of Vegetation change over time using different satellites and indices datasets, for different seasons. For future studies, there is a need to determine level of significances on the trends.

Using different vegetation indices, a detailed study monitoring vegetation response. There is a need to introduce real-time monitoring systems, which may be easy to maintain that could someday be used as a warning system of such extremes. Vegetation drone monitoring could be used to provide real-time monitoring systems.

References

Abramowitz, M. and Stegun, I.A. 1964. *Handbook of mathematical functions*: with formulas, graphs, and mathematical tables (Vol. 55). Courier Corporation.

Abramowitz, M. and Stegun, I.A. 1965. Handbook of mathematical functions with formulas, graphs, and mathematical table. In *US Department of Commerce*. National Bureau of Standards Applied Mathematics series 55.

Adhikari, R. and Agrawal, R.K. 2013. An introductory study on time series modeling and forecasting. *arXiv preprint arXiv*:1302.6613.

Aihui, H.A.N. 2004. Method of Abstracting the Desertification Sensitive Areas through Analysis of the Time Series of MODIS Vegetation Indices [J]. *Forest Resources Management*, 1(2):57-60.

Alexander, L.V., Zhang, X., Peterson, T.C., Caesar, J., Gleason, B., Klein Tank, A.M.G., Haylock, M., Collins, D., Trewin, B., Rahimzadeh, F. and Tagipour, A. 2006. Global observed changes in daily climate extremes of temperature and precipitation. *Journal of Geophysical Research: Atmospheres*, 111(D5).

Alexander, L.V., Hope, P., Collins, D., Trewin, B., Lynch, A. and Nicholls, N. 2007. Trends in Australia's climate means and extremes: a global context. *Australian Meteorological Magazine*, 56(1): 1-18.

Allen, C.D., and Breshears, D.D., 2007. Climate-induced forest dieback as an emergent global phenomenon*. Eos, Transactions American Geophysical Union, 88(47)*: 504-504.

Allen, C.D., Macalady, A.K., Chenchouni, H., Bachelet, D., McDowell, N., Vennetier, M., Kitzberger, T., Rigling, A., Breshears, D.D., Hogg, E.T. and Gonzalez, P. 2010. A global overview of drought and heat-induced tree mortality reveals emerging climate change risks for forests. *Forest ecology and management,* 259(4): 660-684.

Allen, M.R. and Ingram, W.J. 2002. Constraints on future changes in climate and the hydrologic cycle. *Nature*, 419(6903), :224-232.

Al-Mahdi, A.M. and Maina, M.L. 2013. The Role of GIS and Remote Sensing in Mapping the Distribution of Greenhouse Gases. *European Scientific Journal, ESJ*, 9(36).

Arnone, J.A., Jasoni, R.L., Lucchesi, A.J., Larsen, J.D., Leger, E.A., Sherry, R.A., Luo, Y., Schimel, D.S. and Verburg, P.S. 2011. A climatically extreme year has large impacts on C4 species in tallgrass prairie ecosystems but only minor effects on species richness and other plant functional groups. *Journal of Ecol*, 99(3), :678-688.

Auclair, A.N. 1993. Extreme climatic fluctuations as a cause of forest dieback in the Pacific Rim. *Water, Air, and Soil Pollution*, 66(3-4): 207-229.

Bailey LD, van de Pol M. 2016 Tackling extremes: challenges for ecological and evolutionary research on extreme climatic events. *Journal of Animal Ecology. 85*: 85–96.

Bajgain, R., Xiao, X., Wagle, P., Basara, J. and Zhou, Y. 2015. Sensitivity analysis of vegetation indices to drought over two tallgrass prairie sites. *ISPRS Journal of Photogrammetry and Remote Sensing*, 108: 151-160.

Barbosa, H.A., Huete, A.R. and Baethgen, W.E. 2006. A 20-year study of NDVI variability over the Northeast Region of Brazil. *Journal of Arid Environments, 67(2)*: 288-307.

Baudoin, M.A., Vogel, C., Nortje, K. and Naik, M. 2017. Living with drought in South Africa: lessons learnt from the recent El Niño drought period. *International Journal of Disaster Risk Reduction*, 23: 128-137.

Beck, P.S., Atzberger, C., Høgda, K.A., Johansen, B. and Skidmore, A.K. 2006. Improved monitoring of vegetation dynamics at very high latitudes: A new method using MODIS NDVI. *Remote Sensing of Environment, 100(3)*: 321-334.

Beguería, S., Vicente-Serrano, S.M., Reig, F. and Latorre, B. 2014. Standardized precipitation evapotranspiration index (SPEI) revisited: parameter fitting, evapotranspiration models, tools, datasets, and drought monitoring. *International Journal of Climatology*, 34(10): 3001-3023.

Behera, S.K., Luo, J.J., Masson, S., Yamagata, T., Delecluse, P., Gualdi, S. and Navarra, A. 2003. Impact of the Indian Ocean Dipole on the East African short rains: A CGCM study. *CLIVAR exchanges*, 27(4): 3-5.

Behera, S.K., Luo, J.J., Masson, S., Delecluse, P., Gualdi, S., Navarra, A. and Yamagata, T. 2005. Paramount impact of the Indian Ocean dipole on the East African short rains: A CGCM study. *Journal of Climate, 18(21)*: 4514-4530.

Bhuiyan, C., 2004, July. Various drought indices for monitoring drought condition in Aravalli terrain of India. In *Proceedings of the XXth ISPRS Congress, Istanbul, Turkey*: 12-23.

Bjerknes, J. 1966. A possible response of the atmospheric Hadley circulation to equatorial anomalies of ocean temperature. *Tellus*, 18(4) :820-829.

Black, E. 2005. The relationship between Indian Ocean sea–surface temperature and East African rainfall. Philosophical Transactions of the Royal Society of London A: *Mathematical, Physical and Engineering Sciences*, 363(1826): 43-47.

Breshears, D.D., Cobb, N.S., Rich, P.M., Price, K.P., Allen, C.D., Balice, R.G., Romme, W.H., Kastens, J.H., Floyd, M.L., Belnap, J. and Anderson, J.J. 2005. Regional vegetation die-off in response to global-change-type drought. *Proceedings of the National Academy of Sciences*, 102(42): 15144-15148.

Bromley, D. 2002. Comparing corporate reputations: League tables, quotients, benchmarks, or case studies?. *Corporate reputation review*, 5(1): 35-50.

Brotherton, S.J. and Joyce, C.B. 2015. Extreme climate events and wet grasslands: plant traits for ecological resilience. *Hydrobiologia, 750(1)*: 229-243.

Campbell, J.B. 2007. *Introduction to Remote Sensing*, 4th edn. New York, The Guilford Press

Castillo, E. 1988. *Extreme Value Theory in Engineering*, Statistical Modeling and Decision Science, Academic Press Inc., Boston, MA

Cao, C., Ungar, S., Lecomte, P., Fox, N., Xiong, X., Henry, P., Buck, C., Stenssas, G., Zhan, X. and Campbell, P. 2008, July. Toward consistent satellite calibration and validation for GEOSS interoperability. *In Geoscience and Remote Sensing Symposium, 2008. IGARSS 2008. IEEE International*, 1: I-300.

Chang, S., Wu, B., Yan, N., Davdai, B. and Nasanbat, E., 2017. Suitability assessment of satellite-derived drought indices for Mongolian grassland. *Remote Sensing, 9(7)*.: 650.

Chandola, V., Banerjee, A. and Kumar, V. 2009. Anomaly detection: A survey. *ACM computing surveys (CSUR)*, 41(3):1-58.

Chandrasekar, K., Sesha Sai, M.V.R., Roy, P.S. and Dwevedi, R.S. 2010. Land Surface Water Index (LSWI) response to rainfall and NDVI using the MODIS Vegetation Index product. *International Journal of Remote Sensing*, 31(15):3987-4005.

Chen, Z., Elvidge, C.D. and Groeneveld, D.P. 1998. Vegetation change detection using high spectral resolution vegetation indices. Remote Sensing Change detection techniques, 2395.

Chen, A., He, B., Wang, H., Huang, L., Zhu, Y. and Lv, A. 2015. Notable shifting in the responses of vegetation activity to climate change in China. *Physics and Chemistry of the Earth, Parts A/B/C*, (87): 60-66.

Chen, T., Werf, G.R., Jeu, R.A.M., Wang, G. and Dolman, A.J. 2013. A global analysis of the impact of drought on net primary productivity. *Hydrology and Earth System Sciences*, 17(10): 3885-3894.

Chang, J., Hansen, M.C., Pittman, K., Carroll, M. and DiMiceli, C. 2007. Corn and soybean mapping in the United States using MODIS time-series data sets. *Agronomy Journal*, 99(6): .1654-1664.

Chaves, M.M., Flexas, J. and Pinheiro, C. 2009. Photosynthesis under drought and salt stress: regulation mechanisms from whole plant to cell. *Annals of botany*, 103(4): 551-560.

Chikoore, H., Vermeulen, J.H. and Jury, M.R. 2015. Tropical cyclones in the Mozambique Channel: January–March 2012. *Natural Hazards*, 77(3): 2081-2095.

Chikoore, H. 2016. *Drought in Southern Africa: structure, characteristics and impacts* (Doctoral dissertation, University of Zululand).

Chuai, X.W., Huang, X.J., Wang, W.J. and Bao, G. 2013. NDVI, temperature and precipitation changes and their relationships with different vegetation types during 1998–2007 in Inner Mongolia, China. *International Journal of Climatology*, 33(7):1696-1706.

Coles, S., Bawa, J., Trenner, L. and Dorazio, P. 2001*. An introduction to statistical modeling of extreme values*, 208: 208. London: Springer.

Collins, S.L., Belnap, J., Grimm, N.B., Rudgers, J.A., Dahm, C.N., D'odorico, P., Litvak, M., Natvig, D.O., Peters, D.C., Pockman, W.T. and Sinsabaugh, R.L. 2014. A multiscale, hierarchical model of pulse dynamics in arid-land ecosystems. *Annual Review of Ecology, Evolution, and Systematics*, 45: 397-419.

Compo, G.P., Whitaker, J.S., Sardeshmukh, P.D., Matsui, N., Allan, R.J., Yin, X., Gleason, B.E., Vose, R.S., Rutledge, G., Bessemoulin, P. and Brönnimann, S. 2011. The twentieth century reanalysis project. *Quarterly Journal of the Royal Meteorological Society*, 137(654): 1-28.

Congalton, R.G. 1991. A review of assessing the accuracy of classifications of remotely sensed data. *Remote sensing of environment*, 37(1) :35-46

Congalton, R.G., Gu, J., Yadav, K., Thenkabail, P. and Ozdogan, M. 2014. Global land cover mapping: A review and uncertainty analysis. *Remote Sensing*, 6(12):12070-12093.

Cook, C., Reason, C.J. and Hewitson, B.C. 2004. Wet and dry spells within particularly wet and dry summers in the South African summer rainfall region. *Climate Research*, 26(1): 17-31.

Coppin, P., Jonckheere, I., Nackaerts, K., Muys, B. and Lambin, E. 2004. Review ArticleDigital change detection methods in ecosystem monitoring: a review. *Int. J. Remote Sens*, 25(9): 1565-1596

Córdoba, M.A., Fuentes, M., Guinness, J. and Xie, L. 2018. Multivariate Spatial-Temporal Variable Selection with Applications to Seasonal Tropical Cyclone Modeling. *arXiv preprint arXiv:1805.03318*.

CSIRO and Bureau of Meteorology. Climate Change in Australia. Technical Report 2007. www.climatechangeinaustralia.gov.au. Last accessed 10 November, 2017.

Dahlman, L. 2009. Climate variability: Oceanic Niño Index. *Climate Watch Magazine*, *30*. Retrieved from, (https://www.climate.gov/news-features/understanding-climate/climate-variability-oceanic-ni%C3%B1o-index). Last accessed 09 November, 2017.

Dale, V.H., Joyce, L.A., McNulty, S. and Neilson, R.P. 2000. The interplay between climate change, forests, and disturbances. *Science of the Total Environment*, 262(3): 201-204.

Dangermond, J. and Artz, M. 2010. *Climate change is a geographic problem: The geographic approach to climate change*. Esri.

Data, C. 2009. Guidelines on analysis of extremes in a changing climate in support of informed decisions for adaptation. *World Meteorological Organization*.

Death, R.G., Fuller, I.C. and Macklin, M.G. 2015. Resetting the river template: the potential for climate-related extreme floods to transform river geomorphology and ecology. *Freshwater biology*, 60(12): 2477-2496.

Denniston, R.F., Villarini, G., Gonzales, A.N., Wyrwoll, K.H., Polyak, V.J., Ummenhofer, C.C., Lachniet, M.S., Wanamaker, A.D., Humphreys, W.F., Woods, D. and Cugley, J. 2015.

Extreme rainfall activity in the Australian tropics reflects changes in the El Niño/Southern Oscillation over the last two millennia. *Proceedings of the National Academy of Sciences*, 112(15): 4576-4581.

Donat, M.G., Alexander, L.V., Yang, H., Durre, I., Vose, R., Dunn, R.J.H., Willett, K.M., Aguilar, E., Brunet, M., Caesar, J. and Hewitson, B. 2013. Updated analyses of temperature and precipitation extreme indices since the beginning of the twentieth century: the HadEX2 dataset. *J. Geophys. Res: Atmospheres*, 118(5): 2098-2118.

Donat, M.G., Lowry, A.L., Alexander, L.V., O'Gorman, P.A. and Maher, N. 2017. Addendum: More extreme precipitation in the world's dry and wet regions. *Nature Climate Change*, 7(2) :154-158.

Dutta, D., Kundu, A., Patel, N.R., Saha, S.K. and Siddiqui, A.R. 2015. Assessment of agricultural drought in Rajasthan (India) using remote sensing derived Vegetation Condition Index (VCI) and Standardized Precipitation Index (SPI). *The Egyptian Journal of Remote Sensing and Space Science*, 18(1):53-63.

Duadze, S.E.K., 2004. *Land use and land cover study of the savannah ecosystem in the Upper West Region (Ghana) using remote sensing* (Vol. 16). Cuvillier Verlag.

Dyson, L.L. and Van Heerden, J. 2001. The heavy rainfall and floods over the northeastern interior of South Africa during February 2000. *South African Journal of Science*, 97(3-4): 80-86.

Easterling, D.R., Meehl, G.A., Parmesan, C., Changnon, S.A., Karl, T.R. and Mearns, L.O. 2000. Climate extremes: observations, modeling, and impacts. *Science*, 289(5487): 2068-2074.

Ebi, KL and Villalobos Prats, E. 2015. Health in National Climate Change Adaptation Planning. *Annals of Global Health*, 81: 418-426.

Edenhofer, O. ed. 2015. *Climate change 2014: mitigation of climate change* (Vol. 3). Cambridge University Press.

Engelbrecht, F., Adegoke, J., Bopape, M.J., Naidoo, M., Garland, R., Thatcher, M., McGregor, J., Katzfey, J., Werner, M., Ichoku, C. and Gatebe, C. 2015. Projections of rapidly rising surface temperatures over Africa under low mitigation. *Environmental Research Letters*, 10(8): 085004.

Embrechts, P., Klüppelberg, C. and Mikosch, T. 1997. Modelling extremal events, volume 33 of Applications of Mathematics.

Ferreira, A. and de Haan, L. 2015. On the block maxima method in extreme value theory: PWM estimators. *The Annals of statistics*, 43(1): 276-298.

Friedl, M. A., Sulla-Menashe, D., Tan, B., Schneider, A., Ramankutty, N., Sibley, A., and Huang, X. 2010. MODIS Collection 5 global land cover: Algorithm refinements and characterization of new datasets. *Remote Sensing of Environment*, 114(1): 168-182.

Frischknecht, M., Münnich, M. and Gruber, N. 2015. Remote versus local influence of enso on the california current system. *Journal of Geophysical Research: Oceans*, 120(2): 1353-1374.

Fu, B., Li, S., Yu, X., Yang, P., Yu, G., Feng, R. and Zhuang, X. 2010. Chinese ecosystem research network: progress and perspectives. *Ecological Complexity*, 7(2): 225-233.

Gao, B. C. 1996. NDWI-A normalized difference water index for remote sensing of vegetation liquid water from space. *Remote Sensing of Environment*, Vol.58, pp. 257-266.

Garcia-Herrara, R., Diaz, J., Trigo, R.M., Luterbacher, J. and Fischer, E.M. 2010. A review of the European Summer Heat Wave of 2003. *Critical Reviews in Environmental Science and Technology*, 40: 267–306.

Gillett, N.P., Kell, T.D. and Jones, P.D. 2006. Regional climate impacts of the Southern Annular Mode. *Geophysical Research Letters*, *33*(23).

Gitlin, A.R., Sthultz, C.M., Bowker, M.A., Stumpf, S., Paxton, K.L., Kennedy, K., Muñoz, A., Bailey, J.K. and Whitham, T.G. 2006. Mortality gradients within and among dominant plant populations as barometers of ecosystem change during extreme drought. *Conservation Biology*, 20(5): 1477-1486.

Goda, Y., 1989. On the methodology of selecting design wave height. In Coastal *Engineering* :899-913.

Goodin D.G., 2004. Climate committee takes aim at extreme climatic events. *The Network Newsletter* [of LTER], 17(2).

Gordon, H.B., Whetton, P.H., Pittock, A.B., Fowler, A.M. and Haylock, M.R. 1992. Simulated changes in daily rainfall intensity due to the enhanced greenhouse effect: implications for extreme rainfall events. *Climate Dynamics*, 8(2): 83-102.

Green, K., Congalton, R.G. and Tukman, M. 2017. *Imagery and GIS: Best Practices for Extracting Information from Imagery*. Esri Press.

Gregg, J.W., Jones, C.G. and Dawson, T.E. 2003. Urbanization effects on tree growth in the vicinity of New York City. *Nature*, *424*(6945): 183-187.

Griffiths, P., Hostert, P., Gruebner, O., van der Linden, S. 2010. Mapping megacity growth with multi-sensor data. *Remote Sensing of Environment*. 114: 426–439.

Groisman, P.Y. and Knight, R.W. 2008. Prolonged dry episodes over the conterminous United States: New tendencies emerging during the last 40 years. *Journal of Climate,* 21(9):1850-1862.

Gutschick, V.P. and BassiriRad, H. 2003. Extreme events as shaping physiology, ecology, and evolution of plants: toward a unified definition and evaluation of their consequences. *New Phytologist*, 160(1): 21-42.

Guttman, N.B. 1998. Comparing the Palmer drought index and the standardized precipitation index. *JAWRA Journal American Water Resource*, 34(1): 113-121.

Hamada, J.I., Mori, S., Kubota, H., Yamanaka, M.D., Haryoko, U., Lestari, S., Sulistyowati, R. and Syamsudin, F. 2012. Interannual rainfall variability over northwestern Jawa and its relation to the Indian Ocean Dipole and El Niño-Southern Oscillation events. *Sola*, (8): 69-72.

Han, W., Meehl, G.A., Rajagopalan, B., Fasullo, J.T., Hu, A., Lin, J., Large, W.G., Wang, J.W., Quan, X.W., Trenary, L.L. and Wallcraft, A. 2010. Patterns of Indian Ocean sea-level change in a warming climate. *Nature Geoscience*, *3*(8): 546.

Hanley, D.E., Bourassa, M.A., O'Brien, J.J., Smith, S.R. and Spade, E.R. 2003. A quantitative evaluation of ENSO indices. *Journal of Climate*, 16(8): 1249-1258.

Hao, F., Zhang, X., Ouyang, W., Skidmore, A.K. and Toxopeus, A.G. 2012. Vegetation NDVI linked to temperature and precipitation in the upper catchments of Yellow River. *Environmental Modeling and Assessment*, 17(4):389-398.

Hauke, J. and Kossowski, T. 2011. Comparison of values of Pearson's and Spearman's correlation coefficients on the same sets of data. *Quaestiones geographicae*, 30(2): 87-93.

Heim Jr, R.R. 2002. A review of twentieth-century drought indices used in the United States*. Bull. Am. Meteorol. Soc*, 83(8): 1149-1165.

Herold, M., Mayaux, P., Woodcock, C., Baccini, A., Schmullius, C. 2008. Some challenges in global land cover mapping: an assessment of agreement and accuracy in existing 1 km datasets. *Remote Sensing of Environment*. 112: 2538–2556.

Hussein, S.O., Kovács, F. and Tobak, Z. 2017. Spatiotemporal assessment of vegetation indices and land cover for Erbil city and its surrounding using MODIS imageries. *Journal of Environmental Geography,* 10(1-2): 31-39.

Holben, B. and Justice, C. 1981. An examination of spectral band ratioing to reduce the topographic effect on remotely sensed data. *International journal of remote sensing*, 2(2): 115-133.

Hossain, F., Jeyachandran, I. and Pielke, R. 2009. Have large dams altered extreme precipitation patterns? *Eos, Transactions American Geophysical Union*, 90(48): 453-454.

Huang, K., Zhou, T. and Zhao, X. 2014. Extreme Drought-induced Trend Changes in MODIS EVI Time Series in Yunnan, China. In IOP Conference Series: *Environmental Earth Science*. (Vol. 17, No. 1, p. 012070). IOP Publishing.

Huber, D.G. and Gulledge, J. 2011. *Extreme weather and climate change: Understanding the link, managing the risk*. Arlington: Pew Center on Global Climate Change.

Hua, L., Wang, H., Sui, H., Wardlow, B., Hayes, M.J. and Wang, J. 2019. Mapping the spatial-temporal dynamics of vegetation response lag to drought in a semi-arid region. *Remote Sensing*, 11(16): 1873.

Huete, A., Justice, C. and Liu, H., 1994. Development of vegetation and soil indices for MODIS-EOS. *Remote Sensing of Environment*, 49(3): 224-234.

Huete, A.R., Liu, H.Q., Batchily, K., and van Leeuwen, W. 1997, A comparison of vegetation indices over a global set of TM images for EOS-MODIS, *Remote Sensing of Environment*., 59: 440-451

Huete, A., Justice, C. and Van Leeuwen, W. 1999. MODIS vegetation index (MOD13). *Algorithm theoretical basis document*, 3: 213.

Huete, A., Didan, K., Miura, T., Rodriguez, E.P., Gao, X. and Ferreira, L.G. 2002. Overview of the radiometric and biophysical performance of the MODIS vegetation indices. *Remote sensing of environment*, 83(1-2): 195-213.

Hussein, S.O., Kovács, F. and Tobak, Z. 2017. Spatiotemporal assessment of vegetation indices and land cover for Erbil city and its surrounding using MODIS imageries. *Journal of Environmental Geography*, 10(1-2):31-39.

Huyse, L., Chen, R. and Stamatakos, J.A. 2010. Application of generalized Pareto distribution to constrain uncertainty in peak ground accelerations. *Bull. Seismol. Soc. Am*, 100(1): 87-101.

IPCC (2007): Climate Change. The Physical Science Basis. Contribution of Working Group I to the Fourth Assessment Report of the Intergovernmental Panel on Climate Change. Cambridge University Press, Cambridge, United Kingdom and New York, NY, USA.

IPCC (2013) Climate change 2013: the physical science basis. In: Contribution of Working Group I to the Fifth Assessment Report of the Intergovernmental Panel on Climate Change. IPCC, Cambridge, UK and New York, NY: 1535

Jensen, J.R. 1996. *Introduction to Digital Image Processing: A remote sensing perspective, 2nd edn. Piscataway*. New Jersey.

Jensen, J.R. 2007. Remote sensing of vegetation. *Remote Sensing of the Environment: An Earth Resource Perspective. Pearson Prentice Hall, Upper Saddle River, NJ.*

Jentsch, A., Kreyling, J. and Beierkuhnlein, C. 2007. A new generation of climate-change experiments: events, not trends. *Frontiers in Ecology and the Environment*, 5(7): 365-374.

Jentsch, A. and Beierkuhnlein, C. 2008. Research frontiers in climate change: effects of extreme meteorological events on ecosystems. *Comptes Rendus Geoscience*, 340: 621–628.

Jentsch, A., Kreyling, J., Elmer, M., Gellesch, E., Glaser, B., Grant, K., Hein, R., Lara, M., Mirzae, H., Nadler, S.E. and Nagy, L. 2011. Climate extremes initiate ecosystem-regulating functions while maintaining productivity. *Journal of Ecology*, 99(3): 689-702.

Jiang, Z., Huete, A.R., Didan, K. and Miura, T. 2008. Development of a two-band enhanced vegetation index without a blue band. *Remote sensing of Environment*, 112(10): 3833-3845.

Jinghua, Z., Luguang, J., Zhiming, F. and Peng, L. 2012. Detecting effects of the recent drought on vegetation in southwestern China. *Journal of Resource and Ecology*, 3(1): 43-49.

Katz, R.W. and Brown, B.G. 1992. Extreme events in a changing climate: variability is more important than averages. *Climatic change*, 21(3): 289-302.

Karl, T.R., Knight, R.W. and Plummer, N. 1995. Trends in high-frequency climate variability in the 20th century. *Nature*, (377): 217–220.

Karl, T.R., Meehl, G.A., Peterson, T.C., Kunkel, K.E., Gutowski Jr, W.J. and Easterling, D.R., 2008. Executive summary in weather and climate extremes in a changing climate. Regions of focus: North America, Hawaii, Caribbean, and US Pacific Islands. *A Report by the US Climate Change Science Program and the Subcommittee on Global Change Research*.

Karnieli, A., Agam, N., Pinker, R.T., Anderson, M., Imhoff, M.L., Gutman, G.G., Panov, N. and Goldberg, A. 2010. Use of NDVI and land surface temperature for drought assessment: Merits and limitations. *Journal of climate*, 23(3): 618-633.

Kharin, V.V. and Zwiers, F.W. 2005. Estimating extremes in transient climate change simulations. *Journal of Climate*, 18(8): 1156-1173.

Kharin, V.V., Zwiers, F.W. and Zhang, X. 2005. Intercomparison of near-surface temperature and precipitation extremes in AMIP-2 simulations, reanalyses, and observations. *Journal of Climate*, 18(24): 5201-5223.

Kharin, V.V., Zwiers, F.W., Zhang, X. and Hegerl, G.C., 2007. Changes in temperature and precipitation extremes in the IPCC ensemble of global coupled model simulations. *Journal of Climate,* 20(8) :1419-1444.

Kharin, V.V., Zwiers, F.W., Zhang, X. and Wehner, M. 2013. Changes in temperature and precipitation extremes in the CMIP5 ensemble. *Climatic change*, 119(2): 345-357.

Kidston, J., Renwick, J.A. and McGregor, J. 2009. Hemispheric-scale seasonality of the Southern Annular Mode and impacts on the climate of New Zealand. *Journal of Climate*, *22*(18): 4759-4770.

Knight, D.B. and Davis, R.E. 2009. Contribution of tropical cyclones to extreme rainfall events in the southeastern United States. *Journal of Geophysical Research: Atmospheres*, 114(D23).

Kruger, A.C. and Shongwe, S. 2004. Temperature trends in South Africa: 1960–2003. International Journal of Climatology: *A Journal of the Royal Meteorological Society*, 24(15): 1929-1945.

Kubota, H. and Wang, B. 2009. How much do tropical cyclones affect seasonal and interannual rainfall variability over the western North Pacific? *Journal of Climate*, 22(20): 5495-5510.

Lawal, S., Lennard, C. and Hewitson, B. 2019. Response of southern African vegetation to climate change at 1.5 and 2.0° global warming above the pre-industrial level. *Climate Services:* 16: 100134.

Lei, Y. and Duan, A. 2011. Prolonged dry episodes and drought over China. *International Journal of Climatology*, 31(12):1831-1840.

Lenderink, G. and Van Meijgaard, E. 2008. Increase in hourly precipitation extremes beyond expectations from temperature changes. *Nature Geosci*, 1(8): 511.

Levey, K.M. and Jury, M.R. 1996. Composite intraseasonal oscillations of convection over southern Africa. *Journal of Climate*, 9(8): 1910-1920.

Li, C., Leal Filho, W., Yin, J., Hu, R., Wang, J., Yang, C., Yin, S., Bao, Y. and Ayal, D.Y. 2018. Assessing vegetation response to multi-time-scale drought across inner Mongolia plateau. *Journal of cleaner production*, 179: 210-216.

Lillesand, T.M. 1994. Ralph W. Kiefer. *Remote sensing and image interpretation*. 3rd ed. New York: John Wiley.

Lillesand, T.M. and R.W. Kiefer. 2002. *Remote sensing and Image Interpretation*, 4th edition, Joh Wiley and Sons, New York

Lillesand, T., Kiefer, R.W. and Chipman, J. 2014. *Remote sensing and image interpretation*. John Wiley and Sons: 611 – 620.

Limpopo, D.F.E.D., 2004. Limpopo Department of Finance and Economic Development. *Limpopo Province, State of the Environment Report (Phase 1).*

Lin, G., Phillips, S.L. and Ehleringer, J.R. 1996. Monosoonal precipitation responses of shrubs in a cold desert community on the Colorado Plateau. *Oecologia*, 106(1): 8-17.

Linacre, E. and Geerts, B., 1997. *Climates and weather explained*. Routledge.

Lopes, H.F., Nascimento, F.F. and Gamerman, D. 2011. In *preparation with Generalized Pareto models with time-varying tail behaviour*. Technical Report LES: UFRJ.

Lu, D. S, Mausel, P., Brondí´zio, E., and Moran, E. 2004. Change Detection Techniques; *International Journal of Remote Sensing*, 25 (12): 2365– 2407

Lu, D., Tian, H., Zhou, G., Ge, H. 2008. Regional mapping of human settlements in southeastern China with multisensor remotely sensed data. *Remote Sensing of Environment*. 112, 3668–3679

Marshall, J. and Plumb, R.A. 1989. Atmosphere, ocean and climate dynamics: an introductory text (Vol. 43). Academic Press: 259-292.

Maselli, F., Papale, D., Puletti, N., Chirici, G., Corona, P. 2009. Combining remote sensing and ancillary data to monitor the gross productivity of water-limited forest ecosystems. *Remote Sensing of Environment*. 113 (3):657-667

Mason, S.J. and Jury, M.R. 1997. Climatic variability and change over southern Africa: a reflection on underlying processes. *Progress in Physical Geography*, 21(1):23-50.

Masubelele, M.L., Hoffman, M.T., Bond, W.J. and Gambiza, J. 2014. A 50-year study shows grass cover has increased in shrublands of semi-arid South Africa. *Journal of Arid Environments*, 104: 43-51.

Matsushita, B., Yang, W., Chen, J., Onda, Y. and Qiu, G. 2007. Sensitivity of the enhanced vegetation index (EVI) and normalized difference vegetation index (NDVI) to topographic effects: a case study in high-density cypress forest. *Sensors*, 7(11): 2636-2651.

McBride, J.L., Mills, G. and Wain, A.G. 2009. November. The meteorology of Australian heatwaves. In *Modelling and Understanding High Impact Weather: Extended Abstracts of the Third CAWCR Modelling Workshop*: 91-94.

McDowell, N., Pockman, W.T., Allen, C.D., Breshears, D.D., Cobb, N., Kolb, T., Plaut, J., Sperry, J., West, A., Williams, D.G. and Yepez, E.A. 2008. Mechanisms of plant survival and mortality during drought: why do some plants survive while others succumb to drought?. *New phytologist*, 178(4) :719-739.

McElroy, M. and Baker, D.J., 2012. Climate extremes: Recent trends with implications for national security. Harvard University Center for the Environment.

McKee, T. B., N. J. Doesken, and J. Kliest. 1993: The relationship of drought frequency and duration to time scales. In *Proceedings of the 8th Conference of Applied Climatology*, 17(22): 179-183.

McKee, T.B. and Doesken, N.J., J. Kleist. 1995, “Drought Monitoring with Multiple Time Scales,” Preprints. *In 9th Conference on Applied Climatology* (15-20).

McVicar, T.R., Van Niel, T.G., Li, L.T., Roderick, M.L., Rayner, D.P., Ricciardulli, L. and Donohue, R.J. 2008. Wind speed climatology and trends for Australia, 1975–2006: Capturing the stilling phenomenon and comparison with near-surface reanalysis output. *Geophysical Research Letters*, 35(20).

Meehl, G.A., Karl, T., Easterling, D.R., Changnon, S., Pielke, R., Jr, Changnon, D. 2000. An introduction to trends in extreme weather and climate events: observations, socioeconomic impacts, terrestrial ecological impacts, and model projections. Bull. *American Meteorology Society*, 81, :413–416.

Meehl, G.A. and Tebaldi, C. 2004. More intense, more frequent, and longer lasting heat waves in the 21st century. *Science,* 305:994–997.

Meehl, G.A., Stocker, C.M., Bowker, T.F., Collins, C.M., Bowker, W.D., Friedlingstein, C.M., Bowker, P., Gaye, C.M., Bowker, A.T., Gregory, C.M., Bowker, J.M. 2007. Global Climate Projections. Climate Change: The Physical Science Basis. Contribution of Working Group I to the Fourth Assessment Report of the Intergovernmental Panel on Climate Change.

Melillo, J.M., Richmond, T.T. and Yohe, G. 2014. Climate change impacts in the United States. *Third national climate assessment*, 52.

Menenti, M., Jia, L., Azzali, S., Roerink, G., Gonzalez-Loyarte, M. and Leguizamon, S. 2010. Analysis of vegetation response to climate variability using extended time series of multispectral satellite images*. Maselli, F., Menenti, M., Brivio, PA (eds.). Remote Sensing Optical Observations of Vegetation Properties, Chapter 6*: 131-163.

Min, S.K., Zhang, X., Zwiers, F.W. and Hegerl, G.C. 2011. Human contribution to more-intense precipitation extremes. *Nature*, 470(7334):378-381.

Mishra, A.K. and Singh, V.P. 2010. A review of drought concepts. *Journal of hydrology*, 391(1-2): 202-216.

Moncrieff, G.R., Scheiter, S., Slingsby, J.A. and Higgins, S.I., 2015. Understanding global change impacts on South African biomes using Dynamic Vegetation Models. *South African Journal of Botany*, 101:16-23.

Mpandeli, S., Nesamvuni, E. and Maponya, P. 2015. Adapting to the impacts of drought by smallholder farmers in Sekhukhune district in Limpopo province, *South Africa. Journal of Agricultural Science*, 7(2): 115.

Mudelsee, M. 2010. Climate time series analysis: classical statistical and bootstrap methods: atmospheric and oceanographic Sciences Library, vol 42: 474.

Mueller, B. and Seneviratne, S.I. 2012. Hot days induced by precipitation deficits at the global scale. *Proceedings of the national academy of sciences*, 109(31): 12398-12403.

Muller, A., Reason, C.J.C. and Fauchereau, N. 2008. Extreme rainfall in the Namib Desert during late summer 2006 and influences of regional ocean variability. *International Journal of Climatology*, 28(8): 1061-1070.

Murtugudde, R., McCreary, J.P. and Busalacchi, A.J. 2000. Oceanic processes associated with anomalous events in the Indian Ocean with relevance to 1997–1998. *Journal of Geophysical Research: Oceans*, 105(C2): 3295-3306.

Nairn, J. and Fawcett, R. 2011. Defining heatwaves: heatwave defined as a heat-impact event servicing all. *Europe*, (220): 224.

NERC, 1975. Flood Studies Report. Natural Environment Research Council.

Nicholson, S.E. 1997. An analysis of the ENSO signal in the tropical Atlantic and western Indian Oceans. *International Journal of Climatology*, 17(4) :345-375.

Nicholls N, and Larsen S. 2011. Impact of drought on temperature extremes in Melbourne, Australia. *Australian Meteorology and Oceanographic journal. Jun*;61(2) :113-6.

O'Gorman, P.A. and Schneider, T. 2009. The physical basis for increases in precipitation extremes in simulations of 21st-century climate change. *Proceedings of the National Academy of Sciences*, 106(35) :14773-14777.

O'Gorman, P. A. 2012. Sensitivity of tropical precipitation extremes to climate change. *Nature Geosci*. 5:697–700

O'Gorman, P.A. 2015. Precipitation extremes under climate change. *Current climate change reports*, 1(2): 49-59.

Okorie, I.E. and Akpanta, A.C. 2015. Threshold Excess Analysis of Ikeja Monthly Rainfall in Nigeria. *International Journal of Statistics and Applications*, 5(1):15-20.

Overpeck, J.T. and Cole, J.E. 2006. Abrupt change in Earth's climate system. *Annual Review of Environment and Resources*., 31: 1-31.

Owrangi, M.A., Adamowski, J., Rahnemaei, M., Mohammadzadeh, A. and Sharifan, R.A. 2011. Drought monitoring methodology based on AVHRR images and SPOT vegetation maps. *Journal of water resource and protection*, 3(05): 325.

Palmer, W.C. 1965. *Meteorological drought* (Vol. 30). US Department of Commerce, Weather Bureau.

Parmesan, C., T.L. Root, and M.R. Willig. 2000. Impacts of extreme weather and climate on terrestrial biota. Bull. *American Meteorology Society*, 81(3:443-50.

Parmesan, C. and P. Martens. 2008: In press. Climate change, wildlife and human health. Chapter 14 in: SCOPE Assessment: "*Biodiversity, Global Change and Human Health*", [Sala, O.E., C. Parmesan, and L.A. Meyerson (eds.)]. Island Press.

Parmesan, C. and Martens, P. 2009. Climate change, wildlife, and human health. Biodiversity Change and Human Health: From Ecosystem Services to Spread of Disease, 69: 245-266.

Penalba, O.C. and Rivera, J.A. 2016. Precipitation response to El Niño/La Niña events in Southern South America-emphasis in regional drought occurrences. *Advances in Geosciences*, 42.

Piao, S., Wang, X., Ciais, P., Zhu, B., Wang, T.A.O. and Liu, J.I.E. 2011. Changes in satellite-derived vegetation growth trend in temperate and boreal Eurasia from 1982 to 2006. *Global Change Biology*, 17(10): 3228-3239.

Philander, S.G.H., Pacanowski, R.C., Lau, N.C. and Nath, M.J. 1992. Simulation of ENSO with a global atmospheric GCM coupled to a high-resolution, tropical Pacific Ocean GCM. *Journal of Climate*, 5(4): 308-329.

Ponette-González, A.G., Weathers, K.C. and Curran, L.M. 2010. Tropical land-cover change alters biogeochemical inputs to ecosystems in a Mexican montane landscape. *Ecological applications,* 20(7): 1820-1837.

Potop, V. and Možný, M. 2011, September. Examination of the effect of evapotranspiration as an output parameter in SPEI drought index in Central Bohemian region. In *Bioclimate: source and limit of social development. International Scientific Conference, Topoľčianky, Slovakia* (6-9).

Preston-Whyte, R.A. and Tyson, P.D. 1988. Atmosphere and weather of southern Africa. Oxford University Press.

Preston-Whyte, R.A and Tyson P.D. 2000. The weather and climate of southern Africa, Oxford University Press, Cape Town, SA:197

Prus-Glowacki W, Stephan BR. 1994. Genetic-Variation of Pinus sylvestris from Spain in Relation to Other European Populations. *Silvae Genet*, 43(1): 7–14.

Rahayu, A. 2013. Identification of Climate Change with Generalized Extreme Value (GEV) Distribution Approach. *Journal of Physics*: Conference Series 423(1): 012026

Rao, S.A., Chaudhari, H.S., Pokhrel, S. and Goswami, B.N. 2010. Unusual central Indian drought of summer monsoon 2008: role of southern tropical Indian Ocean warming. *Journal of Climate*, 23(19): 5163-5174.

Reason, C.J.C. and Keibel, A. 2004. Tropical cyclone Eline and its unusual penetration and impacts over the southern African mainland. *Weather and forecasting*, 19(5): 789-805.

Reynolds, J.F., Kemp, P.R., Ogle, K. and Fernández, R.J. 2004. Modifying the 'pulse–reserve'paradigm for deserts of North America: precipitation pulses, soil water, and plant responses. *Oecologia*, 141(2): 194-210.

Ropelewski, C.F. and Halpert, M.S. 1987. Global and regional scale precipitation patterns associated with the El Niño/Southern Oscillation. *Monthly weather review*, 115(8): 1606-1626.

Rosenzweig, C., Iglesias, A., Yang, X.B., Epstein, P.R. and Chivian, E. 2001. Climate change and extreme weather events; implications for food production, plant diseases, and pests. *Global change and human health,* 2(2):90-104.

Roux, P.W. and Van der Vyver, J. 1988. *The agricultural potential of the eastern Cape and Cape Midlands*. MN Bruton and FW Gess, Towards an environmental plan for the eastern Cape. Rhodes University, Grahamstown.

Rouault, M. and Richard, Y. 2003. Intensity and spatial extension of drought in South Africa at different time scales. *water SA*, 29(4):489-500.

Royer, P.D., Cobb, N.S., Clifford, M.J., Huang, C.Y., Breshears, D.D., Adams, H.D. and Villegas, J.C. 2011. Extreme climatic event-triggered overstorey vegetation loss increases understorey solar input regionally: Primary and secondary ecological implications. *Journal of Ecology*, 99(3):714-723.

Rutherford, M.C. and Westfall, R.H. 1994. *Biomes of southern Africa: an objective categorization*. National Botanical Institute.

Sabo, P. 1992. Application of the thermal front parameter to baroclinic zones around cut-off lows. *Meteorology and Atmospheric Physics*, 47(2): 107-115.

Saidi, H., Ciampittiello, M., Dresti, C. and Ghiglieri, G. 2013. Observed variability and trends in extreme rainfall indices and Peaks-Over-Threshold series. *Hydrology and Earth System Sciences Discussions*, 10(5): 6049-6079.

Saleska, S.R., Didan, K., Huete, A.R. and Da Rocha, H.R. 2007. Amazon forests green-up during 2005 drought. *Science*, 318(5850): 612-612.

Saji, N.H., Goswami, B.N., Vinayachandran, P.N. and Yamagata, T. 1999. A dipole mode in the tropical Indian Ocean. *Nature*, 401(6751): 360-363.

Saji, N.H. and Yamagata, T. 2003. Structure of SST and surface wind variability during Indian Ocean dipole mode events: COADS observations. *Journal of Climate*, 16(16): 2735-2751.

Seneviratne, S.I., Lehner, I., Gurtz, J., Teuling, A.J., Lang, H., Moser, U., Grebner, D., Menzel, L., Schroff, K., Vitvar, T. and Zappa, M. 2012. Swiss prealpine Rietholzbach research catchment and lysimeter: 32-year time series and 2003 drought event. *Water Resources Research*, 48(6).

Schar, C., Vidale, P.L., Luthi, D., Frei, C., Haberli, C., Liniger, M.A. and Appenzeller, C. 2004.The role of increasing temperature variability in European summer heatwaves. *Nature*, 427, :332–336.

Schmiedel, U., Jürgens, N. and Hoffman, M.T. eds. 2010. Biodiversity in southern Africa. 2. *Patterns and processes at regional scale*. Hess.

Seddon, A.W., Macias-Fauria, M., Long, P.R., Benz, D. and Willis, K.J. 2016. Sensitivity of global terrestrial ecosystems to climate variability. *Nature*, 531(7593), pp.229-232.

Sillmann, J., Kharin, V.V., Zwiers, F.W., Zhang, X. and Bronaugh, D. 2013. Climate extremes indices in the CMIP5 multimodel ensemble: Part 2. Future climate projections. *J. Geophys. Res: Atmospheres*, 118(6): 2473-2493.

Singh, A. 1989. Digital Change Detection Techniques Using Remotely Sensed Data. *International Journal of Remote Sensing*, 10: 989–1003.

Singleton, A.T. and Reason, C.J.C. 2006. Numerical simulations of a severe rainfall event over the Eastern Cape coast of South Africa: sensitivity to sea surface temperature and topography. *Tellus A: Dynamic Meteorology and Oceanography*, 58(3): 335-367.

Singleton, A.T. and Reason, C.J.C. 2007. Variability in the characteristics of cut-off low pressure systems over subtropical southern Africa. *International Journal of Climatology*, 27(3): 295-310.

Smith, M.D. 2011. An ecological perspective on extreme climatic events: a synthetic definition and framework to guide future research. *Journal of Ecology*, 99(3):656-663.

Smith, K. and Ward, R. 1998. *Floods: physical processes and human impacts*. John Wiley and Sons Ltd.

Solomon, S., Qin, D., Manning, M., Chen, Z., Marquis, M., Averyt, K., Tignor, M.M.H.L. and Miller, H. 2007. The physical science basis. Contribution of working group I to the fourth assessment report of the intergovernmental panel on climate change, Cambridge, Cambridge University Press:235-337.

Sönmez, F.K., KÖmÜscÜ, A.Ü., Erkan, A. and Turgu, E. 2005. An analysis of spatial and temporal dimension of drought vulnerability in Turkey using the standardized precipitation index. *Natural Hazards*, 35(2): 243-264.

Song, C., Pei, T. and Zhou, C. 2014. The role of changing multiscale temperature variability in extreme temperature events on the eastern and central Tibetan Plateau during 1960–2008. *International Journal of Climatology*, 34(14): 3683-3701.

Starman, A.B. 2013. The case study as a type of qualitative research. *Journal of Contemporary Educational Studies/Sodobna Pedagogika*, 64(1).

Tahir, M.H., Cordeiro, G.M., Alzaatreh, A., Mansoor, M. and Zubair, M. 2016. A New Weibull–Pareto Distribution: Properties and Applications. *Communications in Statistics-Simulation and Computation*, 45(10) :3548-3567.

Taljaard, J.J. 1985. *Cut-off lows in the South African region*: South African Weather Bureau Technical Paper 14.

Tan, C., Yang, J. and Li, M. 2015. Temporal-spatial variation of drought indicated by SPI and SPEI in Ningxia Hui Autonomous Region, China. *Atmosphere*, 6(10): 1399-1421.

Tebaldi, C., Hayhoe, K., Arblaster, J.M. and Meehl, G.A., 2006. Going to the extremes. *Climatic Change*, 79(3) :185-211.

Thenkabail, P.S., Gamage, M.S.D.N., Smakhtin, V.U. 2004. The Use of Remote Sensing Data for Drought Assessment and Monitoring in Southwest Asia, 85. *International Water Management Institute*. Research Report.

Thompson, D.W., Wallace, J.M. and Hegerl, G.C. 2000. Annular modes in the extratropical circulation. Part II: Trends. *Journal of climate*, 13(5): 1018-1036.

Trenberth, K.E. 1997. The definition of el Niño. *Bulletin of the American Meteorological Society*, *78*(12): 2771-2778.

Trenberth, K.E. and Caron, J.M. 2000. The Southern Oscillation revisited: Sea level pressures, surface temperatures, and precipitation. *Journal of Climate*, 13(24): 4358-4365.

Trenberth, K.E., Caron, J.M., Stepaniak, D.P. and Worley, S. 2002. Evolution of El Niño–Southern Oscillation and global atmospheric surface temperatures. *Journal of Geophysical Research: Atmospheres*, *107*(D8): AAC-5.

Tshiala, M.F., Olwoch, J.M. and Engelbrecht, F.A. 2011. Analysis of temperature trends over Limpopo province, South Africa. *Journal of Geography and Geology*, 3(1) :13.

Tucker, C.J. and Choudhury, B.J. 1987. Satellite remote sensing of drought conditions. *Remote Sensing of Environment*, (23): 243-251.

Tucker, C.J., 1979. Red and photographic infrared linear combinations for monitoring vegetation. *Remote Sensing of Environment*. 8: 127-150

Ummenhofer, C.C. and England, M.H. 2007. Interannual extremes in New Zealand precipitation linked to modes of Southern Hemisphere climate variability. *Journal of Climate*, 20(21): 5418-5440.

Usman, M.T. and Reason, C.J.C., 2004. Dry spell frequencies and their variability over southern Africa. *Climate research*, 26(3):199-211.

Van Lanen, H.A.J., Wanders, N., Tallaksen, L.M. and Van Loon, A.F., 2013. Hydrological drought across the world: impact of climate and physical catchment structure. *Hydrology and Earth System Sciences,* 17: 1715-1732.

van Vliet, A.J.H. and Leemans, R., 2006. Ecological impacts of climate change in The Netherlands. In *Climate change and biodiversity-meeting the challenge; people and nature: plan, adapt and survive: report of the 13th Annual Conference of the European Environment and Sustainable Development Advisory Councils EEAC, Oxford, 7-10 September 2005* (81-83). English Nature.

VIANA, D.R. and Alvalá, R.C.S. 2011. Vegetation index performance for the pantanal region during both dry and rainy seasons. *GEOGRAFIA, Rio Claro*, 36: 143-158.

Vicente-Serrano, S.M., Beguería, S. and López-Moreno, J.I. 2010. A multiscalar drought index sensitive to global warming: the standardized precipitation evapotranspiration index. *Journal of Climate*, 23(7) :1696-1718.

Vicente-Serrano, S.M., Beguería, S. and López-Moreno, J.I. 2011. Comment on "Characteristics and trends in various forms of the Palmer Drought Severity Index (PDSI) during 1900–2008" by Aiguo Dai. *Journal of Geophysical Research: Atmospheres*, 116(D19).

Vincent-Serrano, S.M., Zoubber, A., Lasanta, T. and Pueyo, Y. 2012. Dryness is accelerating degradation of vulnerable shrublands in semiarid Mediterranean environments. *Ecological Monographs*, 82(4) :407-428.

Vose, J., Clark, J.S., Luce, C. and Patel-Weynand, T. 2016. Effects of drought on forests and rangelands in the United States: a comprehensive science synthesis. *Gen. Tech. Rep. WO-93b. Washington, DC: US Department of Agriculture, Forest Service, Washington Office*, *93*: 1-289.

Wang, J. and Meng, Y. 2013. An analysis of the drought in Yunnan, China, from a perspective of society drought severity. *Natural hazards*, 67(2): 431-458.

Wang, W., Ertsen, M.W., Svoboda, M.D. and Hafeez, M. 2016. Propagation of drought: from meteorological drought to agricultural and hydrological drought. *Advances in Meteorology*, 2016.

Webster, P.J., Moore, A.M., Loschnigg, J.P. and Leben, R.R. 1999. Coupled ocean–atmosphere dynamics in the Indian Ocean during 1997–98. *Nature,* 401(6751): 356-360.

Weiss, J.L., Gutzler, D.S., Coonrod, J.E.A. and Dahm, C.N. 2004. Long-term vegetation monitoring with NDVI in a diverse semi-arid setting, central New Mexico, USA. *Journal of Arid Environments*, 58(2): 249-272.

Wehner, M. 2013. Methods of projecting future changes in extremes. In Extremes in a Changing Climate. Springer Netherlands :223-237.

Westra, S., Alexander, L.V. and Zwiers, F.W. 2013. Global increasing trends in annual maximum daily precipitation. *Journal of Climate*, 26(11) :3904-3918.

WenBin, Z.H.U., AiFeng, L.V. and ShaoFeng, J.I.A. 2011. Spatial distribution of vegetation and the influencing factors in Qaidam Basin based on NDVI. *Journal of Arid Land*, 3(2): 85-93.

Wigley, T.M. 2009. The effect of changing climate on the frequency of absolute extreme events. *Climatic Change*, 97(1-2) :67.

Williams, C.A. and Hanan, N.P. 2011. ENSO and IOD teleconnections for African ecosystems: evidence of destructive interference between climate oscillations. *Biogeosciences*, 8(1) :27.

Wilcox, E.M. and Donner, L.J. 2007. The frequency of extreme rain events in satellite rain-rate estimates and an atmospheric general circulation model. *Journal of Climate*, 20(1) :53-69.

Wu, D., Zhao, X., Liang, S., Zhou, T., Huang, K., Tang, B. and Zhao, W. 2015. Time-lag effects of global vegetation responses to climate change. *Global change biology*, 21(9): 3520-3531.

Yang, Y., Xiao, P., Feng, X. and Li, H. 2017. Accuracy assessment of seven global land cover datasets over China. ISPRS *Journal of Photogrammetry and Remote Sensing*, 125: 156-173.

Yeh, S.W., Cai, W., Min, S.K., McPhaden, M.J., Dommenget, D., Dewitte, B., Collins, M., Ashok, K., An, S.I., Yim, B.Y. and Kug, J.S. 2018. ENSO atmospheric teleconnections and their response to greenhouse gas forcing. *Reviews of Geophysics,* 56(1): 185-206.

Yuan, F., Sawaya, K.E., Loeffelholz, B.C. and Bauer, M.E. 2005. Land cover classification and change analysis of the Twin Cities (Minnesota) Metropolitan Area by multitemporal Landsat remote sensing. *Remote sensing of Environment*, 98(2-3): 317-328.

Zarch, M.A.A., Sivakumar, B. and Sharma, A. 2015. Droughts in a warming climate: A global assessment of Standardized precipitation index (SPI) and Reconnaissance drought index (RDI). *Journal of Hydrology*, *526*: 183-195.

Ziervogel, G., New, M., Archer van Garderen, E., Midgley, G., Taylor, A., Hamann, R., Stuart-Hill, S., Myers, J. and Warburton, M. 2014. Climate change impacts and adaptation in South Africa. Wiley Interdisciplinary Reviews: *Climate Change*, 5(5): 605-620.

Zhang, N., Hong, Y., Qin, Q. and Liu, L. 2013. VSDI: a visible and shortwave infrared drought index for monitoring soil and vegetation moisture based on optical remote sensing. *International journal of remote sensing,* 34(13): 4585-4609.

Zhang, Z., Chen, X., Xu, C.Y., Hong, Y., Hardy, J. and Sun, Z. 2015. Examining the influence of river–lake interaction on the drought and water resources in the Poyang Lake basin. *Journal of Hydrology*, 522: 510-521.

Zhang, Q., Zhang, J., Yan, D. and Wang, Y. 2015. Extreme precipitation events identified using detrended fluctuation analysis (DFA) in Anhui, China. *Theoretical and applied climatology*, 117(1-2):169-174.

Zhang, X., Brown, R., Vincent, L., Skinner, W., Feng, Y. and Mekis, E. 2010. Canadian climate trends, 1950-2007. Canadian biodiversity: *ecosystem status and trends*.

Zhang, Q., Kong, D., Singh, V.P. and Shi, P. 2017. Response of vegetation to different time-scales drought across China: Spatiotemporal patterns, causes and implications. *Global and Planetary Change*, 152:1-11.

Zhang, H.K. and Roy, D.P. 2017. Using the 500 m MODIS land cover product to derive a consistent continental scale 30 m Landsat land cover classification. *Remote Sensing of Environment*, 197:15-34.

Zhao, S. and Sun, J., 2007. Study on cut-off low-pressure systems with floods over Northeast Asia. *Meteorol. Atmos. Phys*, 96(1): 159-180.

Zhong, S., Qian, Y., Zhao, C., Leung, R., Wang, H., Yang, B., Fan, J., Yan, H., Yang, X.Q. and Liu, D. 2017. Urbanization-induced urban heat island and aerosol effects on climate extremes in the Yangtze River Delta region of China. *Atmospheric Chemistry & Physics*, 17(8).

Zoungrana, B.J., Conrad, C., Amekudzi, L.K., Thiel, M., Da, E.D., Forkuor, G. and Löw, F. 2015. Multi-temporal landsat images and ancillary data for land use/cover change (LULCC) detection in the Southwest of Burkina Faso, West Africa. *Remote Sensing*, 7(9): 12076-12102. Stop